DOKUZ EYLÜL UNIVERSITY
GRADUATE SCHOOL OF NATURAL AND APPLIED SCIENCE

ELASTO-PLASTIC STRESSES IN A CIRCULAR CYLINDER WITH A BAND OF PRESSURE

A Thesis Presented to the
Graduate School of Natural and Applied Sciences
Dokuz Eylül University

In Partial Fulfillment of the
Requirements for the Doctor of Philosophy
Mechanical Engineering

by
Muhammet CERİT

Advisor
Prof. Dr. Onur SAYMAN

March, 1996 İZMİR

ABSTRACT

Circular cylindrical element with strip pressure in radial direction has widely applications in engineering such as bearings, gears, pulleys and shrink fit. In these machine elements, small permanent deformations occur under the working loads. Determination of elasto-plastic deformations, stress components and residual stresses after removal of loads would make possible the utilization of ultimate level of material capacity.

In the study, elasto-plastic stresses and residual stresses in the isotropic circular cylinder with the strip pressure in radial direction are investigated by the finite element method.

As the stress-strain relationship of the material is nonlinear after the yielding point, in the non-linear region successive incremental loading are carried out, the material is assumed linear, and for each incremental that material behaves linearly. Namely, successive linear analysis carried out for non-linear behavior.

In the investigation, because of the symmetry with respect to geometry, support condition and material properties of the problem, the problem is analyzed by four nodes isoparametric rectangular ring shape finite elements. Finite element mesh generation is carried out on computer automatically. General purpose computer program is used to solve the problem.

In the solution, it is assumed that deformations are small. Solid and hallow sectional cylinders with ratios inner diameter to outer diameter are considered. Stress and strain components are determined for different band pressures. And in the removal of the band pressure residual stresses are calculated. The magnitude of the residual stress can be obtained by superposition of the stresses due to loading and unloading. Values of the band pressure initiating plastic deformation are determined for different diameters by using von-Mises criterion.

Distributions of stress components (equivalent, tangential, radial, axial and shear stress) and residual stress components are plotted along the longitudinal axis on the outer and inner surfaces of the circular cylinder. Deformed shape and displacement of the model are given on the longitudinal section in the circular cylinders. Variations of stress contour components are presented on the longitudinal section along the circular cylinder for different diameter.

Key words: Elasto-plastic stresses analysis, finite element method, axisymmetric finite element, residual stresses, band pressure, circular cylindrical element, plastic deformation.

ÖZET

Çevresi boyunca band basıncına maruz dairesel silindirik elemanlar mühendislik uygulamalarında yaygın kullanım alanı bulmaktadır (rulman, kasnak ve dişli makina elemanlarının sıkı geçme ile bağlanmasında olduğu gibi). Bu form birleştirmelerde, silindirik elemanlar üzerinde, büyük olmayan kalıcı şekil değişiklikleri meydana gelir. Makina elemanlarının bu bölgelerindeki, elasto-plastik şekil değişikliklerinin, gerilme bileşenlerinin ve band basıncının kaldırılmsıyle oluşan artık gerilmelerin önceden belirlenmesi, malzemenin mukavemetinden maksimum seviyede faydalanılmasına imkan sağlar.

Bu çalışmada, çevresi boyunca band basıncı etkisine maruz, izotrop malzemeye sahip dairesel silindirik (dolu ve simetri ekseni boyunca boşaltılmış) elemanlarda meynada gelen elasto-plastik gerilmeler ve artık gerilmeler sonlu elemanlar metodu ile incelendi.

Akma noktasından sonra malzemenin gerilme-zorlanma ilişkisi non-lineer olduğundan, küçük artırımlarla ardışık yükleme yapılmış ve her bir aralıkta malzemenin lineer davrandığı kabul edilmiştir. Diger bir ifade ile nonlineer analizde çok tekrarlı lineer analiz yapılmıştır. Sonlu eleman modeli, geometri, sınır şartları ve yükleme simetrisinden dolayı izoparametrik dört düğümlü dörtgen halka elemanlardan oluşturulmuştur. Sistemin sonlu sayıda elamana bölümlenmesi bilgisayarda otomatik olarak yapılmıştır.

Çözümde, şekil değişimlerinin küçük olduğu durumlar incelenmiştir. Çözümler, dolu ve farklı oranlarda içi boşaltılmış silindirler için yapılmıştır. Farklı band basıncı değerlerinde meydana gelen zorlanma ve gerilme bileşenleri değerleri hesaplanmıştır. Bununla birlikte, silindire etki eden band basıncının kaldırılması halinde silindirde meydana gelen artık gerilmeler hesaplanmıştır. Plastik şekil değişimini başlatan band basıncı değerleri von-Mises akma kriteri esas alınarak belirlenmiş ve grafik olarak sunulmuştur..

Elasto-plastik gerilme analizi sonucunda, farklı band basıncı etkisinde dairesel silindirlerin iç ve dış yüzeylerinde hesaplanan gerilme bileşenlerinin (eşdeğer, teğetsel, radyal, eksenel ve kayma) ve artık gerilme bileşenlerinin değişimleri simetri ekseni boyunca grafikler halinde gösterildi. Modelin şekil değiştirmiş formu ve modeli oluşturan sonlu elemanların yerdeğiştirmeleri kesit üzerinde gösterildi. Elasto-plastik gerilme bileşenlerinin dağılımları ve band basıncın artırılması ile plastik defomasyonun derinleşmesi silindirin boylamasına kesiti üzerinde farklı renklerle gösterildi.

Anahtar sözcükler: Elasto-plastik gerilme analizi, sonlu elemanlar metodu, plastik şekil değişimi, eksenel simetrik eleman, artık gerilmeler, band basıncı, silindirik eleman.

II

ACKNOWLEDGMENTS

I am deeply grateful to Prof. Dr. Onur Sayman for his patient supervision, voluble guidance and continuos encouragement throughout this study.

I am much indebted to Assoc. Prof. Dr. Durmuş Günay SA.Ü Engineering Faculty, for his active support and his continued interest in my work.

Finally, I wish to express my sincere thanks to my family for their tolerance and understanding while preparing this thesis.

<div align="right">Muhammet Cerit</div>

Esentepe - Adapazarı
March 1996

CONTENTS

LIST OF FIGURES

XI

XII

XVI

XVIII

LIST OF TABLES

NOMENCLATURES

a	:Inner radius of the circular cylinder
b	:Outer radius of the circular cylinder
c	:Width of the half band pressure
L	:Length of the half circular cylinder
E	:Modulus of elasticity
G	:Shear modulus of elasticity
υ	:Poisson's ratio
φ	:Interpolation function
$\{F\}^e$	:Column vector of the nodal forces of the element e
$[K]^e$	:Stiffness matrix of the element e
$\{U\}^e$	:Nodal displacement vector of the element e
t_e	:Thickness of element e
$\{F\}$	:Column vector of the nodal forces of the entire system
$[K]$	:Stiffness matrix of the entire system
$\{U\}$	:Nodal displacement vector of the entire system
ξ, η	:Natural coordinate
x,y	:Global coordinate
$\{q\}$	:Displacement vector
$[D]$	:Elasticity matrix of material
$[B]$	:Transformation matrix between strain and displacement
$\{\sigma\}$	:Stress vector
$\{\varepsilon\}$	:Strain vector
r,z,θ	:Cylindrical coordinate
u,w	:Displacement components in r-z coordinate
J	:Jacobian operator
U_d	:Distortion energy
σ_r	:Radial stress
σ_t	:Tangential stress
τ_{rz}	:Shear stress
σ_z	:Axial (longitudinal) stress
σ_{eq}	:Equivalent stress for von-Mises criterion
σ_{ep}	:Elasto-plastic stress
σ_y	:Yield strength
σ_u	:Ultimate strength
σ_f	:Fracture strength

ε_e	:Elastic strain
ε_p	:Plastic strain
K	:Strain hardening coefficient
n	:Strain strengthening exponent
σ_0	:Yield stress
ε_0	:Yield strain
T	:Traction force
P	:Band pressure
P_i, F	:Force
a_1, a_2, a_3	:Constants of the polynomial
$\sigma_1, \sigma_2, \sigma_3$	:Principal stresses
N_1, N_2, N_3, N_4	:Shape functions of quadrilateral element
d.o.f	:Degree of freedom

Note: The other notations have been defined in the chapters.

CHAPTER ONE

INTRODUCTION

A circular cylinder with a band of pressure is encountered on a routine basis. For instance, pressure vessels, roller bearing, assembly of shrink fits etc. In these elements, small permanent deformations occur under the working loads. Determination of elasto-plastic deformations, stress components and residual stresses after removal of loads would make possible the utilization of ultimate level of material capacity. In the study, elasto-plastic stresses and residual stresses in the isotropic circular cylinder with the strip pressure in radial direction are investigated by the finite element method

Shrink fits are found frequently in mechanical engineering. The importance of shrink fits rests on the fact that they are capable of transmitting high moments at low production coast. To better utilize hub material, plastic deformation is admitted in many cases. A generalization of Kollmann's work for linear strain-hardening materials has been given by Gamer and Lance [1]. Furthermore, it has been shown that hub material with an arbitrary nonlinear hardening law can be taken into account without excessive numerical calculations[2].

As the stress-strain relationship of the material is nonlinear after the yielding point, in the non-linear region successive incremental loading are carried out, the material is assumed, and for each incremental that material behaves linearly. Namely, successive linear analysis carried out for non-linear behavior. In the investigation, because of the symmetry with respect to geometry, support condition and material properties of the problem, the problem is analyzed by four nodes axisymmetric isoparametric finite elements. Finite element mesh generation is carried out on computer automatically.

Various computational procedures have been used with success for a limited range of elasto-plastic problems utilizing the finite element approach. Two main formulation appear. In the first, during an increment of loading, the increase of plastic strain is computed and treated as an initial strain for which the elastic stress distribution is adjusted [3,4]. This approach manifestly fails if ideal plasticity is postulated or if the degree of hardening is small. The second approach is that in which the stress-strain relationship in every load increment is adjusted to take into account plastic deformation. The work of Pope [5] Swedlow [6] Marcal and King [7], Reyes and Deere [8] and Popov and others [9] falls into this category. With a properly specified elasto-plastic

1

matrix this incremental elasticity approach can successfully treat ideal as well as hardening plasticity.

Ergatoudis, Irons and Zienkiewicz have investigated the theory of new family of isoparametric elements for use in two dimensional situations[10]. Clough has developed an approximate numerical analysis procedure which is capable of solving the shells of arbitrary shape, boundary conditions and loading[11].

Owen and Salonen have present numerical solutions to three-dimensional elasto-plastic problems illustrating the applicability of isoparametric elements and the other of computation times involved[12].

Elasto-plastic analysis of two-dimensional stress system -plane stress, plane stress and axisymmetrically loaded body of revaluation- has carried out for isotropic materials by finite element method. Studies have been made on the development of the plastic zone, the load-displacement relationship, and the stress and strain distribution during continued loading and residual stresses have been examined[13,14].

In the solution, it is assume that deformations are small. Solid cylinder and hallow sectional cylinders with ratios inner diameter to outer diameter are considered. Stress and strain components are determined for different band pressures. And in the removal of the band pressure residual stresses are calculated values of the band pressure initiating plastic deformation are determined by using criteria of Von-Mises.

Meguid and Klair present elasto-plastic finite element analyses of the simultaneous indentations of a bounded solid[15].

Distributions of stresses components (equivalent, tangential, radial, axial and shear stresses) and residual stresses components are plotted along the cylinder length on the outer surface of cylinder and inner surface of cylinder. Variation of stresses components are presented along the circular cylinder on the cross sectional area as stress contour map legend for different diameter.

In this study, circular cylinder under band pressure is solved by finite element method in elastic region and elasto-plastic region.

In elastic region, M.V. Barton solve this problem by means of fourier series [16]. An analysis of an elastic collar shrunk onto a long elastic shaft is given by H. Okubo[17]. When a short collar is shrunk on a much longer shaft the simple shrink-fit formula are not accurate but, is valid when collar and shaft are of equal lengths. A much better approximation is obtained by considering the problem indicated in figure 1.1 of a long cylinder with a uniform normal pressure P acting on the band ABCD of the surface. The required solution can evidently be obtained by superposing the effects of the two pressure

distribution indicated in figure 1.1. The basic problem is therefore that of pressure P/2 on the lower half of the cylindrical surface and -P/2 on the upper half, the length of the cylinder being infinite..

Barton obtained a different method of using Fourier series. From these curves results can be obtained for the problem of figure 1.1 by superposition.
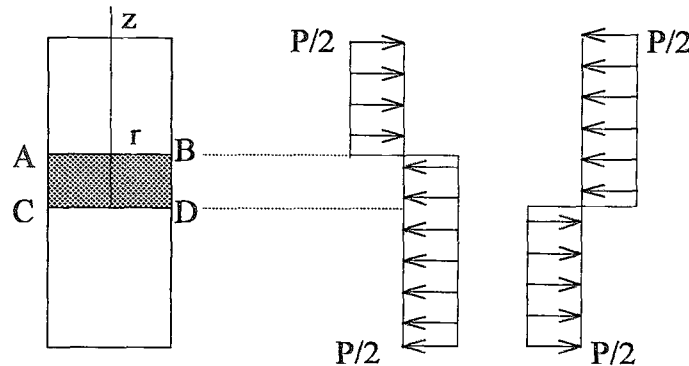
Figure 1.1 A long cylinder with a uniformed normal pressure P

When the width of band pressure is equal to the radius of the cylinder the tangential stress σ_θ at the surface and at the middle of the pressure band reaches a value about 10 per cent higher than the applied pressure, and is, of course, compressive. The axial stress σ_z in the surface just outside the pressure band reaches a tensile value of about 45 per cent of the applied pressure. The shear stress τ_{rz} attains a greatest value, equal to 31.8 per cent of the applied pressure, at the edges of the pressure band AB and CD in figure 1.1 and just below the surface. When the pressure is applied all over the curved surface of the cylinder, of any length, we have simply compressive σ_r and σ_θ equal to the applied pressure, and σ_z and τ_{rz} zero. Solutions have been obtained in a similar manner for a band of pressure in a hole in an infinite solid, and for a band of pressure near one and of a cylinder.

In the study, elasto-plastic stresses and residual stresses in the isotropic circular cylinder with the strip pressure in radial direction are investigated by the finite element method. In the solution, ANSYS program is a general-purpose computer program for finite element analysis was used. The ANSYS program is a general-purpose program, meaning that you can use it for almost any type of finite element analysis in virtually any industry - automobiles, aerospace, railways, machinery, electronics, electromagnetic, sporting goods, power generation, power transmission, and biomechanics to mentioned just a few. General purpose also refers to the fact that the program can be used in all disciplines of engineering -structural, mechanical, electrical, electromagnetic, electronic, thermal, fluid, and biomedical. The ANSYS program is also used as an educational tool in universities and other academic institutions[18,26].

3

In the second chapter, we recall some fundamental concepts needed in the development of the finite element method. Equation of equilibrium, stress-strain relation, strain-displacement relation and some axial symmetric formulation that we interest in that deal with are given.

In the third chapter, a brief overview of the finite element method, historical background and its concept is presented. These are generation of the finite element mesh, the isoparametric elements, shape functions, obtaining the element properties, assembly of the element properties, solving the system equations, calculating of the stresses from the strain.

In the fourth chapter, we developed what are popularly called isoparametric elements and apply them to stress analysis. These elements have proved effective on a wide variety of two dimensional problems in engineering.

In the fifth chapter, some basic concepts of theory of plasticity, total stress-strain relations, Prandl-Reuse relation, Levy-Mises relation, empirical equation for stress-strain curve, yield surface, calculation of the elasto-plastic stress, residual stress for isotropic material and some important failure criteria for isotropic material are given.

In the sixth chapter, we present that what causes nonlinear behavior, types of the nonlinear behavior, nonlinear solution technique, newton-raphson iteration.

In the seventh chapter, definition of the circular cylinder with a band of pressure, finite element model, boundary condition and load condition of the finite element, deformed shape of the finite element model are illustrated in figures. Material properties and dimension of the model are defined. Distribution of elasto-plastic and residual stresses distribution for different diameter of the circular cylinders are shown in figures for different band pressure. Components of contour elasto-plastic stresses are plotted from the obtained results.

In the eighth chapter, results and conclusions have been presented.

In the appendix A, press and shrink fits condition is presented

In the appendix B, circular solid and hallow cylinder under uniform pressure have been formulated.

In the appendix C, computer program is presented in detail. Basic main procedure is presented; input geometric form of the model, select element type, definition of the material properties, generation of the mesh, considering the boundary conditions, loading that is external force, solving the problem, obtaining results (displacements, strains, stresses etc.), and plotting results (deformed shape, stresses contour etc.).

4

CHAPTER TWO

BASIC CONCEPTS OF CONTINUUM SYSTEM

2.1. INTRODUCTION

In this chapter, we recall some fundamental concepts needed in the development of the finite element method. Equations of equilibrium, stress-strain relation, strain-displacement relation and some axial symmetric formulation that we interest in that deal with are given.

2.2. EQUATION OF EQUILIBRIUM

The solution of many elasticity problems, especially for bodies of circular cylinder form, are conveniently formulated in terms of cylindrical coordinates r, θ, z. Let us consider equilibrium condition on the figure 2.1 in the direction r, θ, z.
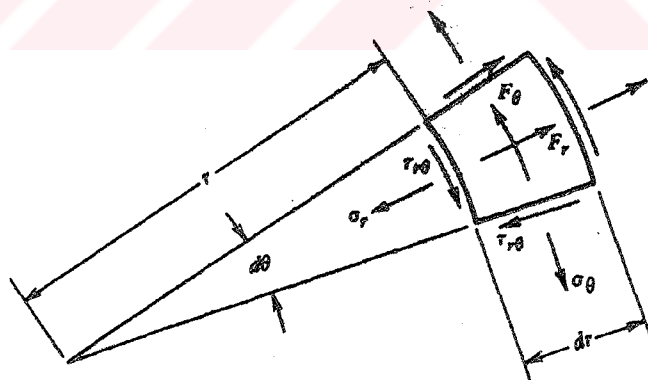
Figure 2.1. Plane differential element in cylindrical coordinate

Total force must be zero for equilibrium in the r, θ, z direction.

$$\sum Fr = 0 \ , \qquad \sum F\theta = 0 \ , \qquad \sum Fz = 0 \ ,$$

$$\frac{\partial \sigma_r}{\partial r} + \frac{1}{r}\frac{\partial \tau_{r\theta}}{\partial \theta} + \frac{\partial \tau_{rz}}{\partial z} + \frac{\sigma_r - \sigma_\theta}{r} + F_r = 0$$

$$\frac{\partial \tau_{r\theta}}{\partial r} + \frac{1}{r}\frac{\partial \sigma_\theta}{\partial \theta} + \frac{\partial \tau_{\theta z}}{\partial z} + \frac{2\partial \tau_{r\theta}}{r} + F_\theta = 0$$

$$\frac{\tau_{rz}}{r} + \frac{1}{r}\frac{\partial \tau_{\theta z}}{\partial \theta} + \frac{\partial \sigma_z}{\partial z} + \frac{\partial \tau_{rz}}{r} + F_z = 0$$

2.3. STRAIN-DISPLACEMENT RELATION
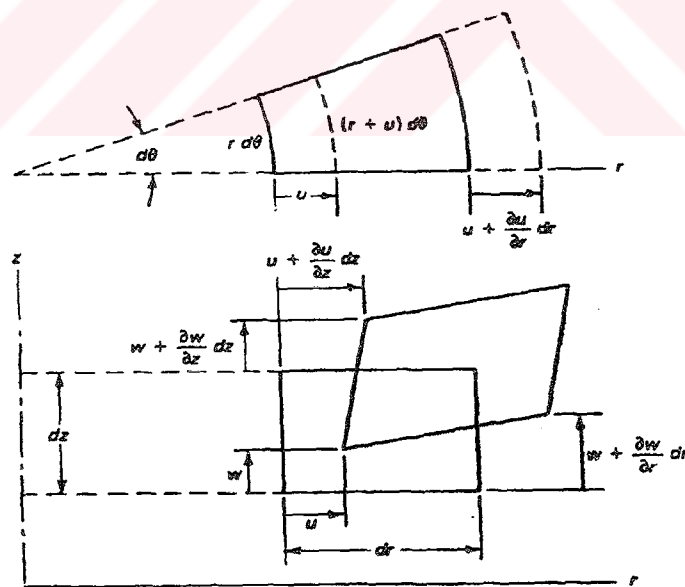
Figure 2.2. Deformation of the elemental volume in the cylindrical coordinate

6

In the cylindrical coordinate, strain-displacement relation are given

$$\varepsilon_r = \frac{\partial u}{\partial r} \qquad\qquad \gamma_{r\theta} = 2\varepsilon_{r\theta} = \frac{1}{r}\frac{\partial u}{\partial \theta} + \frac{\partial v}{\partial r} - \frac{v}{r}$$

$$\varepsilon_\theta = \frac{u}{r} + \frac{1}{r}\frac{\partial v}{\partial \theta} \qquad\qquad \gamma_{\theta z} = 2\varepsilon_{\theta z} = \frac{\partial v}{\partial z} + \frac{1}{r}\frac{\partial w}{\partial \theta}$$

$$\varepsilon_z = \frac{\partial w}{\partial z} \qquad\qquad \gamma_{rz} = 2\varepsilon_{rz} = \frac{\partial u}{\partial z} + \frac{\partial w}{\partial r}$$

2.4. STRESS-STRAIN RELATIONSHIP

For linear elastic materials, the stress-strain come from the generalized Hook's law. For isotropic materials, the two materials properties are Young's modulus (modulus of elasticity) E, Poisson's ratio υ, and shear modules $G = \dfrac{E}{2(1+\upsilon)}$. In the cylindrical coordinate that can be written as;

$$\varepsilon_r = \frac{1}{E}\left[\sigma_r - \upsilon(\sigma_\theta + \sigma_z)\right] \qquad\qquad \gamma_{rz} = \frac{\tau_{rz}}{G}$$

$$\varepsilon_\theta = \frac{1}{E}\left[\sigma_\theta - \upsilon(\sigma_r + \sigma_z)\right] \qquad\qquad \gamma_{r\theta} = \frac{\tau_{r\theta}}{G}$$

$$\varepsilon_z = \frac{1}{E}\left[\sigma_z - \upsilon(\sigma_\theta + \sigma_r)\right] \qquad\qquad \gamma_{\theta z} = \frac{\tau_{\theta z}}{G}$$

From the above equation we can get stress components as following form;

$$\sigma_r = \frac{E}{1+\upsilon}\left[\varepsilon_r + \frac{\upsilon}{1-2\upsilon}(\varepsilon_r + \varepsilon_\theta + \varepsilon_z)\right] \qquad\qquad \tau_{r\theta} = G\gamma_{r\theta}$$

$$\sigma_\theta = \frac{E}{1+\upsilon}\left[\varepsilon_\theta + \frac{\upsilon}{1-2\upsilon}(\varepsilon_r + \varepsilon_\theta + \varepsilon_z)\right] \qquad\qquad \tau_{rz} = G\gamma_{rz}$$

$$\sigma_z = \frac{E}{1+\upsilon}\left[\varepsilon_z + \frac{\upsilon}{1-2\upsilon}(\varepsilon_r + \varepsilon_\theta + \varepsilon_z)\right] \qquad\qquad \tau_{\theta z} = G\gamma_{\theta z}$$

2.5. AXISYMMETRIC ANALYSIS (SOLIDS OF REVOLUTION)

A solid of revolution is generated by the revolving a plane figure about an axis, and it most easily described in cylindrical coordinates r, θ, and z figure 2.3. The geometry is axially symmetric, and if material properties and loads also axially symmetric the problem is mathematically two-dimensional. That is, if geometry, support condition, loads, and material property matrix are all independent of θ, and if the material either is isotropic or has θ as a principal material direction, then static displacements and stresses are independent of θ: Circumferantial displacement v is zero, material points have only u (radial) and w (axial) displacement components, and the nonzero stresses are those shown in figure 2.3.
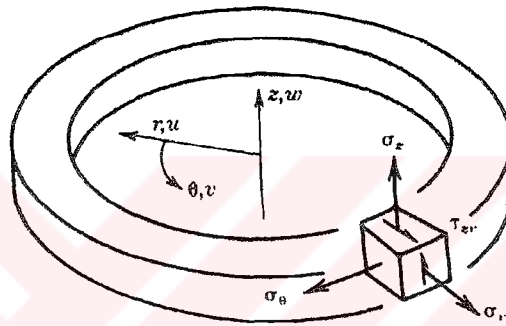
Figure 2.3. Axially symmetric solid isometric view
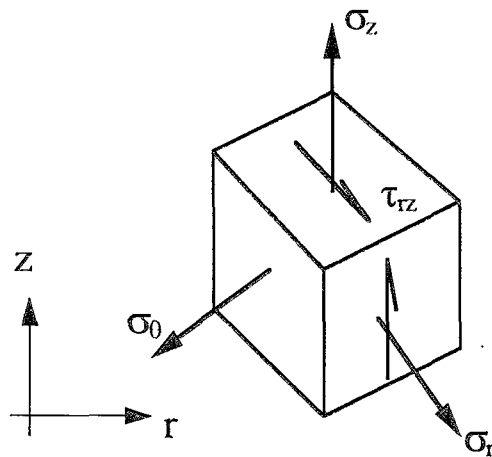
Figure 2.4. Stresses produced by axially symmetric loading

8

Considering the elemental volume, the potential energy can be written in the form

$$\Pi = \frac{1}{2}\int_0^{2\pi}\int_A \sigma^T \varepsilon \, r \, dA \, d\theta - \int_0^{2\pi}\int_A u^T f \, r \, dA \, d\theta - \int_0^{2\pi}\int_L u^T T \, r \, dl \, d\theta - \sum_i u_i^T P_i \qquad (2.1)$$

where r dl dθ is the elemental surface area, and the point load P_i represent a line load distributed around a circle,

$$u = [u, w]^T, \quad f = [f_r, f_z]^T, \quad T = [T_r, T_z]^T, \quad P = [P_r, P_z]^T \qquad (2.2)$$

where f is the body force, T is the surface traction force, u is the displacement and unit volume for axially symmetric element.

$$dV = r \, d\theta \, dz \, dz = r \, d\theta \, dA$$

All variables in the integrals are independent of θ. Thus, equation (2.1) can be written as

$$\Pi = 2\pi\left(\frac{1}{2}\int_A \sigma^T \varepsilon \, r \, dA - \int_A u^T f \, r \, dA - \int_L u^T T \, r \, dl\right) - \sum_i u_i^T P_i \qquad (2.3)$$

We can write the relationship between strains ε and displacements u as

$$\varepsilon = [\varepsilon_r, \varepsilon_z, \gamma_{xy}, \varepsilon_\theta]^T \qquad (2.4)$$

$$\varepsilon = \left[\frac{\partial u}{\partial r}, \frac{\partial w}{\partial z}, \frac{\partial u}{\partial z}+\frac{\partial w}{\partial r}, \frac{u}{r}\right]^T \qquad (2.5)$$

The stress vector is correspondingly defined as

$$\sigma = [\sigma_r, \sigma_z, \tau_{rz}, \sigma_\theta]^T \qquad (2.6)$$

The stresses-strains relations are given in the usual form.

$$\sigma = D \, \varepsilon \tag{2.7}$$

where D is (4x4) symmetric material matrix in which E is modulus of elasticity and υ is the Poisson's ratio.

$$D = \frac{E(1-\upsilon)}{(1+\upsilon)(1-2\upsilon)} \begin{bmatrix} 1 & \dfrac{\upsilon}{1-\upsilon} & 0 & \dfrac{\upsilon}{1-\upsilon} \\ \dfrac{\upsilon}{1-\upsilon} & 1 & 0 & \dfrac{\upsilon}{1-\upsilon} \\ 0 & 0 & \dfrac{1-2\upsilon}{2(1-\upsilon)} & 0 \\ \dfrac{\upsilon}{1-\upsilon} & \dfrac{\upsilon}{1-\upsilon} & 0 & 1 \end{bmatrix} \tag{2.8}$$

CHAPTER THREE

FINITE ELEMENT METHOD

3.1. INTRODUCTION

The finite element method is a very powerful and elegant technique that is numerical procedure for analyzing structure and continua. This technique has rapidly become a popular method for the computer solution of complex problems in engineering.

The finite element method originated as a method of stress analysis. Today finite elements are also used to analyze problem of heat transfer, fluid flow, lubrication, electric and magnetic fields, and many others. Finite element calculation are performed on personal computers, mainframe and all size in between. Result are rarely exact. However, errors are decreased by processing more equation, and results accurate enough for engineering purposes are obtainable at reasonable cost.

With this method the structure is divided into a network of small elements connected to each other at node points. Each element is of simple geometry and therefore is much easier to analyze than the actual structure. In essence, we approximate a complicated solution by a model that consists of piecewise-continuos simple solution.

Method was originally developed for two dimensional (plane stress) situation. A three dimensional structure causes orders of magnitude increase in the number of simultaneous equation; but by using high order elements and faster computers these problems are being handled by the finite element method. Figure 3.1 Shows some of the element types available for finite element analysis. These are triangle element, quadrilateral element, axial symmetric triangle or quadratic element, tetrahedron element, hexahedral element, shell element etc.

An important ingredient in a finite element analysis is the behavior of the individual elements. A few good elements may produce better results than many poorer elements. We can see that several element types are possible by considering Figure 3.2. Function φ, which might represent any of several physical quantities, varies smoothly in the actual structure. A finite element model typical yields a piecewise- smooth representation of φ. Within each element φ is a smooth function that is usually
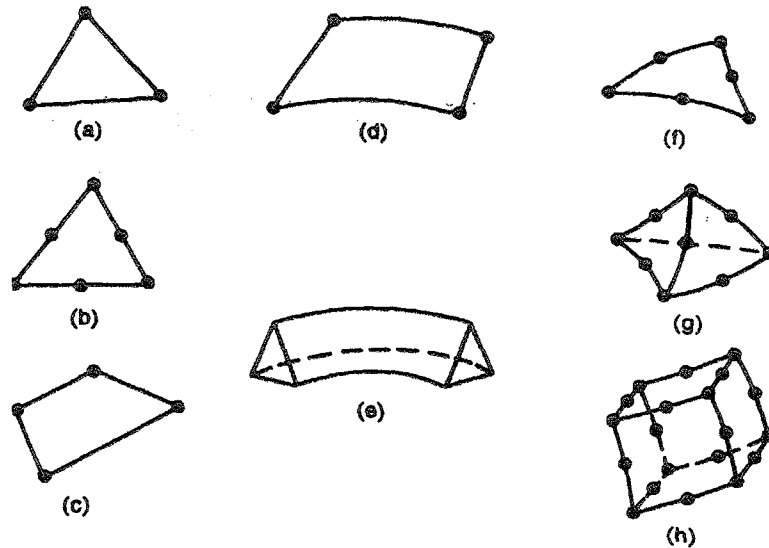
Figure 3.1. Some common elements used in the finite element method analysis

represented by a single polynomial. For the polynomial three node triangle, the bilinear function

$$\varphi = a_1 + a_2x + a_3y \tag{3.1}$$

is appropriate, where the a_i are constants.

How can the user decide which element to use? Unfortunately, the answer is not simple. An element that is good in one problem (such as magnetic fields) may poor in another (such as stress analysis). Even in specific problem area, an element behave well or badly, depending on the particular geometry, loading and boundary conditions. A competent user of finite element must be familiar with how various elements behave under various conditions.

We may now venture some definition. The finite element method is a method of piecewise approximation φ in which the approximating function φ is formed by connecting simple functions, each defined over a small region (element). A finite element is a region in space in which a function φ is interpolated from nodal values of φ on the boundary of the region in such a way that interelement continuity of φ tends to be maintained in the assemblage.

12
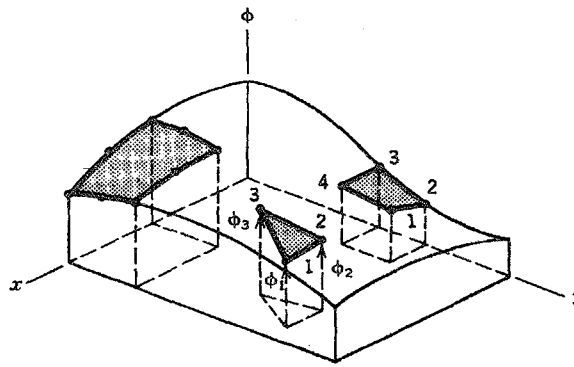
Figure 3.2. A function φ=φ(x,y) that varies smoothly over a rectangular region in the xy plane, and typical elements that might be used to approximate it.

A finite element analysis typically involves the following step

- Divide the structure or continuum into finite elements.
- Formulate the properties each element. In stress analysis, this means determining nodal loads associated with all element deformation states that are allowed.
- Assemble elements to obtain the finite element model of the structure
- Apply the known loads: nodal forces and/or moments in stress analysis.
- In stress analysis, specify how the structure is supported. This step involves setting several nodal displacement to known values (which often are zero).
- Solve simultaneous linear algebraic equations to determine nodal degree of freedom (d.o.f) nodal displacements in stress analysis.
- In stress analysis, calculate element strains from the nodal d.o.f. and the element displacement field interpolation, and finally calculate stresses from strains. Output interpolation programs, called postprosesor, help the user sort the output and display it in graphical form figure 3.3.

The power of the finite element method resides principally in its versatility. The method can be applied to various physical problems. The body analyzed can have arbitrary shape, loads, and support conditions. The mesh can mix elements of different types, shapes and physical properties. This great versatibility is contained within a single computer program. User prepared input data controls the selections of problem type, geometry, boundary condition, element selection, and so on.

An other attractive feature of finite elements is the close physical resemblance between the actual structure and its finite element model. The model is not simply an abstraction. This seems especially true in structural mechanics, and may account for the finite element method having its origins there.

a) Bearing hausing model   b) Deformed shape   c) Stress contour
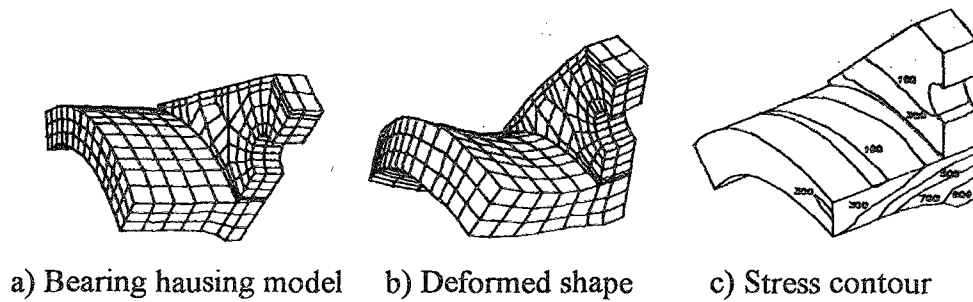
Figure 3.3. Finite element mesh and computed deformation and stresses in a portion of a bearing house.

The finite element method also has disadvantages. A specific numerical result is found for a specific problem. A finite element analysis provides no closed form solution that permits analytical study of the effects of chancing various parameters. A computer, a reliable program, and intelligent use are essential. A general purpose program has extensive documentation, which can not be ignored. Experience and good engineering judgment are needed in order to define a good model. Many input data are required and voluminous output must be stored and understood.

3.2. GENERATION OF FINITE ELEMENT MESH

The first step in a finite element analysis is to select the type of the elements and the corresponding finite element mesh. There are no fixed rules on how to make decisions. Clearly, for a given type of element the accuracy increases with decreasing element and, in general, one will use small elements in regions where the unknown function-stress, say- varies rapidly. This means that a sound physical understanding of the problem considered is of fundamental importance for a realistic analysis. However, the decision on element types and size is more delicate then that. Every analysis involves the use resources, whether they are measured in terms of money or manpower, and even though we aim at an accurate analysis, we do not want it to be more accurate than required. For some problems, we are interest in detailed information on the behavior even in local regions, while for others we only want to obtain a rather general and crude indication of the overall response. As engineers we must therefore use our judgment in order to obtain that optimum choice for element type and element mesh which balances the requirement of reliable results whit that of course effectiveness.

All finite elements are based on rather simple polynomial interpolations of the unknown function within the element. For a given type of element this means that the smaller the elements, the greater the accuracy. However, it also implies that any dimension of an

14

element should be kept as small as possible, i.e. it is not only the size, but also the form of the element which is importance. As an example, assume that quadrilateral shown in figure 3.4.a is to divided into two triangular elements.

<div align="center">(a)   (b)   (c)</div>
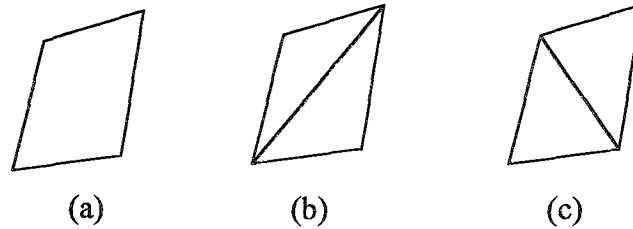
Figure 3.4. a- Quadrilateral element   b- inferior decision   c- desirable division

It is obvious that the division in figure 3.4.c is better than 3.4.b, since largest dimension of the element figure 3.4.c is smaller than that given by 3.4.b. The Ratio between the largest and smallest dimension of an element is called the aspect ratio and in a good finite element mesh, the aspect ratio is as close as possible to unity.
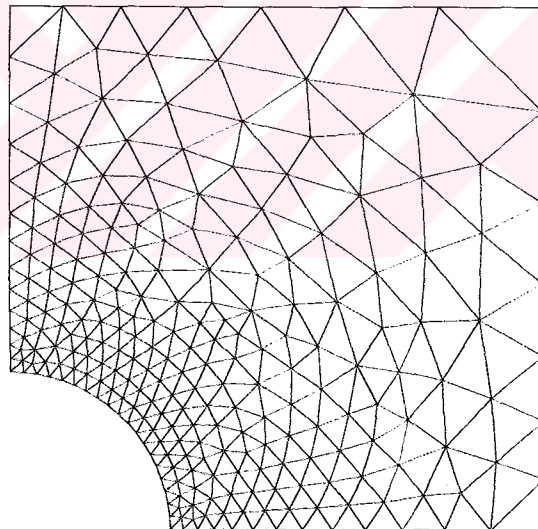
Figure 3.5. Mesh refinement for the finite element analysis

In order to obtain an efficient solution scheme, we want to use few elements in regions where unknown function varies slowly, but many elements in regions where it varies rapidly. Two possibilities, which allow for such a mesh refinement and which fulfill the continuity requirement are illustrated figure 3.5 for the three-node triangular element.

3.3. ISOPARAMETRIC ELEMENTS

The isoparametric formulation makes it possible to generate that are non rectangular and have curved sides. These shapes have obvious uses in grading a mesh from coarse to fine, in modeling curved boundaries. The isoparametric family includes elements for plane, solid, plate, and shell problems. There are also special elements for fracture mechanics and element for nonstructural problems.

In formulating isoparametric elements, natural coordinate systems must be used (systems ξ, η and ξ, η, ζ in figure 3.6). Displacements are expressed in terms of natural coordinates, but must be differentiated with respect to global coordinates x, y and z.

The term isoparametric means same parametric. In other words, the degree of interpolation on coordinates are the same on displacements.
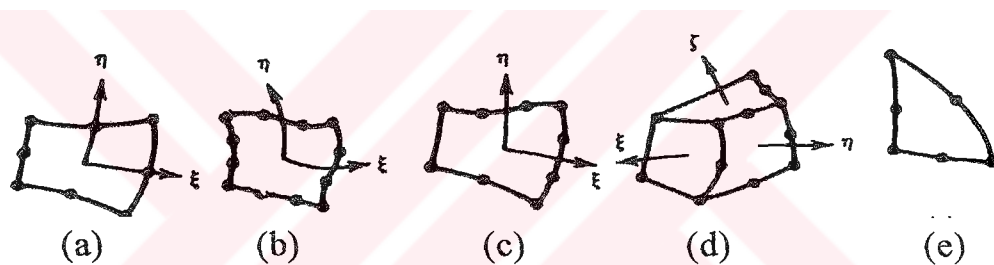
Figure 3.6. Some of the isoparametric elements. a- Quadratic plane element. b- Cubic plane element. c- A degraded cubic element. The left and lower sides can be joined to linear and quadratic elements. d- Quadratic solid element with some linear edges. e- A quadratic plane triangle.

3.4. INTERPOLATION FUNCTIONS

The functions used to represent the behavior of field variable within an element are called interpolation function, shape function or approximation functions. Although it is conceivable that many types of functions could serve as interpolation functions, only polynomials have received widespread use. The reason is that relatively easy to manipulate mathematically, in other words, they can be integrated or differentiated without difficulty.

16

3.4.1. Interpolation Function of Rectangular Elements

Interpolation function have been developed for one, two, and three dimensional elements. Here only two dimensional interpolation function will be shown for a rectangular element.

The basic ideas can be illustrated by a simple example in two dimensions. Suppose that we wish to construct a rectangular element with nodes positioned at the corners of the element . If we assign one value of interpolation function to each node, the element then has four degrees of freedom, and we may select as an interpolation model a four term polynomial such as

$$\varphi = a_1 + a_2x + a_3y + a_4xy \qquad (3.2)$$

3.4.2. Natural and Global Coordinates

A natural coordinate system that relies on the element geometry for its definition and whose coordinates range between zero and unity within the element is known as a local coordinate system.

The basic purpose of the natural coordinate system is to be described the location of the point inside an element in terms of coordinates associated with the node of the element. It will become evident that the natural coordinates are functions of the global Cartesian coordinate system in which the element is defined.

a) Natural coordinates   b) Global coordinates
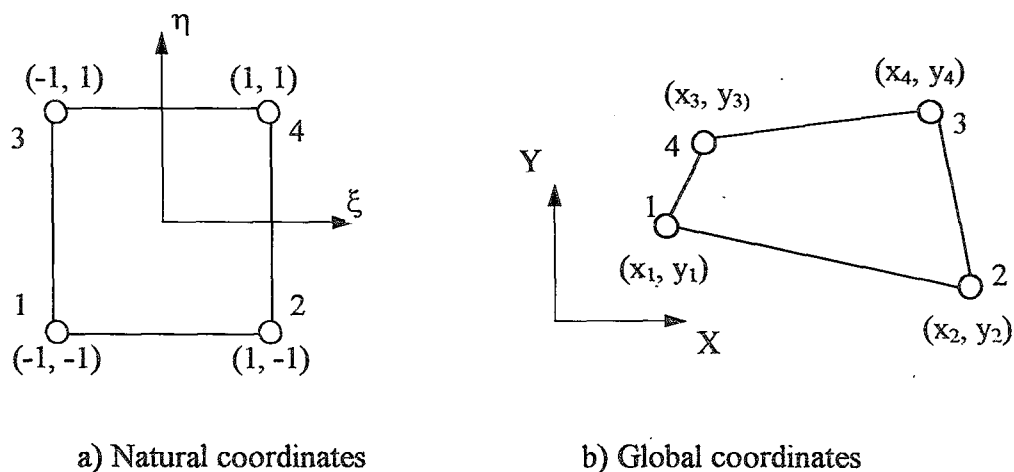
Figure 3.7. Mapping into four-node isoparametric quadrilateral element

17

Consider a mapping of the one region into another region in figure 3.7. A square region in the η,ξ-coordinate system is bounded by the lines $\eta=\pm 1$ and $\xi=\pm 1$. This region is termed mapped domain. We want to map this region into another region defined in the x,y-coordinate system. The region in the x,y-plane is called global domain.

$$x = \begin{bmatrix} x(\xi,\eta); & y = y(\xi,\eta) \end{bmatrix} \tag{3.3}$$

for every point given by its η,ξ-coordinate system in the parent domain, there exists a corresponding point given by its x,y-coordinates in the global domain.

It is evident that if the general form of the region in the global domain could be used as a conforming element, we have achieved the objective mentioned above.

3.5. OBTAINING THE ELEMENT PROPERTIES

For the one element, the force-displacement equations are written as

$$\{F\}^e = [K]^e \{U\}^e \tag{3.4}$$

where $\{F\}^e$ is a column vector of the nodal forces of the element e, $[K]^e$ is the stiffness matrix of the element, and $\{U\}^e$ is nodal displacement vector.

3.6. ASSEMBLY OF THE DISCRETE SYSTEM

The complete force displacement equations for discretized elastic solid are assembled from the sets of equations. The system equations have the same form as the element equations except that they are expanded in dimension to include all nodes Hence discretized system has n nodes, the system equations become

$$\{F\} = [K] \{U\} \tag{3.5}$$

where $\{F\}$ and $\{U\}$ are 2n*1 column vector of the nodal forces, 2n*1 column vector of the nodal displacement respectively, and [K] is 2n*2n stiffness matrix for the entire system.

3.7. BOUNDARY CONDITION

The equation of the system resulting from eq (3.5) can be solved once the prescribed support displacements have been substituted.

The process of specifying the boundary conditions and the procedure for modification for specified displacements is tied to the method adopted to store global arrays, e.g., stiffness and mass matrices. In our computer program only those coefficients whitin a non-zero profile in the global arrays are stored.

Clearly, without substitutions of a minimum number of prescribed displacements to present rigid body movements of the structure, it is impossible to solve this system, because the displacements can not be uniquely determined by the forces.

The non-zero nodal forces or displacements associated with each degree of freedom must be specified. In our program these are both stored in the array {F} and the destination between load and displacements is made by comparing the corresponding value of the boundary restrained condition for each degree of freedom. This physically obvious fact will mathematically be interpreted in the matrix [K] being singular, i.e., the prescription of appropriate displacements after the assembly by deleting appropriate rows and columns of the various matrices.

3.8. OBTAINING THE ELEMENT DISPLACEMENT

After the stiffness matrix [K] and the force vector {F} are obtained and all the boundary conditions are inserted, the equations of the system can be solved for the unknown displacements.

The Gauss elimination methods has been used in the equations of the system. A very important aspect in the computer implementation of the Gauss solution procedure is that a minimum solution time should be used. In addition, the high speed storage requirement should be as small as possible avoid the use of the back-up storage. However, for large system it will nevertheless be necessary to use back-up storage, and for this reason it should also be possible to modify the solution algorithm for effective out of core solution.

3.9. DETERMINATION OF THE STRESSES

Stress {σ} in an element can be calculated when its nodal d.o.f {q} are known. We can write from the basic relation between stress and strain, and displacement to find the stress any point of the element.

$$\{\sigma\} = [D] [B] \{U\} \qquad\qquad (3.6)$$

where [D] elasticity (material) matrix element, [B] is the transformation matrix between strain and displacement, {U} displacement vector.

This relation gives the stresses at any point of the element, in practice, the element stresses are only calculated and printed at some specific points. These may be the center of the element, the nodal point locations or numerical integration points used in the evaluation of the element stiffness matrix.

Another observation in the stress calculation is that the stresses some point in an element can be significantly more accurate when compared whit the exact solution than at other points. In particular, it has been observed that the stress may be considerably more accurate at the Gauss integration points than at the nodal points of element.

The objective in practice is usually to obtain best stress predictions possible once the nodal point displacements have been evaluated for this purpose, if the difference between the element boundary stress is not too large, it may be appropriate to simple average them. In an alternate approach, the stresses are only calculated within the elements and then interpolation procedure is employed to predict the stresses at the element boundaries or other desired points.

CHAPTER FOUR

STIFFNESS MATRIX DERIVATION OF THE QUADRILATERAL ELEMENT

4.1. INTRODUCTION

In this chapter, we developed what are popularly called isoparametric elements and apply them to stress analysis. These elements have proved effective on a wide variety of two and three dimensional problems in engineering. We present the two-dimensional four node quadrilateral in detail. We can view the isoparametric family of elements in a unified manner due to the simple and versatile manner in which shape functions can be derived, followed by the generation of the element stiffness matrix using numerical integration.

A very important phase of a finite element analysis is the calculation of the finite element matrices. In most practical analysis, the use of isoparametric finite element more effective. The principal idea of the isoparametric finite element formulation is to achieve the relationship between the element displacements at any point and the element nodal point displacements directly through the use of interpolation functions.

4.2. TWO DIMENSIONAL ISOPARAMETRIC ELEMENTS
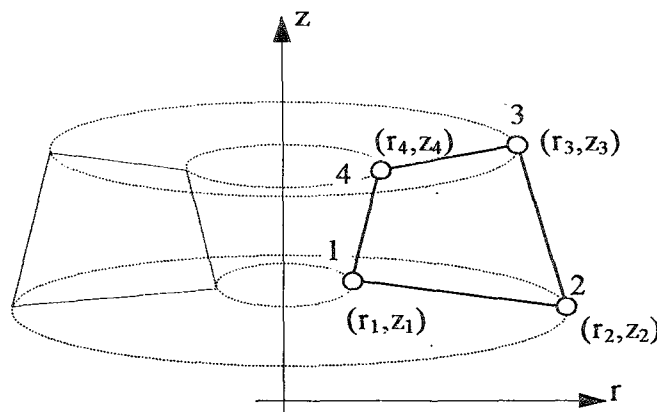
Figure 4.1 Axisymmetric four node quadrilateral element in the r,z-coordinates

The two-dimensional region defined by the revolving area is divided into rectangular elements. Though each element is completely represented by the area in the r,z-plane, it is ring-shaped solid of revolution obtained by revolving by the rectangle about the z axis. A typical element is shown in figure 4.1.
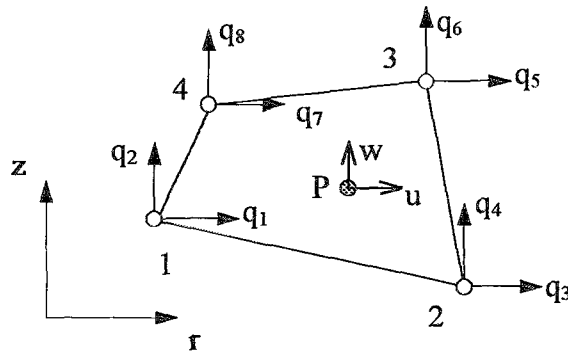
Figure 4.2 Four node quadrilateral element in the r,z-coordinate

Consider the general quadrilateral element shown in figure 4.2. The local nodes are numbered as 1,2,3,4 a counterclockwise fashion as shown, and (r_i, z_i) are the coordinates of node i. The vector

$$q = \begin{bmatrix} q_1, & q_2, & q_3, & q_4, & q_5, & q_6, & q_7, & q_8 \end{bmatrix}^T \qquad (4.1)$$

denotes the element displacement vector. The displacement of an interior P located at (r,z) is represented as

$$u = \begin{bmatrix} u(r,z), & w(r,z) \end{bmatrix}^T \qquad (4.2)$$
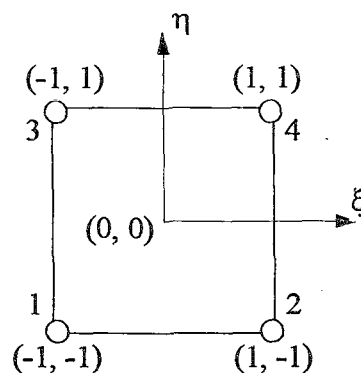
Figure 4.3. Four node quadrilateral element natural ξ, η-coordinates

22

4.3. SHAPE FUNCTIONS FOR FOUR NODE QUADRILATERAL ELEMENT

The master element is defined in ξ,η coordinates (natural coordinates), and is square shaped. The element consists of four node all of which are located on the boundary figure 4.4. The lagrange shape functions N_i, where i=1,2,3,4 are defined such that N_i is equal to unity at node i and is zero at other nodes. In particularly, we refer to the master element shown in figure 4.4 consider the definition of N_1-N_4:

N_1=1 at node 1

N_1=1 at node 1 and 0 at other nodes

Thus, N_1 has to vanish along the lines ξ=+1 , η=+1 and $\xi+\eta = -$ in figure 4.3.

$$N_1 = C\,(1-\xi)(1-\eta)(1+\xi+\eta)$$

At node 1, $N_1 = 1$, $\xi = \eta = -1$. Thus, $C = -\dfrac{1}{4}$ We thus have

$$N_1 = -\frac{1}{4}(1-\xi)(1+\eta)(1+\xi+\eta)$$

$$N_2 = -\frac{1}{4}(1+\xi)(1-\eta)(1-\eta+\xi)$$

$$N_3 = -\frac{1}{4}(1+\xi)(1+\eta)(1-\xi-\eta)$$

$$N_4 = -\frac{1}{4}(1-\xi)(1+\eta)(1+\xi-\eta)$$

(4.3)

Now, we express the displacement field with in the element in terms of the nodal values. Thus, $U = [u,\ w]^T$ represents the displacement components of a point located at $(\xi,\ \eta)$, and q, dimension (8x1), is the element displacement vector, then

$$u = \sum_{i_1=1}^{i_n=4} N_i u_i \quad , \qquad w = \sum_{i_1=1}^{i_n=4} N_i w_i$$

(4.4)

$$u = N_1 q_1 + N_2 q_3 + N_3 q_5 + N_4 q_7$$

$$w = N_1 q_2 + N_2 q_4 + N_3 q_6 + N_4 q_8$$

(4.5)

which can be written in the matrix form as

$$u = Nq \qquad (4.6)$$

where

$$N = \begin{bmatrix} N_1 & 0 & N_2 & 0 & N_3 & 0 & N_4 & 0 \\ 0 & N_1 & 0 & N_2 & 0 & N_3 & 0 & N_4 \end{bmatrix} \qquad (4.7)$$

in the isoparametric formulation, we use the same shape function N_i to also express the coordinates of a point whitin the element in terms of nodal coordinates. Thus

$$r = \sum_{i_1=1}^{i_n=4} N_i r_i \quad , \qquad z = \sum_{i_n=1}^{i_n=4} N_i z_i \qquad (4.8)$$

or

$$r = N_1 r_1 + N_2 r_2 + N_3 r_3 + N_4 r_4$$

$$z = N_1 z_1 + N_2 z_2 + N_3 z_3 + N_4 z_4 \qquad (4.9)$$

Subsequently, we will need to express the derivatives of a function (r, z) coordinates in terms of its derivatives in (ξ, η) coordinates. A function $f = f(r, z)$ in view of eqs(4.9) can be considered to be an implicit function of ξ and η as

$$f = [r(\xi, \eta), \quad z(\xi, \eta)] \text{ or }$$

$$u = u[r(\xi\ \eta), \ z(\xi\ \eta)]$$

$$w = w[r(\xi\ \eta), \ z(\xi\ \eta)] \qquad (4.10)$$

$$\frac{\partial u}{\partial r} = \sum_{i_1=1}^{i_n=4} \frac{\partial N_i}{\partial r} u_i \quad , \qquad \frac{\partial u}{\partial z} = \sum_{i_1=1}^{i_n=4} \frac{\partial N_i}{\partial z} u_i$$

$$\frac{\partial w}{\partial r} = \sum_{i_1=1}^{i_n=4} \frac{\partial N_i}{\partial r} w_i \quad , \qquad \frac{\partial w}{\partial z} = \sum_{i_1=1}^{i_n=4} \frac{\partial N_i}{\partial z} w_i \qquad (4.11)$$

Consider for instance the set of local coordinates (ξ, η) and a corresponding set of global coordinates (r, z). By the usual rule of partial differentiation we can write instance (ξ, η) derivatives as

Using the chain rule of differentiation, we have

$$\frac{\partial N_i}{\partial \xi} = \frac{\partial N_i}{\partial r}\frac{\partial r}{\partial \xi} + \frac{\partial N_i}{\partial z}\frac{\partial z}{\partial \xi} \qquad \frac{\partial N_i}{\partial \eta} = \frac{\partial N_i}{\partial z}\frac{\partial z}{\partial \eta} + \frac{\partial N_i}{\partial z}\frac{\partial z}{\partial \eta} \qquad (4.12)$$

which can be written in matrix form as

$$\begin{Bmatrix} \dfrac{\partial N_i}{\partial \xi} \\ \dfrac{\partial N_i}{\partial \eta} \end{Bmatrix} = \begin{bmatrix} \dfrac{\partial r}{\partial \xi} & \dfrac{\partial z}{\partial \xi} \\ \dfrac{\partial r}{\partial \eta} & \dfrac{\partial z}{\partial \eta} \end{bmatrix} \begin{Bmatrix} \dfrac{\partial N_i}{\partial r} \\ \dfrac{\partial N_i}{\partial z} \end{Bmatrix} = J \begin{Bmatrix} \dfrac{\partial N_i}{\partial r} \\ \dfrac{\partial N_i}{\partial z} \end{Bmatrix} \qquad (4.13)$$

where J is the Jacobian matrix

$$J = \begin{bmatrix} \dfrac{\partial r}{\partial \xi} & \dfrac{\partial z}{\partial \xi} \\ \dfrac{\partial r}{\partial \eta} & \dfrac{\partial z}{\partial \eta} \end{bmatrix} \qquad (4.14)$$

In view of equation(4.5) and equation(4.9), we have

$$J = \frac{1}{4}\begin{bmatrix} -(1-\eta)r_1 +(1-\eta)r_2 +(1+\eta)r_3 +(1+\eta)r_4 & -(1-\eta)z_1 +(1-\eta)z_2 +(1+\eta)z_3 +(1+\eta)z_4 \\ -(1-\xi)r_1 +(1-\xi)r_2 +(1+\xi)r_3 +(1+\xi)r_4 & -(1-\xi)z_1 +(1-\xi)z_2 +(1+\xi)z_3 +(1+\xi)z_4 \end{bmatrix} \qquad (4.15)$$

$$J = \begin{bmatrix} J_{11} & J_{12} \\ J_{21} & J_{22} \end{bmatrix} \qquad (4.16)$$

Inverting J we can write

$$\begin{Bmatrix} \dfrac{\partial N_i}{\partial r} \\ \dfrac{\partial N_i}{\partial z} \end{Bmatrix} = J^{-1} \begin{Bmatrix} \dfrac{\partial N_i}{\partial \xi} \\ \dfrac{\partial N_i}{\partial \eta} \end{Bmatrix} \qquad (4.17)$$

We can obtain J^{-1} in the following form

$$J^{-1} = \frac{1}{\det J} \begin{bmatrix} \dfrac{\partial z}{\partial \eta} & -\dfrac{\partial r}{\partial \eta} \\ -\dfrac{\partial z}{\partial \xi} & \dfrac{\partial r}{\partial \xi} \end{bmatrix} = \frac{1}{\det J} \begin{bmatrix} J_{22} & -J_{12} \\ -J_{21} & J_{11} \end{bmatrix} \tag{4.18}$$

where

$$\det J = \frac{\partial r}{\partial \xi} \frac{\partial z}{\partial \eta} - \frac{\partial r}{\partial \eta} \frac{\partial z}{\partial \xi} \tag{4.19}$$

Introducing the above transformation relationship into the strain-displacement relations equation

4.4. ELEMENT STIFFNESS MATRIX

The stiffness matrix for the quadrilateral element can be derived from the strain energy in the body, given by

$$U = \int_V \frac{1}{2} \sigma^T \varepsilon \, dV = \sum_e t_e \int_e \frac{1}{2} \sigma^T \varepsilon \, dA \tag{4.20}$$

where t_e thickness of element e. The strain-displacement relations are

$$\varepsilon = \begin{Bmatrix} \varepsilon_r \\ \varepsilon_z \\ \gamma_{rz} \\ \varepsilon_\theta \end{Bmatrix} = \begin{Bmatrix} \dfrac{\partial u}{\partial r} \\ \dfrac{\partial w}{\partial z} \\ \left(\dfrac{\partial u}{\partial z} + \dfrac{\partial w}{\partial r} \right) \\ \dfrac{u}{r} \end{Bmatrix} \tag{4.21}$$

$$\begin{Bmatrix} \dfrac{\partial u}{\partial r} \\ \dfrac{\partial u}{\partial z} \end{Bmatrix} = \frac{1}{\det J} \begin{bmatrix} J_{22} & -J_{12} \\ -J_{21} & J_{11} \end{bmatrix} \begin{Bmatrix} \dfrac{\partial u}{\partial \xi} \\ \dfrac{\partial u}{\partial \eta} \end{Bmatrix} \tag{4.22.a}$$

26

smilarly

$$\begin{Bmatrix} \dfrac{\partial w}{\partial r} \\ \dfrac{\partial w}{\partial z} \end{Bmatrix} = \dfrac{1}{\det J} \begin{bmatrix} J_{22} & -J_{12} \\ -J_{21} & J_{11} \end{bmatrix} \begin{Bmatrix} \dfrac{\partial w}{\partial \xi} \\ \dfrac{\partial w}{\partial \eta} \end{Bmatrix} \tag{4.22.b}$$

Equations(4.21)and (4.22.a and 4.22.b) yield

$$\varepsilon = A \begin{Bmatrix} \dfrac{\partial u}{\partial \xi} \\ \dfrac{\partial u}{\partial \eta} \\ \dfrac{\partial w}{\partial \xi} \\ \dfrac{\partial w}{\partial \eta} \\ \dfrac{u}{r} \end{Bmatrix} \tag{4.23}$$

where A is given by

$$A = \begin{bmatrix} \dfrac{J_{22}}{\det J} & -\dfrac{J_{12}}{\det J} & 0 & 0 & 0 \\ 0 & 0 & -\dfrac{J_{21}}{\det J} & \dfrac{J_{11}}{\det J} & 0 \\ -\dfrac{J_{21}}{\det J} & \dfrac{J_{11}}{\det J} & \dfrac{J_{22}}{\det J} & -\dfrac{J_{12}}{\det J} & 0 \\ 0 & 0 & 0 & 0 & 1 \end{bmatrix} \tag{4.24}$$

Now, from the interpolation equations we have

$$\begin{Bmatrix} \dfrac{\partial u}{\partial \xi} \\ \dfrac{\partial u}{\partial \eta} \\ \dfrac{\partial w}{\partial \xi} \\ \dfrac{\partial w}{\partial \eta} \\ \dfrac{u}{r} \end{Bmatrix} = Gq \tag{4.25}$$

27

$$G = \frac{1}{4}\begin{bmatrix} -(1-\eta) & 0 & (1-\eta) & 0 & (1+\eta) & 0 & (1+\eta) & 0 \\ -(1-\xi) & 0 & -(1+\xi) & 0 & (1+\xi) & 0 & (1-\xi) & 0 \\ 0 & -(1-\eta) & 0 & (1-\eta) & 0 & (1+\eta) & 0 & -(1+\eta) \\ 0 & -(1-\xi) & 0 & -(1+\xi) & 0 & (1+\xi) & 0 & (1-\xi) \\ \dfrac{(1-\xi)(1-\eta)}{r} & 0 & \dfrac{(1+\xi)(1-\eta)}{r} & 0 & \dfrac{(1+\xi)(1+\eta)}{r} & 0 & \dfrac{(1-\xi)(1+\eta)}{r} & 0 \end{bmatrix} \quad (4.26)$$

Equation (4.23 and 4.25) now yield

$$\varepsilon = Bq \qquad\qquad (4.27)$$

where

$$B = \begin{bmatrix} \dfrac{\partial N_i}{\partial r} & 0 \\ 0 & \dfrac{\partial N_i}{\partial z} \\ \dfrac{\partial N_i}{\partial z} & \dfrac{\partial N_i}{\partial r} \\ \dfrac{N_i}{r} & 0 \end{bmatrix} = AG \qquad\qquad (4.28)$$

The relation $\varepsilon = Bq$ is the desired result. The strain in the element is expressed in terms of its nodal displecement. The stress is now given by

$$\sigma = DBq = D\varepsilon \qquad\qquad (4.29)$$

where D is an material matrix. The strain energy in equation(4.20) becomes

$$U_d = \sum_e \tfrac{1}{2} q^T \left[2\pi \int_{-1}^{1} \int_{-1}^{1} B^T D\, B\ \det J\ d\xi\, d\eta \right] q = \sum_e \tfrac{1}{2} q^T k^e q \qquad\qquad (4.30)$$

The quantity inside the parentheses is the element stiffness matrix,

$$k^e = 2\pi \int_{-1}^{1} \int_{-1}^{1} B^T D\, B\ \det J\ d\xi\, d\eta \qquad\qquad (4.31)$$

28

4.5. OBTAINING THE FORCE VECTOR

In the finite element solution, the forces that acts the elements are carried to the nodal points of the elements. Constant traction force $T=[T_r, T_z]^T$, a force per unit area, is applied on edge 2-3 of the quadrilateral element. Along this edge, we have $\xi=1$. If we use in equation (4.3) this becomes $N_1=N_4=0$, $N_2=(1-\eta)/2$, $N_3=(1+\eta)/2$. Note that the shape functions are linear functions along the edges. Consequently, from the potential, the element traction load vector is readily given by

$$T^e = \frac{t_e \ell_{2-3}}{2}\begin{bmatrix}0 & 0 & T_r & T_z & T_r & T_z & 0 & 0\end{bmatrix}^T \qquad (4.32)$$

Where ℓ_{2-3} length of the edge 2-3. For varying distributed loads, we may express T_r and T_z in terms of values nodes 2 and 3 using shape functions.. Numerical integration can be used in this case.

4.6. NUMERICAL INTEGRATION

The stiffness matrix equation and the force equations can be calculated by integration. It is very difficult to obtain these integrations by the analytical method. So the numerical integration is used to calculate the stiffness matrix and the forces.

In equation 4.31, quantities B and J in the above integral are involved functions of ξ and η, and so the integration has to be performed numerically. In this study, the gauss numerical integration is chosen.

Consider the problem of numerically evaluating a one-dimensional integral of the form

$$I = \int_{-1}^{+1} f(\xi)\, d\xi \qquad (4.33)$$

The gaussian quadrature approach for evaluating I is given below. This method has proved most useful in finite element work. Extension to integrals in two and three dimensions follow readily. Consider the n-point approximation

$$I = \int_{-1}^{+1} f(\xi)\, d\xi = w_1 f(\xi_1) + w_2 f(\xi_2) + \ldots + w_n f(\xi_n) \qquad (4.34)$$

where w_1, w_2, ... w_n are the weights and ξ_1, ξ_2, ... ξ_n are the sampling points or gauss points. The idea behind Gausian quadrature is to select the n Gauss points and n weights such that Eq. 4.34 provides an exacts answer for polynomials $f(\xi)$ of as large a degree as possible.

CHAPTER FIVE

ELASTO-PLASTIC FINITE ELEMENT ANALYSIS FOR ISOTROPIC MATERIAL

5.1. INTRODUCTION

The theory of plasticity deals with the behavior of materials at strains where Hook's law is no longer valid. A number of aspect of plastic deformation makes the mathematical formulation of a theory of plasticity more difficult than the description of the behavior of an elastic solid. For example, plastic deformation is not reversible process like elastic deformation. Elastic deformation depends only on the initial and final states of stress and strain, while the plastic strain depends on the loading path by which the final state is achieved.

Moreover, in the plastic deformation there is no easily measured constant relating stress to strain as with Young's modulus for elastic deformation. Also several aspects of real material behavior such as plastic anisotropy etc. can not be treated easily by plastic theory. Nevertheless, the theory of plasticity has been one of the most active areas of continuum mechanics and considerable has been made in developing a theory which can solve important engineering theory.

The theory of plasticity is concerned with a number of different type of problems. From the viewpoint of design, plasticity is concerned with predicting the maximum load which can be applied to a body without causing excessive yielding. The yield criterion must be expressed in terms of stress in such a way that it is valid for all state of stress. The designer is also concerned with plastic deformation in problems where the body purposely stressed beyond the yield stress into the plastic region. For example, plasticity must be considered in designing for processes such as autofrettage, shrink fitting, and the overspending of rotor disks. The consideration of small plastic strains allows economies in building construction through the use of the theory of limit design.

Plastic behavior of solid is characterized by a non-unique stress-strain relationship. Indeed, one defination of plasticity may be presence of irrecoverable strains on load removal.

5.2. MATERIAL PROPERTIES

5.2.1. Flow Curve

A true stress- strain is frequently called flow curve because it gives true stress required to cause the metal flow plastically to any given strain. The simplest and most common experiment, as well as the most important, is the standard tensile test. The mechanical properties of materials used in engineering are determined by tests performed on small cylindrical test specimen. The standard tensile test is used to obtain a variety of characteristics and strengths that are used in design. The specimen is then mounted in test machine and slowly loaded in tension while the load and strain are observed. At the conclusion, results are plotted as a stress-strain diagram figure 5.1.
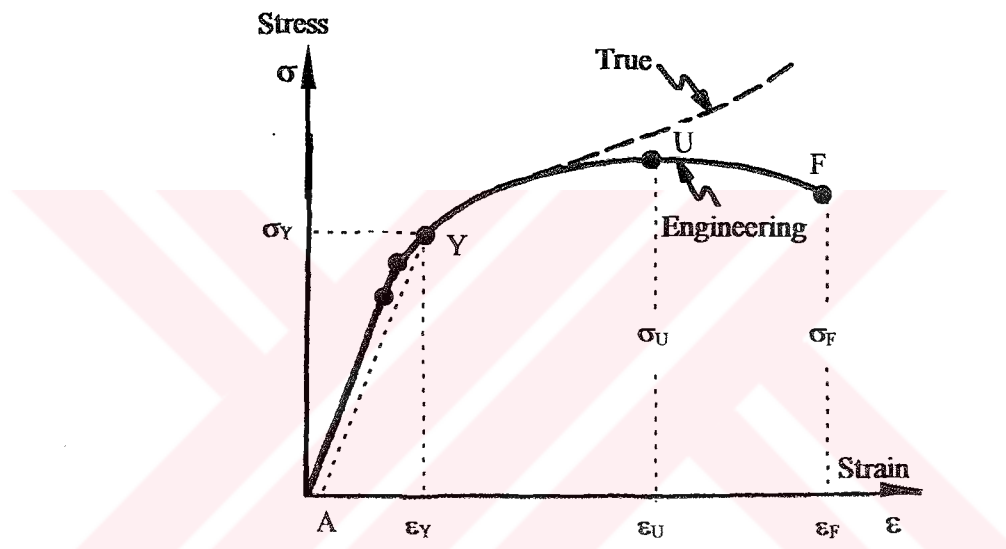
Figure 5.1 Engineering and true stress-strain diagram

In this diagram, initially the relation between stress and strain is essentially linear. This linear part of the curve extends up to the point P, which is called the proportional limit. Point E is called the elastic limit. No permanent set will be observable in the specimen if the load is removed at this point. Between P and E the diagram is not perfectly straight line, even though the specimen is elastic. Thus Hook's law, which states that stress is proportional to strain, applies only up to proportional limit.

During the tension test, many materials reach a point at which the strain begins to increase very rapidly without a corresponding increase in stress. This point Y is called the yield point. Not all material have an obvious yield point. For this reason, yield strength σ_Y is often defined by an offset method. Such a yield strength corresponds to a definite or stated amount of permanent set, usually 0.2 or 0.5 percent of original gauge length.

31

The ultimate or tensile strength σ_U corresponds to point U and is the maximum stress reached on the stress-strain diagram. Some materials exhibit a downward trend after the maximum stress is reached. These fracture at point F on the diagram. Others, such as some of the cast irons and high strength steels, fracture while the stress-strain locus is still rising.

The most important characteristic of the true stress-strain diagram figure 5.1 is that the true stress increasing all the way to fracture. Since the cross-sectional area of the specimen is decreasing with load. This means that the load and cross sectional area must be measured simultaneously during the test. If the specimen has necked, especially care must be taken to measure the area smallest part. In plotting the true stress-stain diagram it is customary to use a term called true strain or logarithmic strain. True strain is the sum of the incremental elongation divided by the current length of the filament,

$$\bar{\varepsilon} = \int_{l_0}^{l_i} \frac{dl}{l} = \ln \frac{l_i}{l_0} = \ln(\varepsilon + 1) \tag{5.1}$$

4.2.2. Plastic Deformation

The best current explanation of relationships between stress and strain is by Datsko.[1] He describes the plastic region of the true stress-true strain diagram by the equation

$$\sigma = K\varepsilon_p^n \tag{5.2}$$

where, σ true stress, K strain-strengthening coefficient or strength coefficient, ε_p true plastic strain, n strain-strengthening exponent.

Consider stress-strain diagram of figure 5.2. Here a material has been stressed beyond the yield strength at Y to some point I, in the plastic region, and the load removed. At this point the material has a permanent plastic deformation ε_p. If the load corresponding to point I is now reapplied, the material is elastically deformed by the amount ε_e. Thus at point I the total unit strain consists of the two components ε_e and ε_p and is given

$$\varepsilon = \varepsilon_e + \varepsilon_p \tag{5.3}$$

This material can be unloaded and reloaded any number of times from and to point I, and it is found that the action always occurs along the straight line which is approximately parallel to the initial elastic line OY.

---

[1] Joseph Datsko, "Solid Materials," Chap.7 in Joseph E. Singhley and Charles R.Mischke (eds.), Standard Handbook of Machine Design, McGraw-Hill, New York, 1986. See also Joseph Datsko, "New look at Material Strength," Machine Design, vol 58, no.3, Feb. 6, 1986 , pp. 81-85.
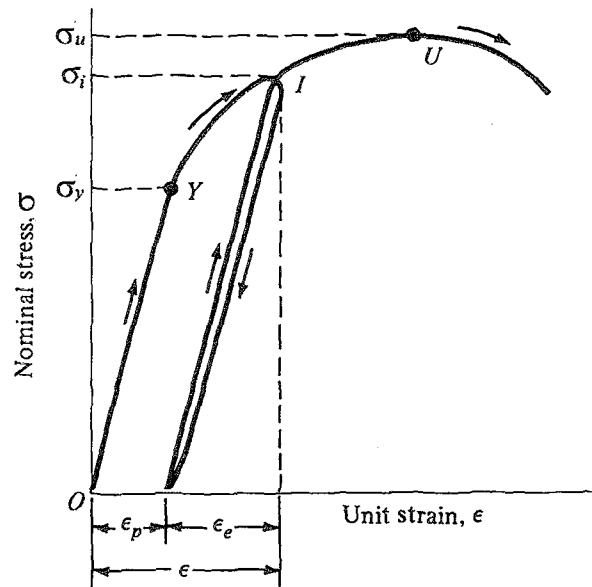
Figure 5.2. Stress-strain diagram showing unloading and reloading

5.2.3. Empirical Equations for Stress-Strain Curves

It is sometimes useful to represent the stress strain-curve of a given material by an equation obtained empirically by fitting the experimental data. One of the first such empirical equation was proposed by Ludwik. It has the form

$$\sigma = \sigma_0 + K\varepsilon_p^n \tag{5.4}$$

A frequently used form, due to Ramberg and Osgood, is

$$\varepsilon = \varepsilon_e + \varepsilon_p \tag{5.5.a}$$

$$\varepsilon = \frac{\sigma_o}{E} + k\left(\frac{\sigma}{E}\right)^n \tag{5.5.b}$$

where ε_o the yield strain, σ_o the yield stress, E the elastic modulus,

33

5.3. FAILURE THEORIES

When a part is loaded so that the stress state is uniaxial, then the stress and strength can be compared directly to determine to degree of safety, or to learn whether the part will fail. The method is simple because there is only one value of stress and there is only one value strength, be it yield strength, ultimate strength, shear strength.

The problem becomes more complicated when the stress state is biaxial or triaxial. In such cases there are a multitude of stresses, but still one significant strength. So how the we learn whether the part is safe or not, and if so, how safe? A number of failure theories have been proposed to help answer this question. Now we shall present name of some theories and we shall give more information about distortion energy (or von Mises) theory.

* Maximum normal stress theory or Rankine theory
* Maximum normal strain theory or Saint Venant's theory
* Maximum shear stress theory or Teresca criterion
* Distortion energy theory or shear energy theory, octahedral shear stress theory, von Mises-Hencky theory
* Maximum strain energy theory or Beltrami's energy theory
* Mohr theory of yielding
* Internal friction theory or Coulomb criterion

5.3.1. Distortion Energy Theory   (von Mises Energy Theory)

We will discuss von Mises yield criterion that is used to solve our problem. Briefly, the distortion energy theory assumes that yielding begins when the distortion energy equals the distortion energy at yield in simple tension.
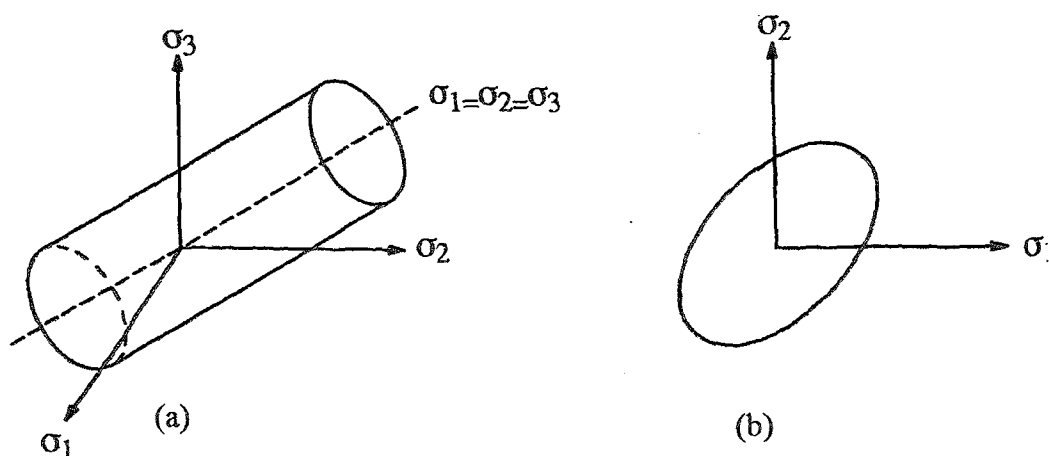
Figure 5.3. Yield surface three and two-dimensional space

It is convenient, when using this theory to work with an equivalent stress, σ_e, defined as the value of uniaxial tensile stress that would produce the same level of distortion energy hence according to the theory, as the actual stresses involved. In terms of the existing principal stresses , the equation for equivalent stresses is

$$\sigma_e = \frac{\sqrt{2}}{2}\left[\left(\sigma_1 - \sigma_2\right)^2 + \left(\sigma_2 - \sigma_3\right)^2 + \left(\sigma_3 - \sigma_1\right)^2\right]^{1/2} \tag{5.6}$$

For the biaxial case this reduces

$$\sigma_e = \left(\sigma_1^2 + \sigma_2^2 - \sigma_1\sigma_2\right)^{1/2} \tag{5.7}$$

Once the equivalent stress is obtained, this is compared with the yield strength from standard tensile test. If σ_e exceeds σ_0 yielding is predicted. The strain energy of distortion per unit volume for a body subjected to a triaxial state of stress is given

$$U_d = \frac{1}{12G}\left[\left(\sigma_x - \sigma_y\right)^2 + \left(\sigma_y - \sigma_z\right)^2 + \left(\sigma_x - \sigma_z\right)^2 + 6\left(\tau_{xy}^2 + \tau_{xz}^2 + \tau_{yz}^2\right)\right] \tag{5.8}$$

in the case principal stress

$$U_d = \frac{1}{12G}\left[\left(\sigma_1 - \sigma_2\right)^2 + \left(\sigma_2 - \sigma_3\right)^2 + \left(\sigma_3 - \sigma_1\right)^2\right] \tag{5.9}$$

In simple tension,

$$U_d = \frac{1}{6G}\sigma_0^2 \tag{5.10}$$

When these two equation are equal

$$\frac{1}{6G}\sigma_0 = \frac{1}{12G}\left[\left(\sigma_1 - \sigma_2\right)^2 + \left(\sigma_2 - \sigma_3\right)^2 + \left(\sigma_3 - \sigma_1\right)^2\right] \tag{5.11}$$

$$\sigma_0{}^2 = \frac{1}{2}\left[\left(\sigma_1 - \sigma_2\right)^2 + \left(\sigma_2 - \sigma_3\right)^2 + \left(\sigma_3 - \sigma_1\right)^2\right] \tag{5.12}$$

for the biaxial case $\sigma_3 = 0$

$$\sigma_1{}^2 - \sigma_1\sigma_2 + \sigma_2{}^2 = \sigma_0{}^2 \tag{5.13}$$

This equation defines as an ellipse, called von Mises ellipse in the σ_1 σ_2 plane as shown in figure 5.3.b. For the three dimension, equation plots as a cylinder surfaces in the σ_1 σ_2 σ_3 space as shown in figure 5.3.a

Experiments have shown that the distortion energy theory is in the better agreement with data from the yielding of the bodies under combined stress than any of the other theories. In general, the distortion energy theory is recommended for defining yielding of ductile materials.

5.4. SOME BASIC CONCEPTS OF PLASTICITY

5.4.1 Yield Surface and Normality

It is quite generally postulated as experimental fact, that yielding can occur only if the stress $\{\sigma\}$ satisfy the general yield criterion

$$F(\sigma, K) = 0 \tag{5.14}$$
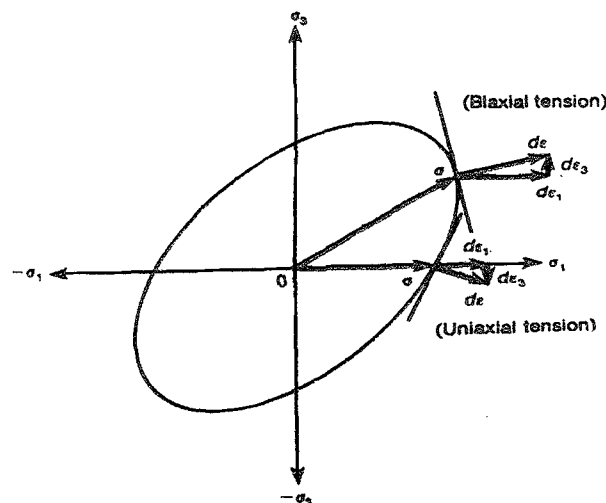
Figure 5.4. Yield surface and normality criterion in two dimensional stress space

In this vectorial notation is used for stress components and K is a hardening parameter. This yield condition can be visualized as a surface in n-dimensional hyper space of stress with the position of the surface dependent on the instantaneous value of the parameter K.

The relationship that have been developed for yield criteria and can be represented geometrically by a cylinder oriented at equal angles to the $\sigma_1, \sigma_2, \sigma_3$ axes. A state of stress which gives a point inside of the cylinder represent elastic behavior. Yielding begins when the state of stress reaches the surface of cylinder, which is called the yield surface. The radius of the cylinder is stress deviator. Plastic deformation occurs we can consider that the yield surface expands outward, maintaining its geometric shape.

The yield surface shown in figure 5.3.a is a circular cylinder if it's represent the von Mises' yield criterion. If a plane is passed through this surface parallel to the σ_2 axis, it intersects on the σ_1 σ_3 plane as an ellipse figure 5.3.b

The normality rule also is useful in constructing experimental yield loci. Figure 5.4 shows that total strain vector dε is normal to the yield locus.

5.4.2. Plastic Stress-Strain Relation

In the plastic region the strains in general are not uniquely determined by the stresses but depend on the entire history of loading. Therefore, in plasticity it is necessary to determine the differentials or increments of plastic strain throughout the loading path and then obtain the total strain by integration or summation.

. For the particular class of loading paths in which all the stresses increase in the same ratio, proportional loading,

$$\frac{d\sigma_1}{\sigma_1} = \frac{d\sigma_2}{\sigma_2} = \frac{d\sigma_3}{\sigma_3} \tag{5.15}$$

the plastic strains are independent of the loading path and depend only on the final state of stress.

There are two general categories of plastic stress strain relationship. Incremental or flow theories relate the stresses to the plastic strain increments. Deformation or total strain theories relate the stresses to the plastic strain. Deformation theory simplifies the solution of plasticity problems, but the plastic strains in general cannot be considered independent of loading path.

5.4.2.1. Levy-Mises Equations

The relationship between stress and strain for an ideal plastic solid, where the elastic strains are negligible, are called flow rules or the Levy-Mises equations. If we consider yielding under uniaxial tension, then $\sigma_1 \neq 0$, $\sigma_2 = \sigma_3 = 0$ and $\sigma_m = \sigma_1/3$ Only the deviatoric stresses cause yielding

$$\sigma_1^\circ = \sigma_1 - \sigma_m = \frac{2\sigma_1}{3} \quad \text{and} \quad \sigma_2^\circ = \sigma_3^\circ = \frac{-\sigma_1}{3} \qquad (5.16.a)$$

from which we find

$$\sigma_1^\circ = -2\sigma_2^\circ = -2\sigma_3^\circ \qquad (5.16.b)$$

from the condition of constancy of volume in plastic deformation

$$d\varepsilon_1 = -2d\varepsilon_2 = -2d\varepsilon_3 \qquad (5.17.a)$$

so that

$$\frac{d\varepsilon_1}{d\varepsilon_2} = -2 = \frac{\sigma_1^\circ}{\sigma_2^\circ} \qquad (5.17.b)$$

This can be generalized to the Levy-Mises equation

$$\frac{d\varepsilon_1}{\sigma_1^\circ} = \frac{d\varepsilon_2}{\sigma_2^\circ} = \frac{d\varepsilon_3}{\sigma_3^\circ} = d\lambda \qquad (5.18)$$

These equations express the fact that at any instant of deformation the ratio of the plastic strain increments to the current deviatoric stresses is constant. This equations can be written in terms of actual stresses.

$$d\varepsilon_1 = \tfrac{2}{3} d\lambda \left[\sigma_1 - \tfrac{1}{2} \left(\sigma_2 + \sigma_3 \right) \right] \qquad (5.19)$$

To evaluate $d\lambda$ we utilize the effective strain

$$d\bar{\varepsilon} = \tfrac{2}{3} d\lambda \bar{\sigma} \qquad (5.20)$$

The Levy-Mises equations then become

$$d\varepsilon_1 = \frac{d\bar{\varepsilon}}{\bar{\sigma}}\left[\sigma_1 - \tfrac{1}{2}(\sigma_2 + \sigma_3)\right]$$

$$d\varepsilon_2 = \frac{d\bar{\varepsilon}}{\bar{\sigma}}\left[\sigma_2 - \tfrac{1}{2}(\sigma_1 + \sigma_3)\right] \qquad (5.21)$$

$$d\varepsilon_3 = \frac{d\bar{\varepsilon}}{\bar{\sigma}}\left[\sigma_3 - \tfrac{1}{2}(\sigma_1 + \sigma_2)\right]$$

4.4.2.2. Prandtl-Reuss Equation

The Levy-Mises equations can only be applied to problems of large plastic deformation because they neglect elastic strains. To treat the important, but more difficult problems in the elastic-plastic region it is necessary to consider both elastic and plastic component of strain.

The total strain increment is the sum of an elastic strain increment $d\varepsilon^e$ and a plastic strain increment $d\varepsilon^p$.

$$d\varepsilon_{ij} = d\varepsilon_{ij}{}^e + d\varepsilon_{ij}{}^p \qquad (5.22)$$

Where, elastic strain increment is given by

$$d\varepsilon_{ij}{}^e = \frac{1+\upsilon}{E}d\sigma_{ij}' + \frac{1+2\upsilon}{E}\frac{d\sigma_{kk}}{3}\delta_{ij} \qquad (5.23)$$

the plastic strain increment is given by the Levy-Mises equations which can be written

$$d\varepsilon_{ij}{}^p = \frac{3}{2}\frac{d\bar{\varepsilon}}{\bar{\sigma}}\sigma_{ij}' \qquad (5.24)$$

Thus, the stress, strain relations for an elastic-plastic solid are given by

$$d\varepsilon_{ij} = \frac{1+\upsilon}{E}d\sigma_{ij}' + \frac{1+2\upsilon}{E}\frac{d\sigma_{kk}}{3}\delta_{ij} + \frac{3}{2}\frac{d\bar{\varepsilon}}{\bar{\sigma}}\sigma_{ij}' \qquad (5.25)$$

5.5. SOLUTION OF PLASTICITY PROBLEM

The Levy-Mises and Prandtl-Reuss equations provide relation between the increments of plastic strain and stresses. The basic problem is to calculate next increment of plastic strain for a given state of stress when the loads are increased incrementally. If all of the increments of strain are known, then the total plastic strain is simple determined by summation. To do this we have available a set of plastic stress-strain relationships, either above equation, a yield criterion, and a basic relationship for the flow behavior of the material in terms of a true stress-strain curve. In addition, a complete solution also must satisfy the equation of equilibrium, the strain-displacement relations, and the boundary conditions. Finite element analysis should make plasticity analysis of engineering problems more commonplace by means of digital computer.

5.6. RESIDUAL STRESS FOR ISOTROPIC MATERIAL

The stress that remains in a structural member upon removal of external loads is called residual stress. This type of stress is always attributable to nonuniform plastic deformation. Residual stresses generally arise when conditions in the outer layer of a material differ from those internally. The presence of residual stress may be harmful or, if properly controlled, may result in substantial benefit.

The magnitude and distribution of residual stresses can be obtained by superposition of the stresses due to loading and the reverse, or rebound, stresses due to unloading. (The strains corresponding to the latter are the reverse, or rebound, strains). The reverse stress pattern is assumed to be fully elastic and hence can be obtained by using Hook's law.

It is probably true to say that all engineering components contain stresses before being subjected to service loading conditions owing to the history of the material prior such service. These stresses, produced as a result of mechanical working of the material, heat treatment, chemical treatment, joining procedure, etc., are termed residual stresses and they can have a very significant effect on the fatigue life of the components. These residual stresses are locked into the component in the absence of external loading and represent a datum stress over which the service load stresses are subsequently superimposed. If, by fortune or design, the residual stresses are of opposite sign to the service stresses then part of the service load goes to reduce the residual stress to zero before the combined stress can again rise towards any likely failure value; such residual stresses are thus extremely beneficial to the strength of the component and significantly higher fatigue strengths can result. If, however the residual stresses are of the same sign as the applied stress, e.g. both tensile, then a smaller service load is required to produce failure than would have been the case for a component with a zero stress level initially; the strength and fatigue life in this case is thus reduced. Thus, both magnitude and sign of

the residual stresses are important to fatigue life considerations, and method these quantities are introduced below.

Whilst engineers have been aware of residual stresses for many years it is only recently that substantial efforts have been made to investigate their magnitudes and distribution with depth in components and hence their influence on performance and service life. This is probably due to the conservatism of old design procedures which generally incorporated sufficiently large safety factors to mask the effects of residual stresses on component integrity. However with current drives for economy of manufacture coupled with enhanced product safety and reliability, design procedure have become far more stringent and residual stress effects can no longer be ignored. Principally, the designer consider the effect of residual stress on structural or component failure but there is also need for detailed consideration of distortion and stability factors which are also closely related to residual stress levels.

CHAPTER SIX

NONLINEAR STRUCTURAL ANALYSIS TECHNIQUE

6.1. INTRODUCTION

When a force (F) is applied to structural system, that system will displace some corresponding amount (u). The predictability of relationship between F and u allows engineers to calculate the response of structures to given sets of loads. In many engineering applications, the relationship between F and u can be described by the linear equation known as Hook's Law:

$$F=Ku \tag{6.1}$$

In this equation, the proportionality constant K represents the structural system. As long as a structure's stiffness remains constant, that structure is said to be linear, because its behavior can be analyzed using linear equations. Many engineering structural systems are designed to remain linear (or linearly so) whitin their normal range of service loads. Standard linear equation solvers are developed to enable engineers to analyze complex linear structures. However, there are significant classes of engineering applications for which the relationship between force and displacement is not constant. A plot of F versus u for such systems are not a straight line; hence, such systems are said to be nonlinear. The behavior of such systems can not be represented directly with a set of linear equations.
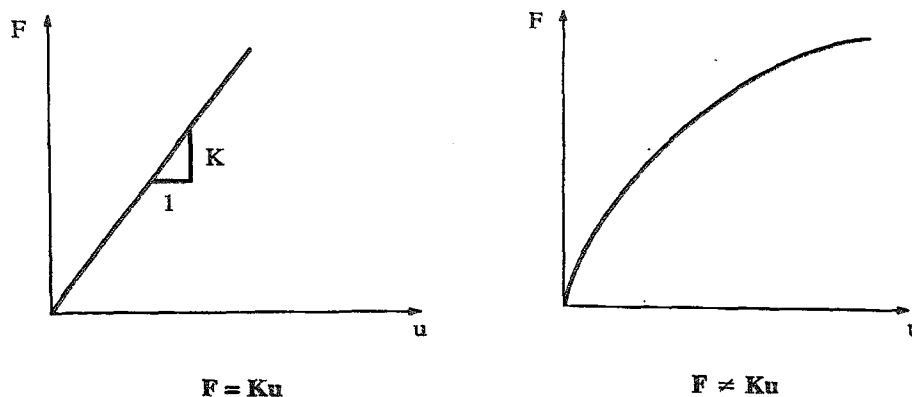
Figure 6.1 Linear and nonlinear response

6.2. WHAT CAUSES OF NONLINEAR BEHAVIOR?

There are many potentials causes of nonlinear behavior. We can group them into three main categories. In many structural systems, different kinds of nonlinearities can be acting simultaneously. For example, in the forging operation shown in figure 6.2. The work piece will experience contact (change status), plasticity (material nonlinearity), and large deformations (geometric nonlinearity), all at the same time.
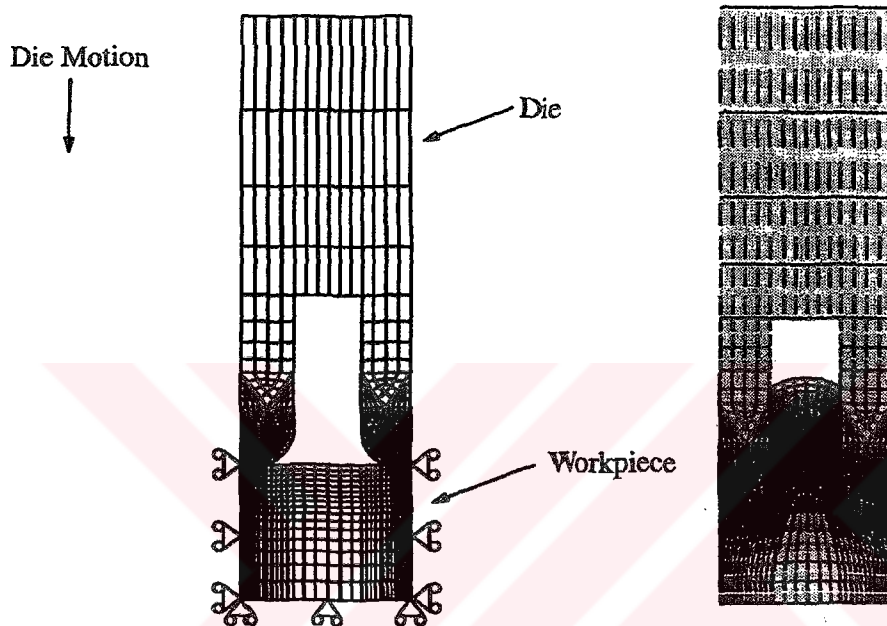
Figure 6.2 Different kinds of nonlinearities can be acting simultaneously all at the same time

6.2.1. Changing Status

Many common structural features exhibit nonlinear behavior that is status-dependent. For example, a tension only cable is either slack or taut; a roller support is either in contact or not in contact; permafrost is either frozen or thawed.

6.2.2. Geometric Nonlinearities

If a structure experiences large deformation, its changing geometric configuration can cause the structure to respond nonlinearly. An example would be the fishing rod shown in figure 6.3. Under light lateral loads, the road tip is extremely flexible (low lateral stiffness). As lateral load increases, the road deflects so much that the moment arm decreases appreciable, causing the road tip to exhibit increasing stiffness at higher load.

43
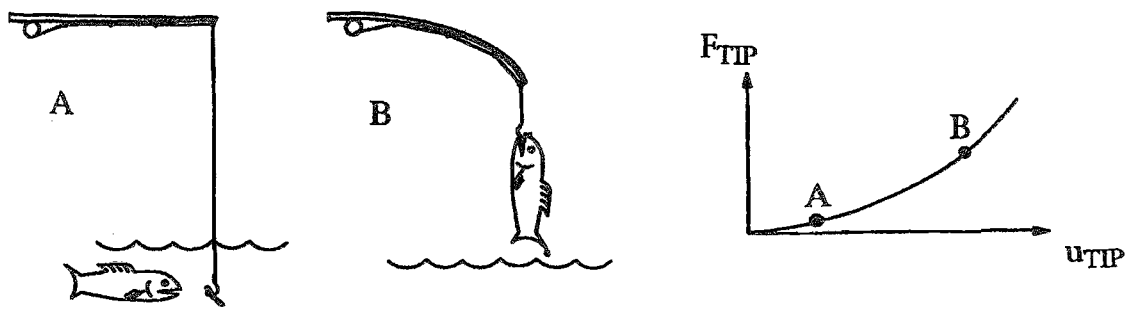
Figure 6.3 A fishing rod demonstrates geometric nonlinearity

6.2.3. Material Nonlinearities

Nonlinear stress-strain relationships are a common cause of nonlinear structural behavior. Many factors can influence a material's stress-strain properties, including load history (as in elasto-plastic response), environmental condition (such a temperature), and the amount of time that a load is applied (as in creep response). Elastic material such rubbers can also behave nonlinearly like figure 6.4.
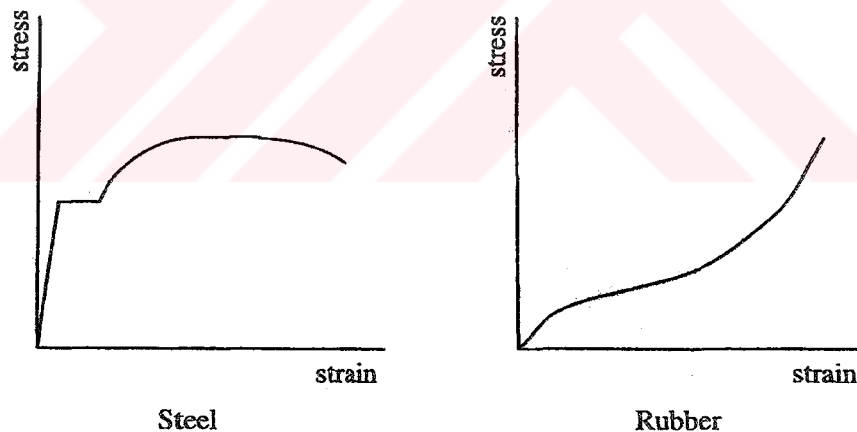
Figure 6.4. Material nonlinearity steel and rubber

Most common engineering materials exhibit a linear stress-strain relationship up to a stress level known as the proportional limit. Beyond this limit, the stress-strain relationship will become nonlinear, but will not necessarily become inelastic. Plastic behavior, characterized by nonrecoverable strain begins when stresses exceed the material's yield point. Because there is a usually little different between the yield point and the proportional limit, our computer program assumes that these two points are coincident in plastic analysis.

Plasticity is a nonconservative, path-dependent phenomenon. In other words, the sequence in which loads are applied and in which plastic responses occur affects the final solution result. Because of the plastic response, we apply loads as a series of small incremental load steps

6.3. BASIC NONLINEAR SOLUTION TECHNIQUE

6.3.1 .Nonlinear analysis with a linear solver

A nonlinear system cannot be analyzed directly with a linear equation solver. However, it can be analyzed by using a series of linear approximation, with corrections.

Each linear approximation requires a separate pass, or iteration, through the program's linear equation solver. Each new iteration is about as expensive as a single linear analysis solution.

Special techniques are required to keep track of information generated during each iteration (information such a displacement, plastic strains, etc.), As well as to calculate the corrections necessary to derive the iterative analysis to a converged solution. The iterative process that is used to solve, correct, and re-solve a nonlinear analysis is called the Newton-Raphson method. Each iteration generated in this process is known as a Newton-Raphson iteration, or an equilibrium iteration.
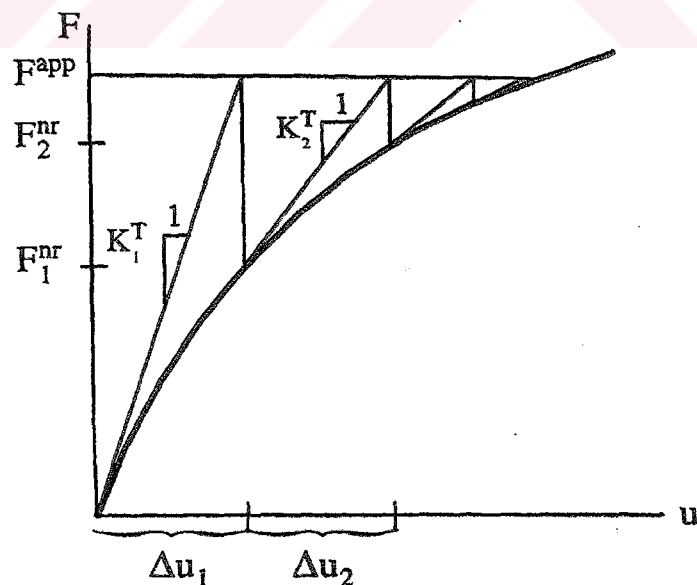

Figure 6.5. Working the Newton-Raphson iteration method

6.3.2. Newton-Raphson Procedure

The finite element discretize process yields a set of simultaneous equations:

$$[K]\{U\} = \{F^a\} \qquad (6.2)$$

where
$[K^a]$: coefficient matrix
$\{u\}$: vector of unknown DOF(degree of freedom) values
$[F^a]$: vector of applied loads

If the coefficient matrix $[K]$ is itself a function of the unknown DOF values (or their derivatives) then equation (1.1) is a nonlinear equation. The Newton-Raphson is a iterative process of solving the nonlinear equations and can be written as:

$$[K^T]\{\Delta u\} = \{F^{app}\} - \{F^{nr}\} \qquad (6.3)$$

where
$[K^T]$: the tangent stiffness matrix
$\{\Delta u\}$: the displacement increment
$\{F^{app}\}$: the applied load vector
$\{F^{nr}\}$: the Newton-Raphson restoring force (the loads generated by the current element stresses)
$(\{F^{app}\}-\{F^{nr}\})$ is called the residual.

For the full Newton-Raphson method, the program updates the tangent stiffness matrix $([K^T])$ and the residual $(\{F^{app}\}-\{F^{nr}\})$ at each iteration, and then re-solves the equation given above.

1. Assume $\{u_0\}$. $\{u_0\}$ is usually the converged solution from the previous step. On the first step $\{u_0\}=\{0\}$.
2. Compute the updated tangent matrix $[K_i^T]$ and restoring load $\{F_i^{nr}\}$ from configuration $\{u_i\}$.
3. Calculate $\{\Delta u_i\}$ from equation (6.2)
4. Add $\{\Delta u_i\}$ to $\{u_i\}$ in order to obtain the next approximation.
5. Repeat steps 2 to 4 until convergence is obtained.

Convergence is achieved once $(\{F^{app}\}-\{F^{nr}\})$ is less than a convergence criterion that you set. In physical terms, if $\{F^{app}\}$ does not equal $\{F^{nr}\}$, the system is not equilibrium. Once the amount of disequilibrium becomes acceptable small, the solution is considered to be converged.

That can be shown how the Newton-Raphson method works from the following force deflection graph for a one degree of freedom (DOF) system in figure 6.5.

In this schematic, the first iteration yields a displacement Δu_1(using the initial elastic stiffness and the applied load F^{app}). The nonlinear response yields a force value F^{nr}_1 for this displacement. The second iteration yields Δu_2 (using the updated tangent matrix and the residual load). Subsequent iterations quickly drive the analysis to a converged solution.

CHAPTER SEVEN

ELASTO-PLASTIC STRESSES IN A CIRCULAR CYLINDER WITH A BAND OF PRESSURE

7.1. CONSTRUCTION OF THE THEORETICAL MODEL

7.1.1. Definition of the Problem

The general arrangement of the circular cylinder with a band of pressure investigated is shown in figure 7.1. Circular cylinder with a band of pressure has symmetry with respect to loading condition, geometric properties, and material properties. On account of the symmetry only quarter of the circular cylinder, which is shaded, was analysed as indicated in figure 7.1
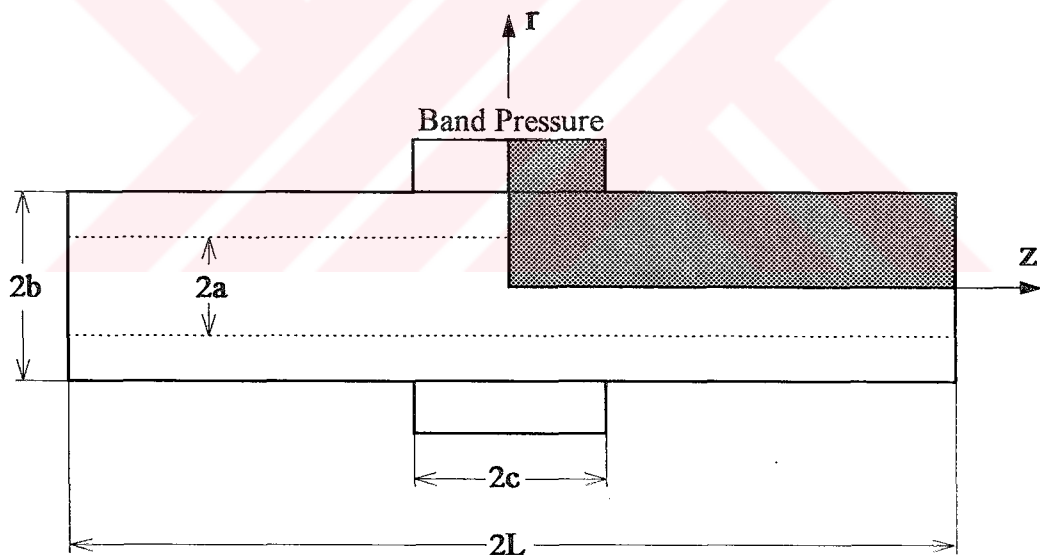

Figure 7.1. A Circular cylinder with a hole under band pressure

2b : outer diameter of the cylinder

2a : inner diameter of the cylinder

2c : width of the band pressure
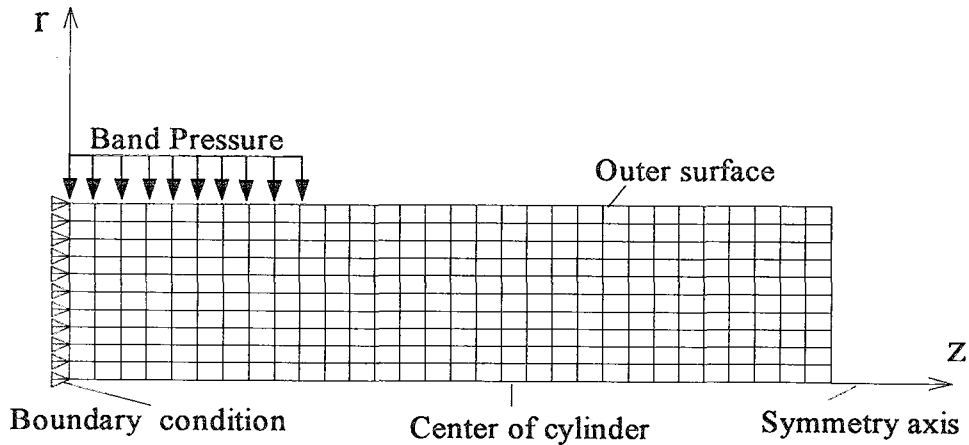
2L : Length of the cylinder

48

Figure 7.2. Finite element model and boundary condition of the quarter of circular solid (without hole) cylinder subjected to band pressure

7.1.2. Finite Element Model and Boundary Condition

Elasto-plastic stresses in the circular cylinder without hole subjected to band pressure are investigated for isotropic material. Band pressure acts as an uniform loading. The horizontal displacements are zero in the y-direction. These are boundary conditions and are shown as simple support in figure 7.2. In the solution, two dimensional isoparametric rectangular ring shape elements are used. Finite element models of the quarter of the circular cylinder (solid or with a hole) consists of 300 elements.

7.1.3. Material Properties of the Circular Cylinder

In the solution of the problem, the material is selected as isotropic and steel. Mechanical properties of selected material is given in table 7.1.

Table 7.1. Material properties of the circular cylinder

Elasticity modulus	E=200000 MPa
Tangent modulus	E_T=3000 MPa
Poisson's ratio	υ=0.3
Yield point of material	σ_y=200 MPa

49

7.2. ELASTO-PLASTIC ANALYSIS IN THE CIRCULAR SOLID CYLINDER SUBJECTED TO BAND PRESSURE

Circular solid cylinder dimension are given in table 7.2. External band pressure is loaded on the surface of solid cylinder in the radial direction. Band pressure is loaded incrementally as small step. Beyond the yield point or around the yield point different band pressures are loaded on the circular solid cylinder. This pressure magnitude is given in table 7.3.

Table 7.2. Dimension of the finite element model of the circular solid cylinder

Inner radius of cylinder	a=0 mm
Outer radius of cylinder	b=20 mm
Width of band pressure	c=20 mm
Length of cylinder	L=60 mm

Table 7.3. Band pressure which are loaded on the solid cylinder surface

Band Pressure P
P=170 MPa,   P=200 MPa,   P=220 MPa,   P=240 MPa

Deformed shape of the circular solid cylinder of the finite element method under band pressure is obtained in the postprocessing section of computer program by means of plot display command.
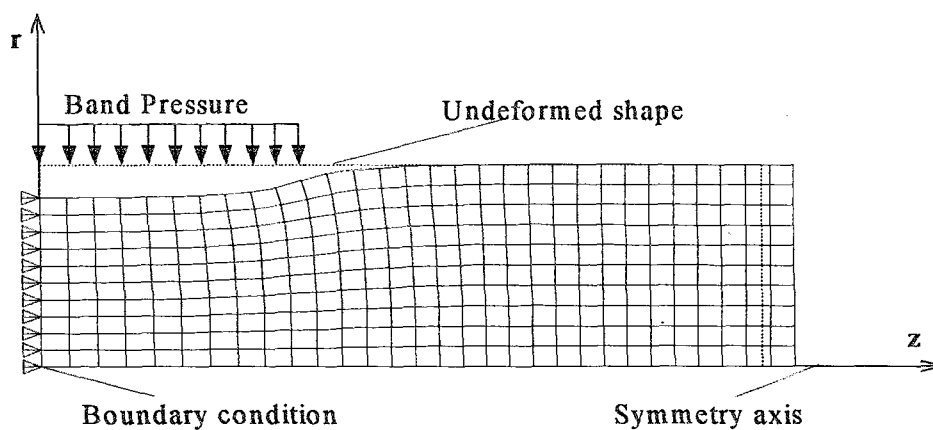

Figure 7.3. Defomed shape of the finite element model quarter of the circular solid cylinder subjected to band pressure

50

Stress components (tangential stress σ_θ, radial stress σ_r, axial stress σ_z, equivalent stress σ_{eq}, elasto-plastic stress σ_{ep}, and shear stress τ_{rz}) and strain components (tangential strain ε_θ, radial strain ε_r, axial strain ε_z, equivalent strain ε_{eq}, total elasto-plastic strain ε_{Total} and shear strain γ_{rz}) are obtained from the computer by means of finite element method at each node.

For band pressure P=220 MPa, all of the stresses components are shown as contour legend with different color on cross section of the circular solid cylinder in figures 7.4-7.8. And also vector plot of displacement on the longitudinal section of the circular solid cylinder subjected to band pressure for P=220 MPa is shown in figure 7.9. Moreover, elasto-plastic equivalent stress contour on the longitudinal section of the circular solid cylinder subjected to band pressure respectively, P=180 MPa, P=200 MPa, P=220 MPa, P=240 MPa are shown as contour legend with different color on longitudinal section of the circular solid cylinder in figure 7.10. When band pressure is equal to 176 MPa yielding begins in the circular solid cylinder. When pressure increases elasto-plastic region getting deeper and deeper.

In the circular solid cylinder, we have investigated all region and especially critical local region (surface of cylinder and center of cylinder). Therefore, distributions of the stresses components are plotted center and outer surface of the circular cylinder for different band pressure in figures. The stress components (tangential stress σ_θ, radial stress σ_r, axial stress σ_z and shear stress τ_{rz}) distributions through the length of the circular solid cylinder under band pressure respectively, P=170 MPa, P=200 MPa, P=220 MPa along outer surface and symmetry axis of cylinder are shown on the same graph in figure 7.11-7.16. Variations of the elasto-plastic stress over the yielding stress through the length of the circular solid cylinder subjected to different band pressure along outer surface and symmetry axis of the cylinder are ploted in figure 7.17-7.18. Variations of the equivalent stress through the length of the circular solid cylinder under different band pressure along outer surface and symmetry axis of the cylinder are shown in figure 7.19-7.20. Variations of the tangential and axial stress through the length of the circular solid cylinder under different band pressure along outer surface and symmetry axis of the cylinder are shown in figure 7.21-7.24.

Variations of the total equivalent strain and tangential strain through the length of the circular solid cylinder under different band pressure along outer surface and symmetry axis of the cylinder are ploted 7.25-7.28.

Variations of the tangential residual and equivalent stress through the length of the circular solid cylinder under different band pressure along outer surface and symmetry axis of the cylinder are shown in figure 7.29-7.32
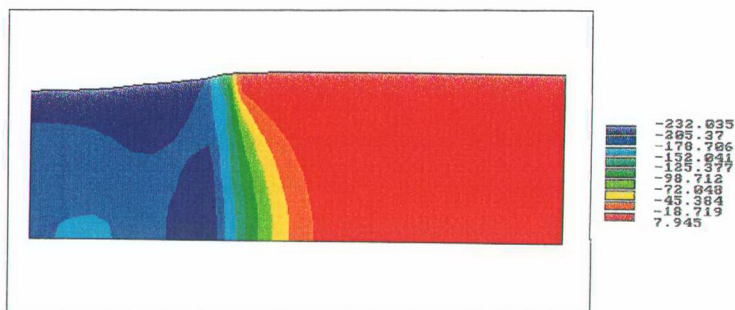
Figure 7.4. Radial stress contour on the longitudinal section of the circular solid cylinder subjected to band pressure P=220 MPa
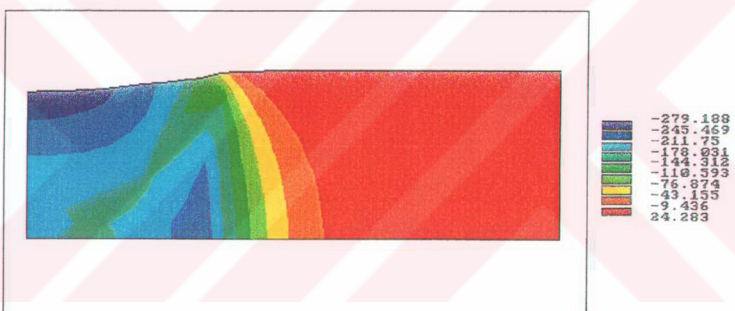

Figure 7.5. Tangential stress contour on the longitudinal section of the circular solid cylinder subjected to band pressure P=220 MPa
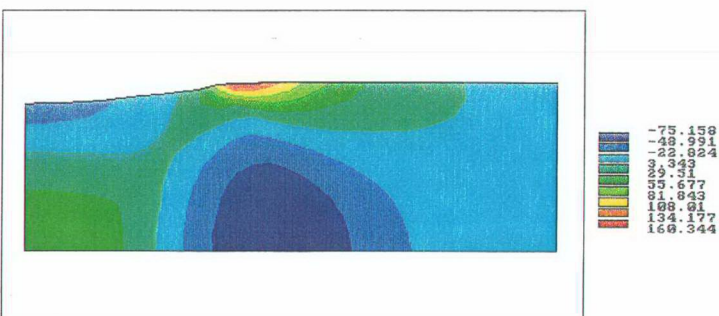

Figure 7.6. Axial stress contour on the longitudinal section of the circular solid cylinder subjected to band pressure P=220 MPa
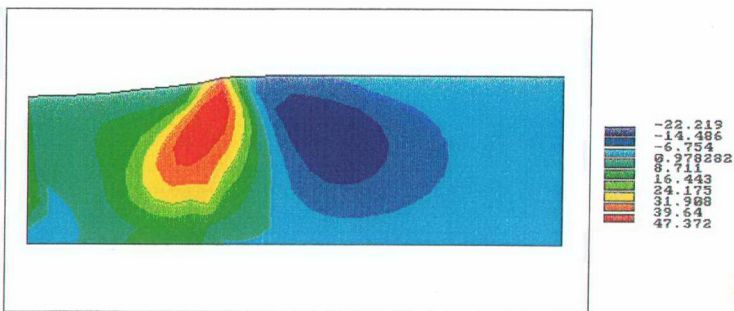
Figure 7.7. Shear stress contour on the longitudinal section of the circular solid cylinder subjected to band pressure P=220 MPa

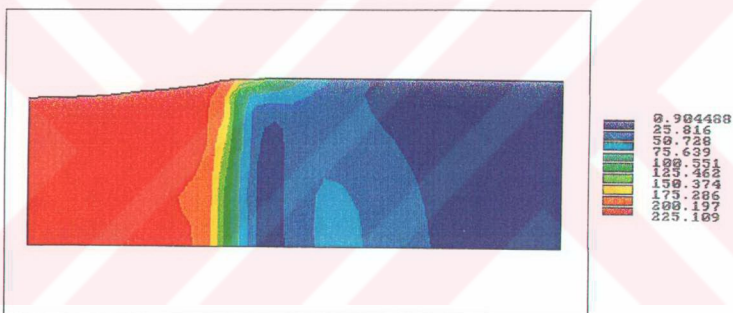
Figure 7.8. Equivalent stress contour on the longitudinal section of the circular solid cylinder subjected to band pressure P=220 MPa
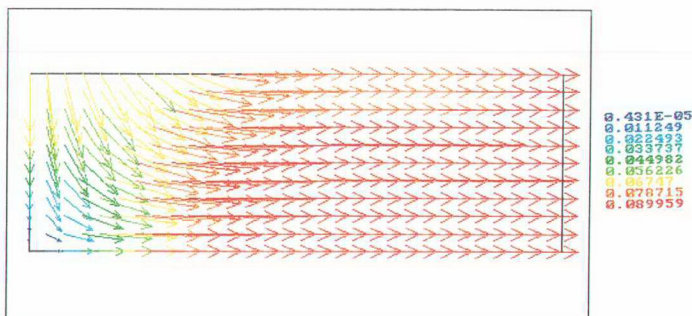

Figure 7.9. Vector plot of displacement on the longitudinal section of the circular solid cylinder subjected to band pressure P=220 MPa
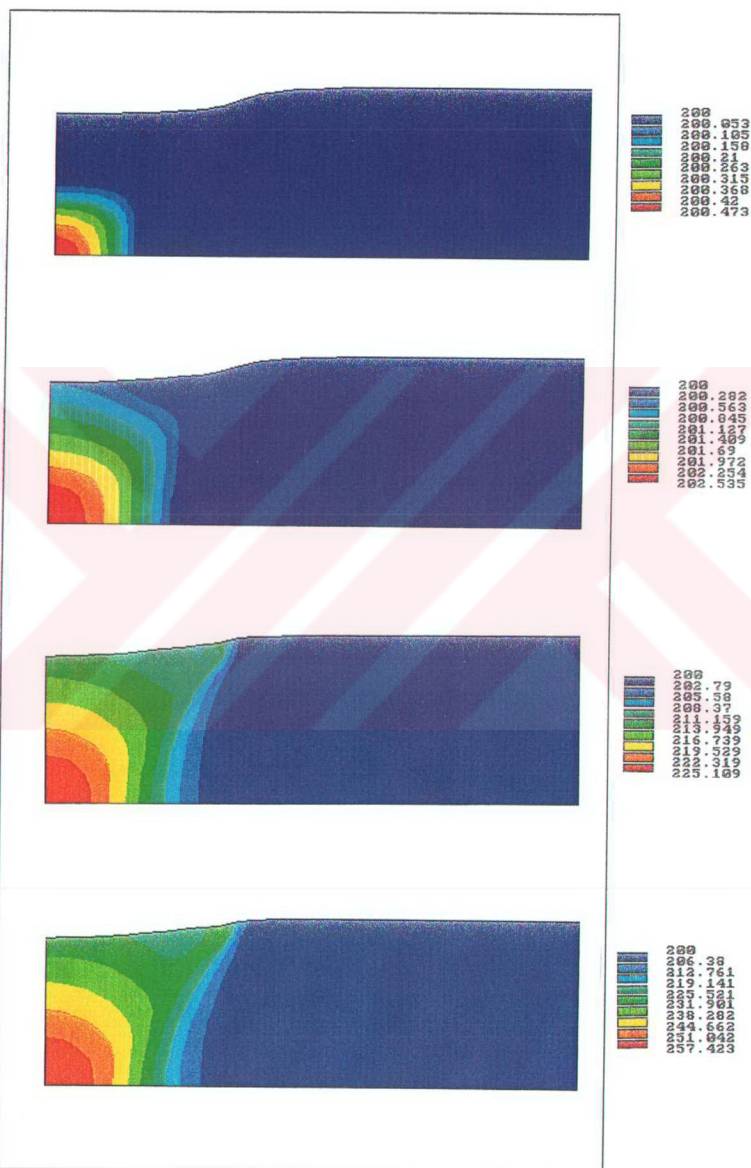
Figure 7.10. Elasto-plastic equivalent stress contour on the longitudinal section of the circular solid cylinder subjected to band pressure respectively P=180 MPa, P=200 MPa, P=220 MPa, P=240 MPa
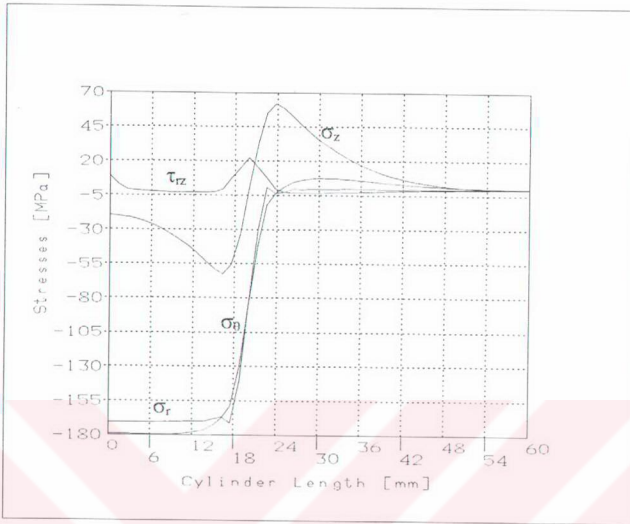
Figure 7.11. The stress components distributions through the length of the circular solid cylinder under band pressure P=170 MPa at r=b (along outer surface of cylinder)
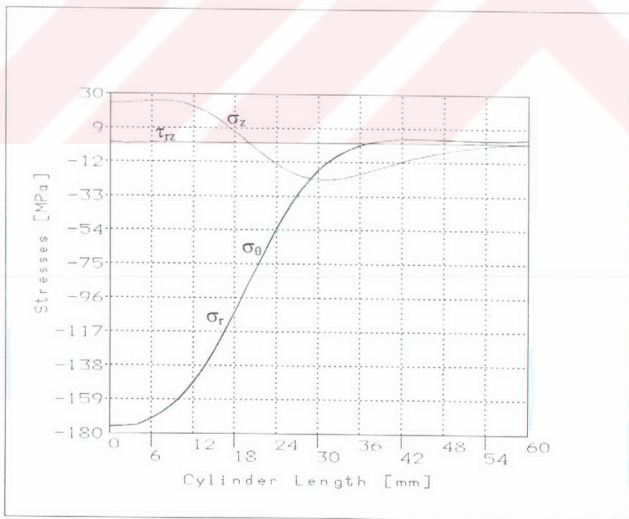

Figure 7.12. The stress components distributions through the length of the circular solid cylinder under band pressure P=170 MPa at r=0 (along symmetry axis of the cylinder)

55

Figure 7.13. The stress components distributions through the length of the circular solid cylinder under band pressure P=200 MPa at r=b (along outer surface of the cylinder)

Figure 7.14. The stress components distributions through the length of the circular solid cylinder under band pressure P=200 MPa at r=0 (along symmetry axis of the cylinder)
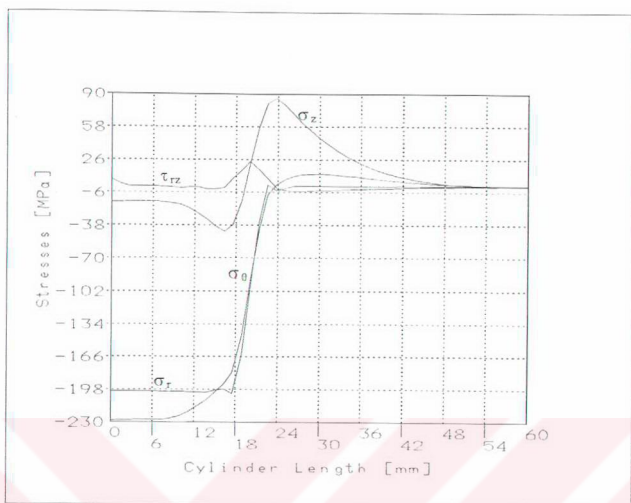
56

Figure 7.15. The stress components distributions through the length of the circular solid cylinder under band pressure P=220 MPa at r=b (along outer surface of the cylinder)
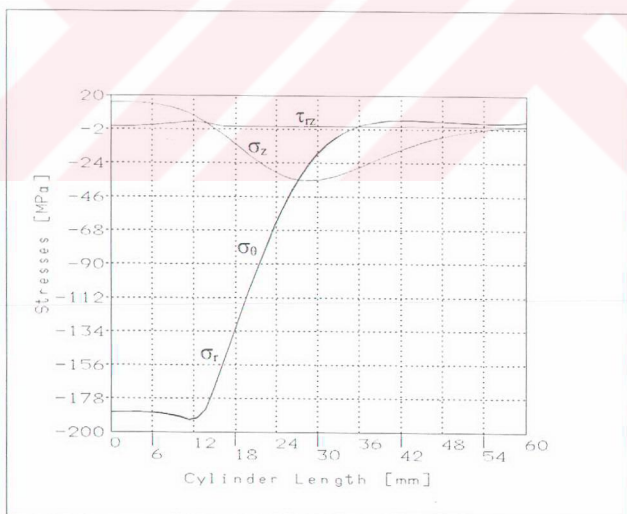

Figure 7.16. The stress components distributions through the length of the circular solid cylinder under band pressure P=220 MPa at r=0 (along symmetry axis of the cylinder)
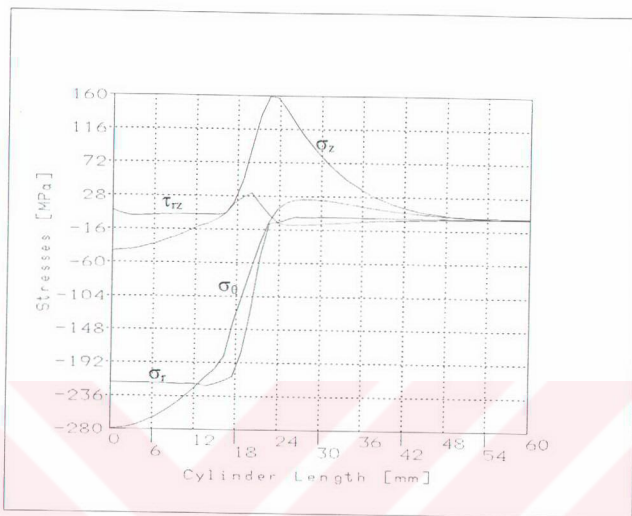
Figure 7.17. Variations of the elasto-plastic stress through the length of the circular solid cylinder under different band pressure at r=b (along outer surface of the cylinder)

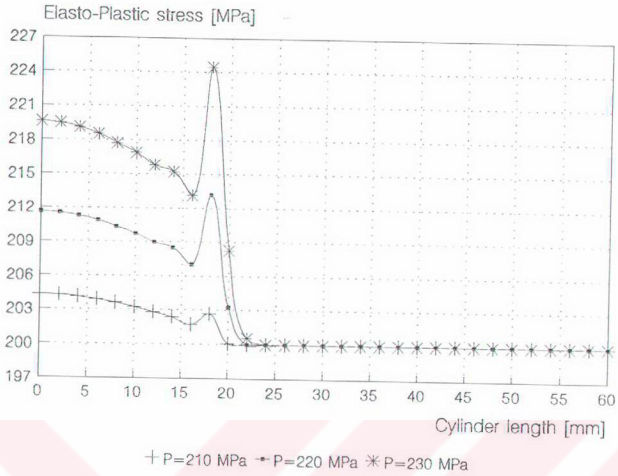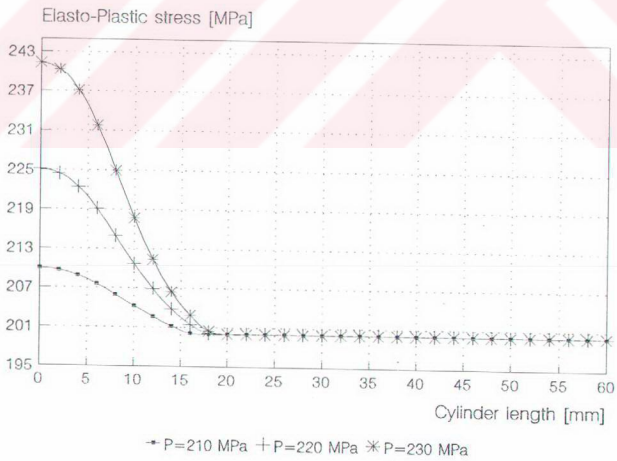**Figure 7.18.** Variations of the elasto-plastic stress through the length of the circular solid cylinder under different band pressure at r=0 (along symmetry axis of the cylinder)
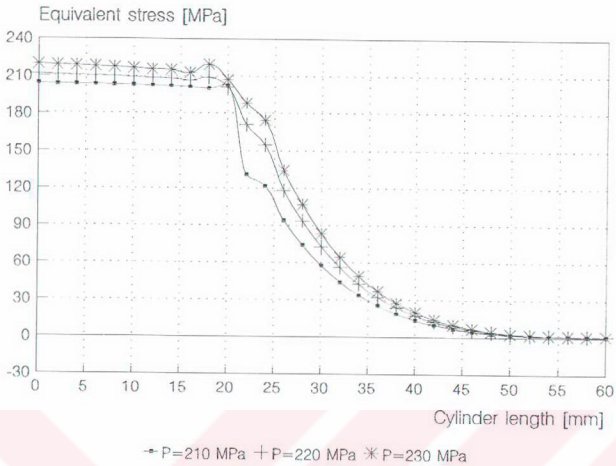
Figure 7.19. Variations of the equivalent stress through the length of the circular solid cylinder under different band pressure at r=b (along outer surface of the cylinder)

Figure 7.20. Variations of the equivalent stress through the length of the circular solid cylinder under different band pressue at r=0 (along symmetry axis of the cylinder)

Figure 7.21. Variations of the tangential stress through the length of the circular solid cylinder under different band pressure at r=b (along outer surface of the cylinder)

Figure 7.22. Variations of the tangential stress through the length of the circular solid cylinder under different band pressure at r=0 (along symmetry axis of the cylinder)

Figure 7.23. Variations of the axial stress through the length of the circular solid cylinder under different band pressure at r=b (along outer surface of the cylinder)
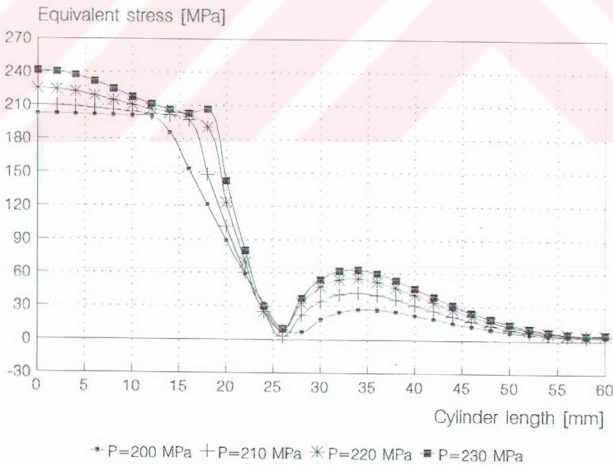

Figure 7.24. Variations of the axial stress through the length of the circular solid cylinder under different band pressure at r=0 (along symmetry axis of the cylinder)

Figure 7.25. Variations of the equivalent strain through the length of the circular solid cylinder under different band pressure at r=b (along outer surface of the cylinder)

Figure 7.26. Variations of the equivalent strain through the length of the circular solid cylinder under different band pressure at r=0 (along symmetry axis of the cylinder)
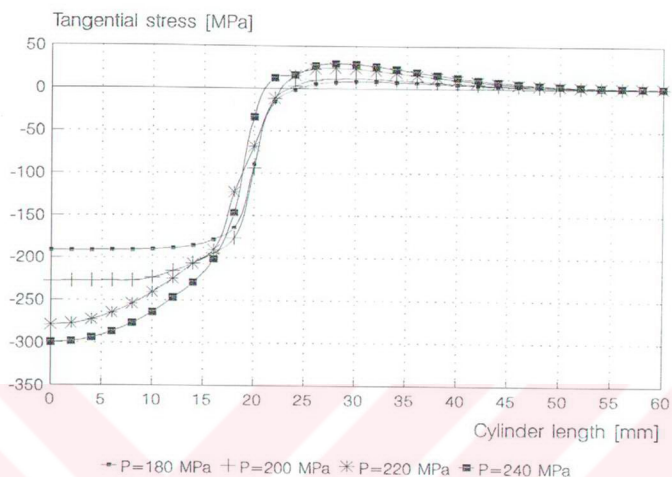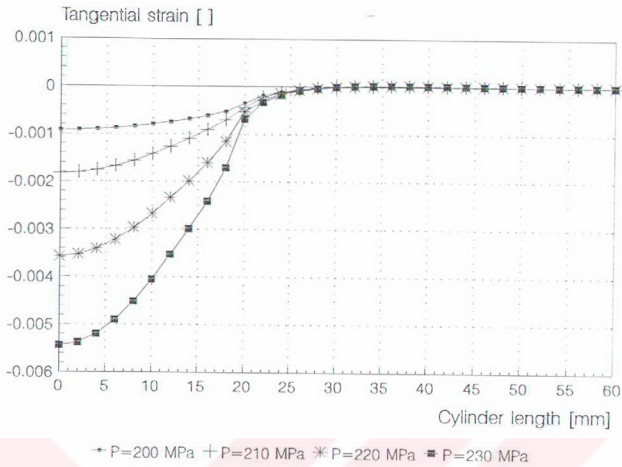
Figure 7.27. Variations of the tangential strain through the length of the circular solid cylinder under different band pressure at r=b (along outer surface of the cylinder)
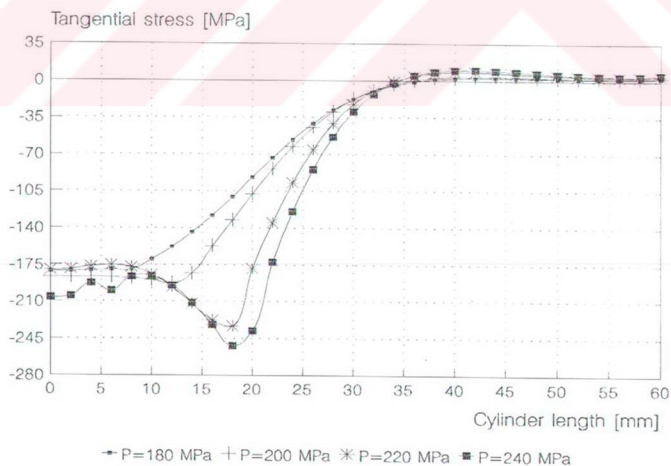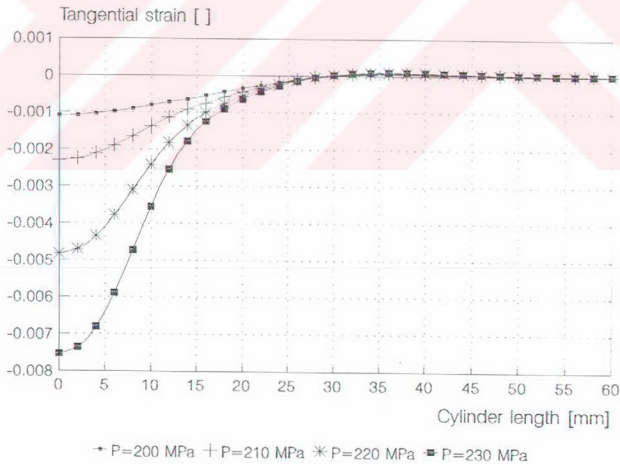

Figure 7.28. Variations of the tangential strain through the length of the circular solid cylinder under different band pressure at r=0 (along symmetry axis of the cylinder)
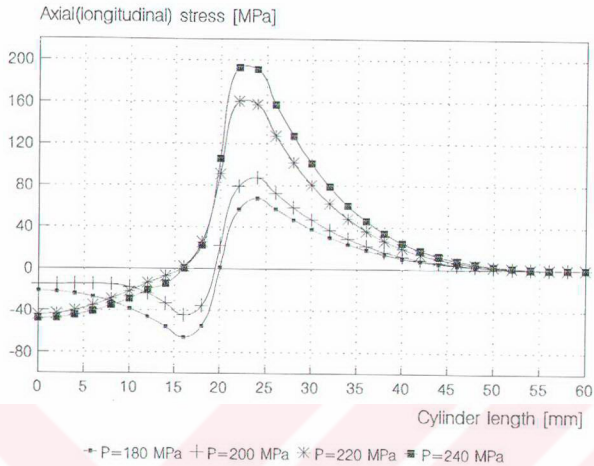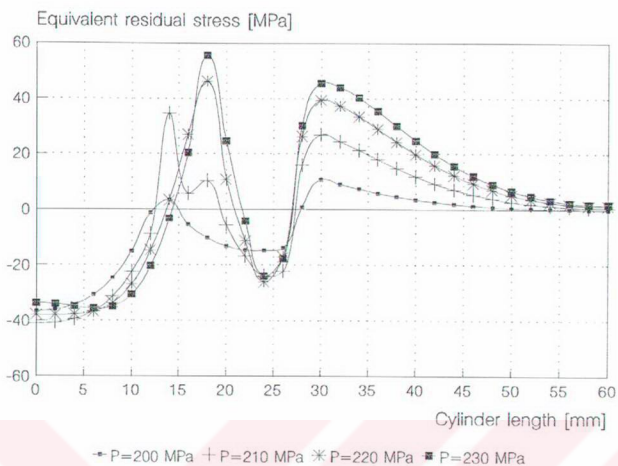
Figure 7.29. Variations of the equivalent residual stress through the length of the circular solid cylinder under different band pressure at r=b (along outer surface of the cylinder)

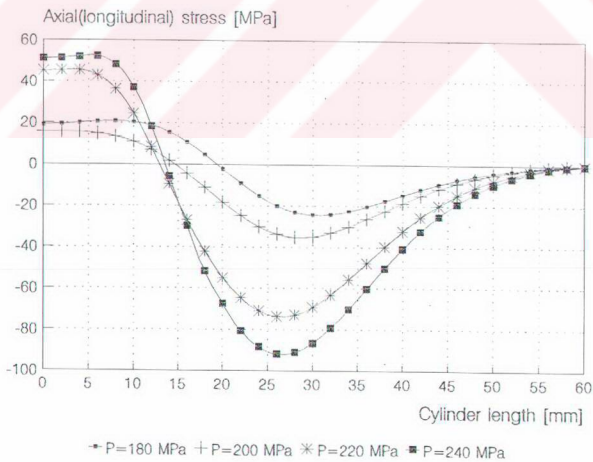**Figure 7.30.** Variations of the equivalent residual stress through the length of the circular solid cylinder under different band pressure at r=0 (along symmetry axis of the cylinder)
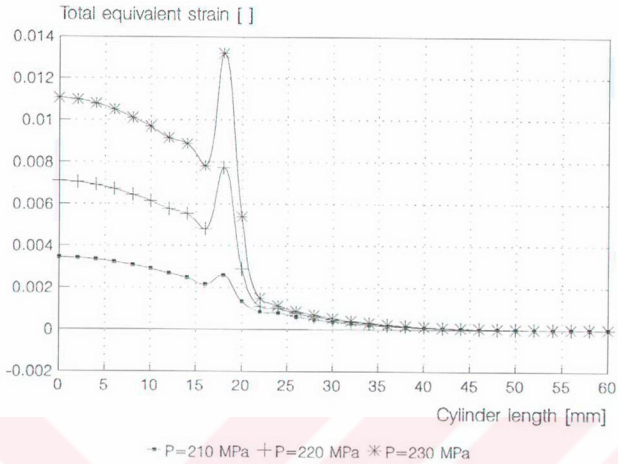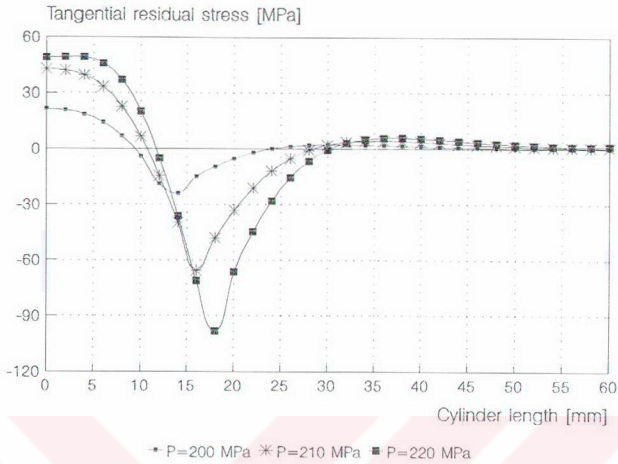
Figure 7.31. Variations of the tangential residual stress through the length of the circular solid cylinder under different band pressure at r=b (along outer surface of the cylinder)
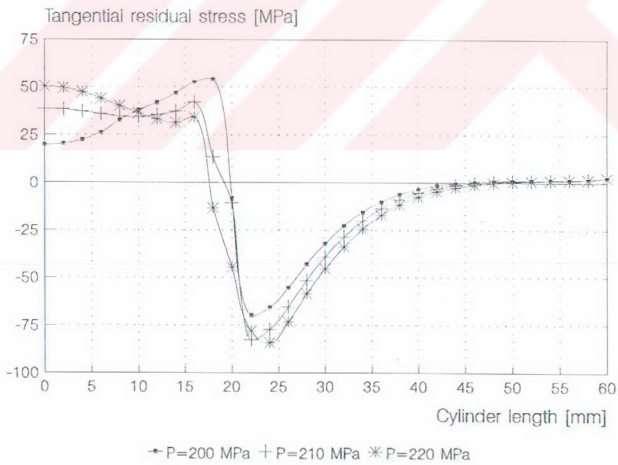
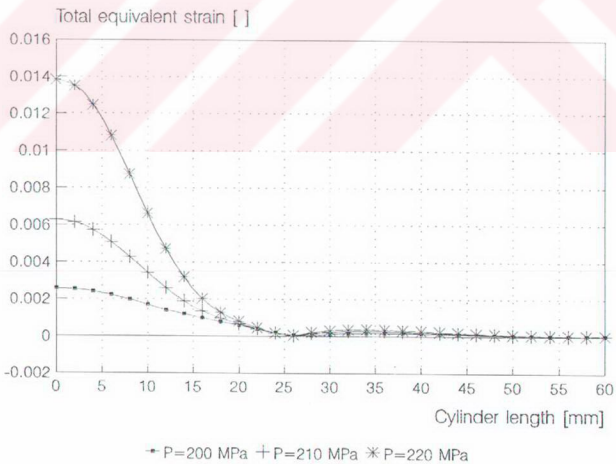**Figure 7.32.** Variations of the tangential residual stress through the length of the circular solid cylinder under different band pressure at r=0 (along symmetry axis of the cylinder)

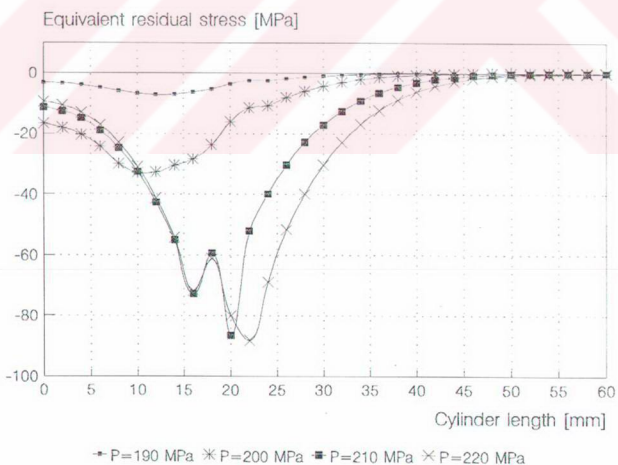## 7.3. ELASTO-PLASTIC ANALYSIS IN THE CIRCULAR CYLINDER WITH HOLE SUBJECTED TO BAND PRESSURE

Elasto-plastic stresses in the circular cylinder with hole subjected to band pressure are investigated for different diameters that are shown in the table 7.4. In the solution of the problem, the material is selected as isotropic. Mechanical properties of selected material are given in table 7.2.

Table 7.4 Dimensions of circular cylinder with a hole subjected to band pressure

	a	b	c	L
a=0.25 b	5mm	20mm	20mm	60mm
a=0.50 b	10mm	20mm	20mm	60mm
a=0.75 b	15mm	20mm	20mm	60mm
a=0.90 b	18mm	20mm	20mm	60mm

Band pressure act as a uniform loading. The horizontal displacements are zero in the r-direction. These are boundary conditions that are shown as simple support in figure 7.33.

Figure 7.33 Finite element model and boundary codition of the quarter of cylinder with a hole under band pressure

Circular cylinders with a hole dimensions are given in table 7.2. External band pressure is loaded on the surface of the cylinder in the radial direction. Band pressure is loaded incrementally as small step. Beyond the yield point or around the yield point different band pressure are loaded on the circular cylinder with a hole. This pressure magnitude is given in table 7.5.

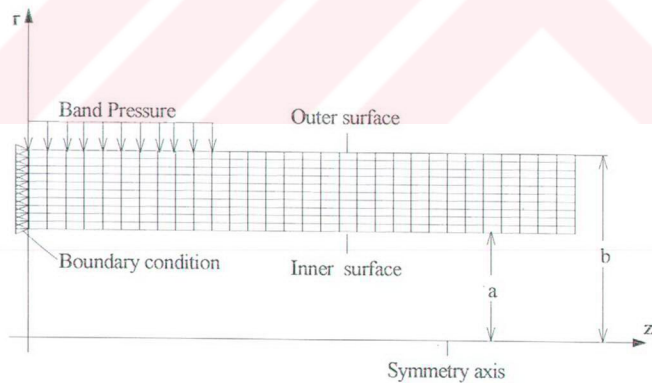Table 7.5. Magnitude of band pressure which are acted on the circular cylinder with a hole

	Band Pressure			
a=0.25 b	100 MPa	140 MPa	160 MPa	180 MPa
a=0.50 b	80 MPa	110 MPa	120 MPa	130 MPa
a=0.75 b	45 MPa	50 MPa	55 MPa	60 MPa
a=0.90 b	20 MPa	21 MPa	22 MPa	23 MPa
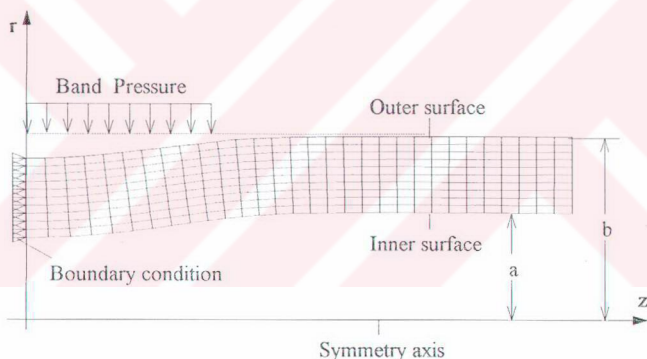
Figure 7.34 Deformed shape of the finite element model of the quarter of the circular cylinder with a hole subjected to band pressure

Deformed shape of the circular cylinder with a hole subjected to band pressure for inner radius a=10 mm and outer radius b=20 mm are given in figure 7.34. Stress components are obtained from the computer by means of finite element method at each node.

All of the stress components are shown as contour legend with different color on longitudinal section of the circular cylinder with a hole (a=5mm, a=10 mm, a=15 mm, a=18 mm) in figures. For different hole vector plot of displacement on the longitudinal section of the circular cylinder with a hole are shown in figures. Moreover, elasto-plastic equivalent stress contour on the longitudinal section of the circular cylinder with a hole for different band pressure are shown as contour legend with different color in figures for different hole.

Figure 7.35. Radial stress contour on the longitudinal section of the circular cylinder with a hole (a=5mm) subjected to band pressure P=200 MPa

Figure 7.36. Tangential stress contour on the longitudinal section of the circular cylinder with a hole (a=5mm) subjected to band pressure P=200 MPa
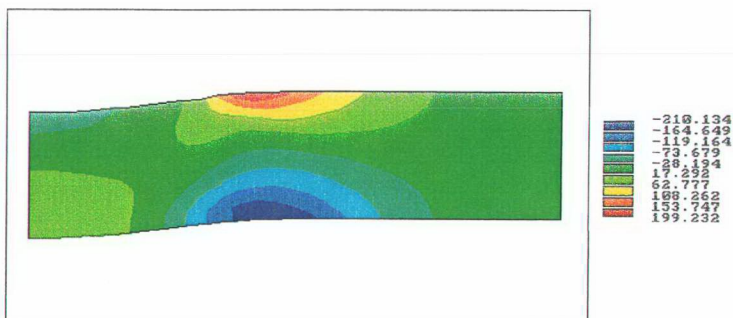
Figure 7.37. Axial stress contour on the longitudinal section of the circular cylinder with a hole (a=5mm) subjected to band pressure P=200 MPa
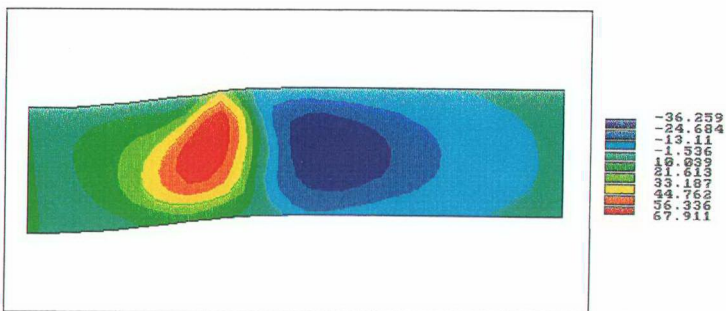
Figure 7.38. Shear stress contour on the longitudina section of the circular cylinder with a hole (a=5mm) subjected to band pressure P=200 MPa
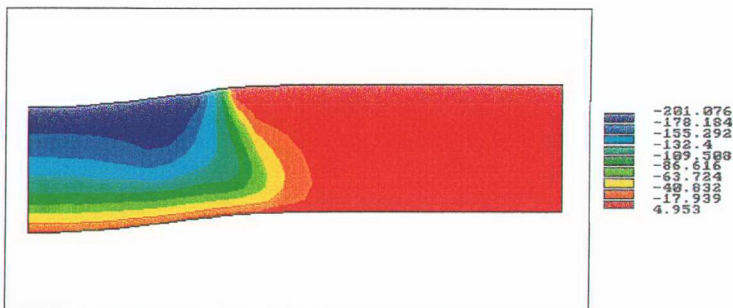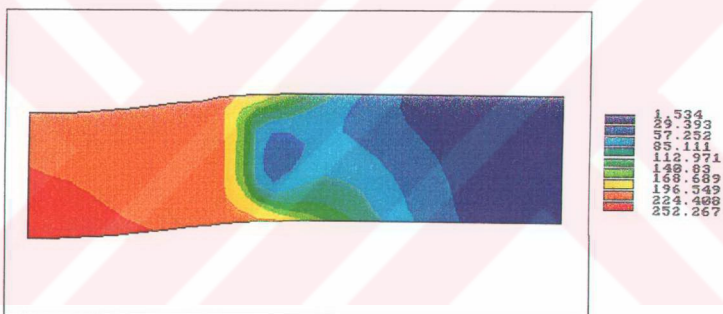

Figure 7.39. Equivalent stress contour on the longitudinal section of the circular cylinder with a hole (a=5mm) subjected to band pressure P=200 MPa
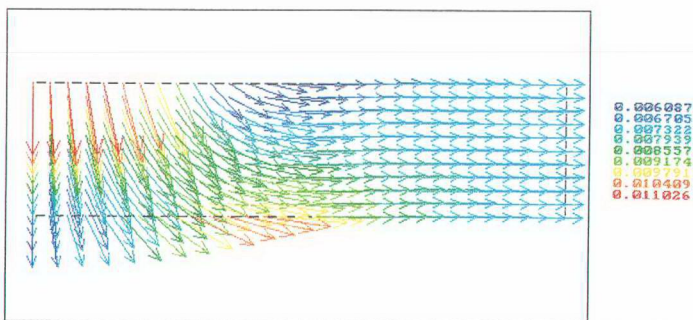
Figure 7.40. Vector plot of displacement on the longitudinal section of the circular cylinder with a hole (a=5mm) subjected to band pressure P=200 MPa

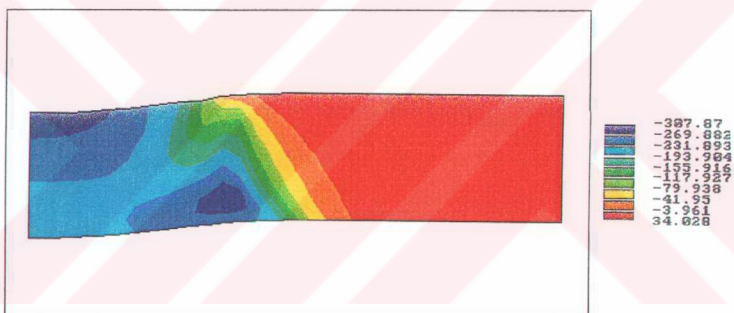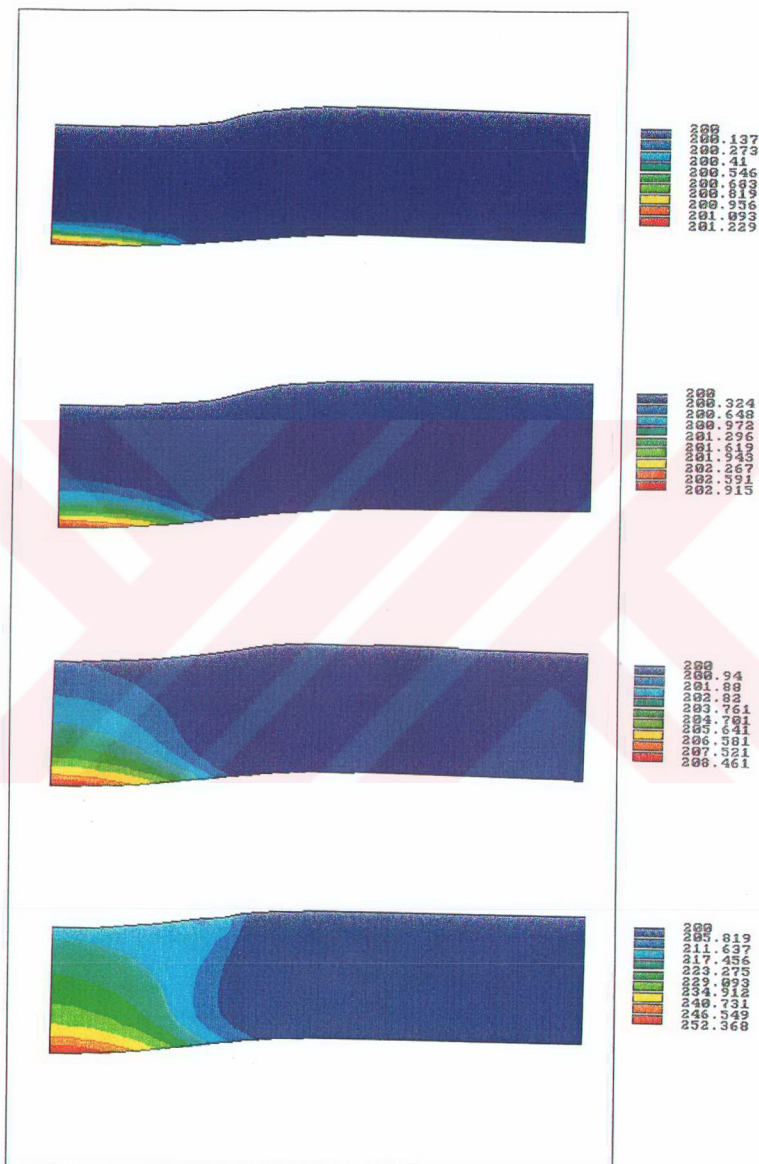Figure 7.41. Elasto-plastic equivalent stress contour on the longitudinal section of the circular cylinder with a hole (a=5mm) subjected to band pressure respectively, P=125 MPa, P=150 MPa, P=175 MPa, P=200 MPa
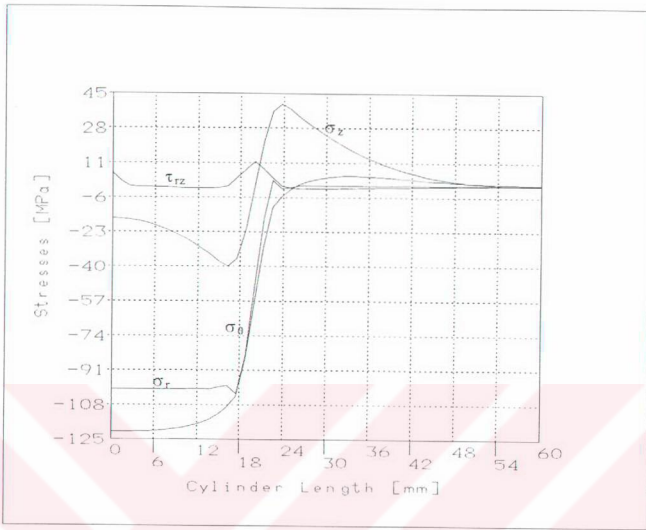
Figure 7.42. The stress distributions through the length of the circular cylinder with a hole (a=5mm) under band pressure P=100 MPa at a=0.25b along the outer surface
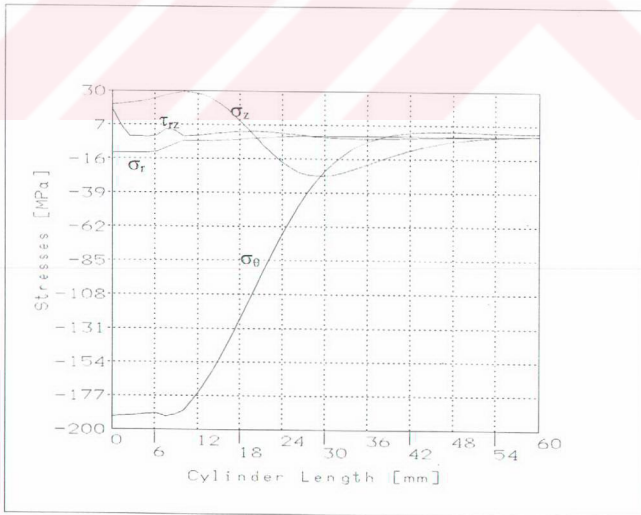
Figure 7.43. The stress distributions through the length of the circular cylinder with a hole (a=5mm) under band pressure P=100 MPa at a=0.25b along the inner surface
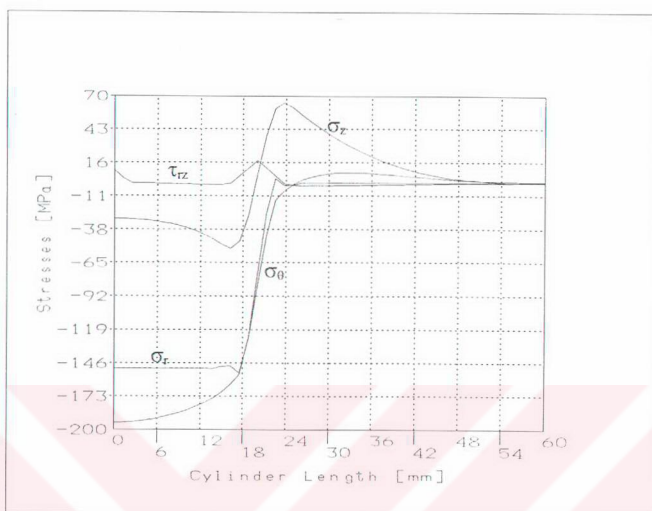
Figure 7.44. The stress distributions through the length of the circular cylinder with a hole (a=5mm) under band pressure P=100 MPa at a=0.25b along the outer surface
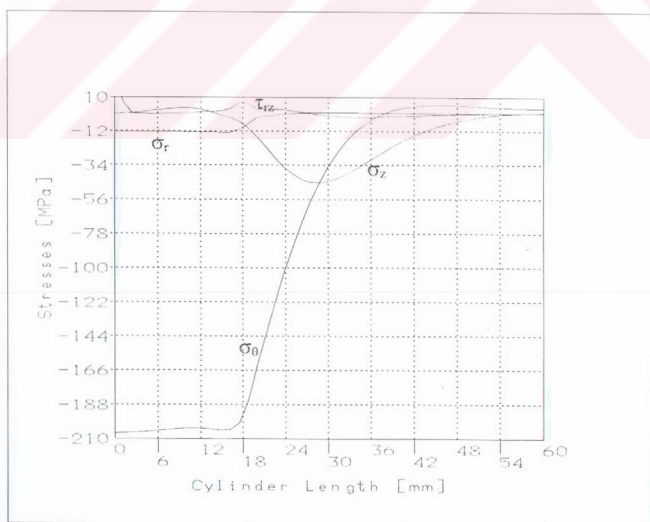
Figure 7.45. The stress distributions through the length of the circular cylinder with a hole (a=5mm) under band pressure P=150 MPa at a=0.25b along inner surface

Figure 7.46. The stress distributions through the length of the circular cylinder with a hole (a=5mm) under band pressure P=180 MPa at a=0.25b along the outer surface

Figure 7.47. The stress distributions through the length of the circular cylinder with a hole (a=5mm) under band pressure P=180 MPa at a=0.25b along the inner surface
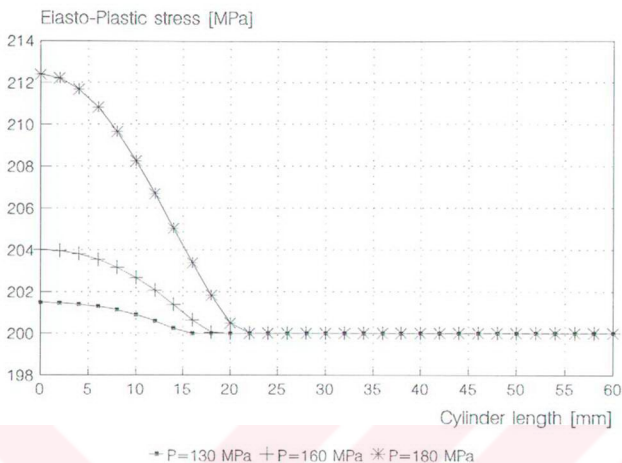
Figure 7.48. Variations of the elasto-plastic stress through the length of the circular cylinder with a hole (a=5mm) under different band pressure along the inner surface
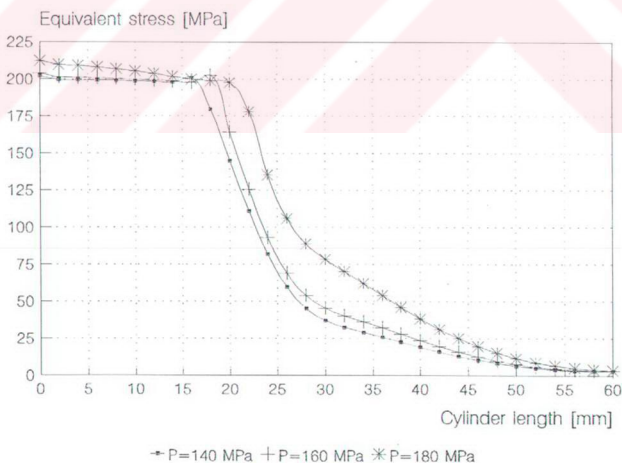
Figure 7.49. Variations of the equivalent stress through the length of the circular cylinder with a hole (a=5mm) under different band pressure along the inner surface
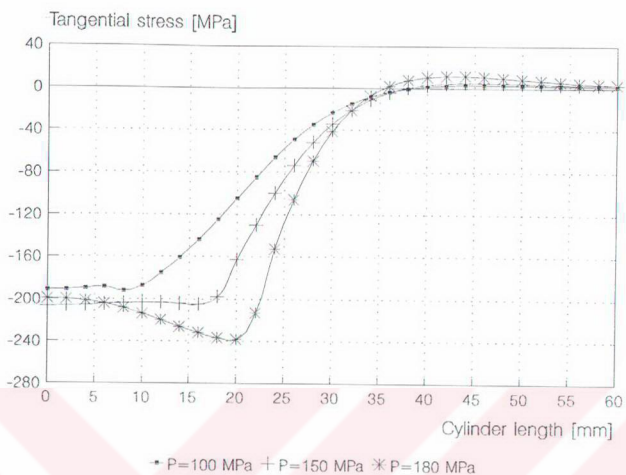
Figure 7.50. Variations of the tangential stress through the length of the circular cylinder with a hole (a=5mm) under different band pressure along the inner surface
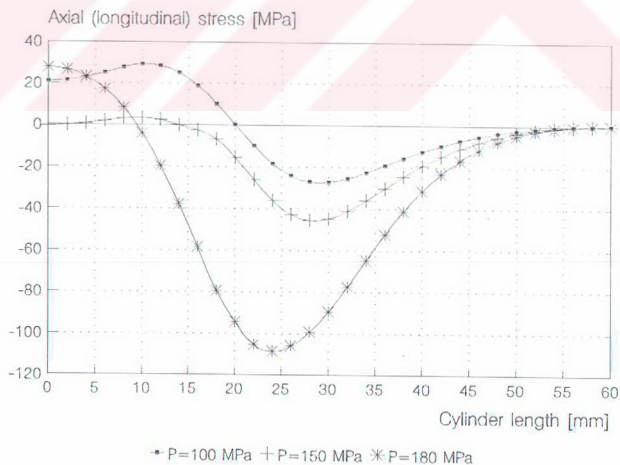
Figure 7.51. Variations of the axial stress through the length of the circular cylinder with a hole (a=5mm) under different band pressure along the inner surface

Figure 7.52. Variations of the equivalent residual stress through the length of the circular cylinder with a hole (a=5mm) under different band pressure along the inner surface

Figure 7.53. Variations of the tangential residual stress through the length of the circular cylinder with a hole (a=5mm) under different band pressure along the inner surface

Figure 7.54. Variations of the total equivalent strain through the length of the circular cylinder with a hole (a=5mm) under different band pressure along the inner surface

Figure 7.55. Variations of the tangential strain through the length of the circular cylinder with a hole (a=5mm) under different band pressure along the inner surface
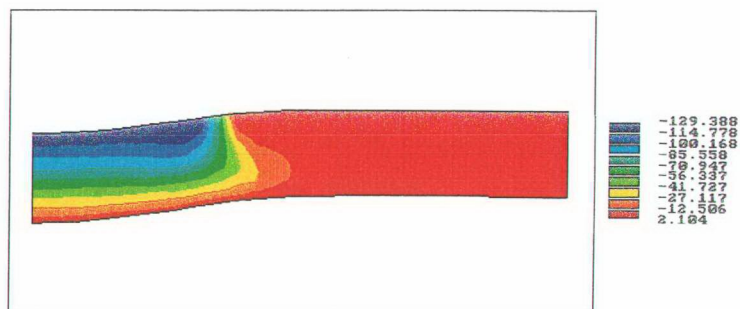
Figure 7.56. Radial stress contour on the longitudinal section of the circular cylinder with a hole (a=10mm) subjected to band pressure P=130 MPa

Figure 7.57. tangential stress contour on the longitudinal section of the circular cylinder with a hole (a=10mm) subjected to band pressure P=130 MPa

Figure 7.58. Axial stresses contour on the longitudinal section of the circular cylinder with a hole (a=10mm) subjected to band pressure P=130 MPa

Figure 7.59. Shear stress contour on the longitudinal section of the circular cylinder with a hole (a=10mm) subjected to band pressure P=130 MPa

Figure 7.60. Equivalent stress contour on the longitudinal section of the circular cylinder with a hole (a=10mm) subjected to band pressure P=130 MPa

Figure 7.61. Vector plot of displacement on the longitudinal section of the circular cylinder with a hole (a=10mm) subjected to band pressure P=130 MPa

Figure 7.62. Elasto-plastic equivalent stress contour on the longitudinal section of the circular cylinder with a hole (a=10mm) subjected to band pressure respectively P=100 MPa, P=110 MPa, P=120 MPa, P=130 MPa
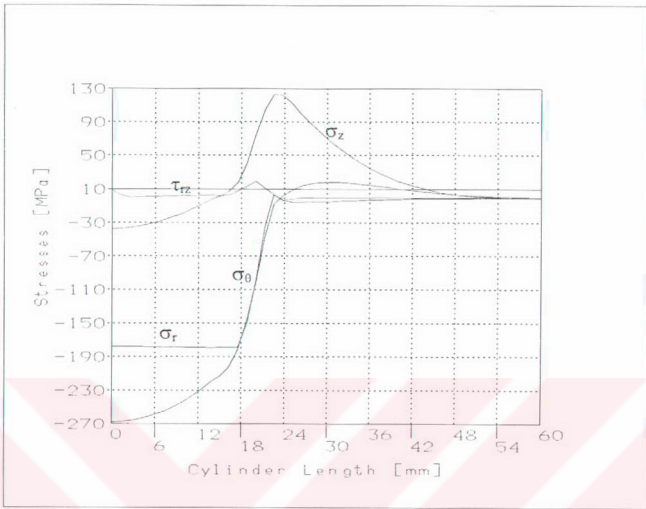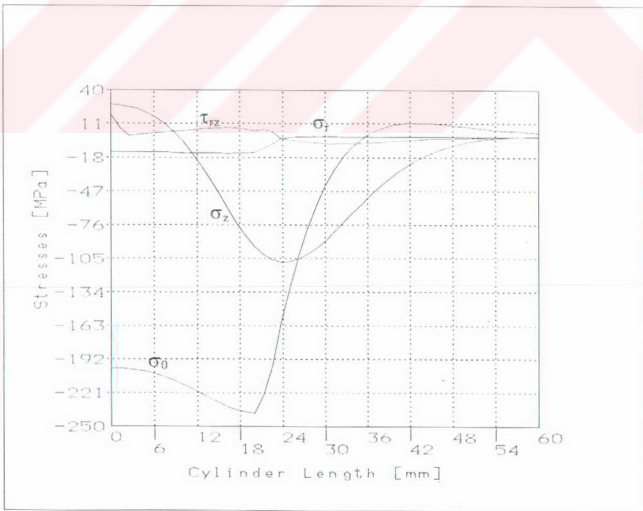
Figure 7.63. The stress distributions through the length of the circular cylinder with a hole (a=10mm) under band pressure P=80 MPa at r=0.5b along the outer surface


Figure 7.64. The stress distributions through the length of the circular cylinder with a hole (a=10mm) under band pressure P=80 MPa at r=0.5b along the inner surface

Figure 7.65. The stress distributions through the length of the circular cylinder with a hole (a=10mm) under band pressure P=110 MPa at a=0.5b along the outer surface

Figure 7.66. The stress distributions through the length of the circular cylinder with a hole (a=10mm) under band pressure P=110 MPa at a=0.5b along the inner surface

Figure 7.67. The stress distributions through the length of the circular cylinder with a hole (a=10mm) under band pressure P=130 MPa at a=0.5b along the outer surface

Figure 7.68. The stress distributions through the length of the circular cylinder with a hole (a=10mm) under band pressure P=130 MPa at a=0.5b along the inner surface

Figure 7.69. Variations of the elasto-plastic stress through the length of the circular cylinder with a hole (a=10mm) under different band pressure along the inner surface

Figure 7.70. Variations of the equivalent stress through the length of the circular cylinder with a hole (a=10mm) under different band pressure along the inner surface
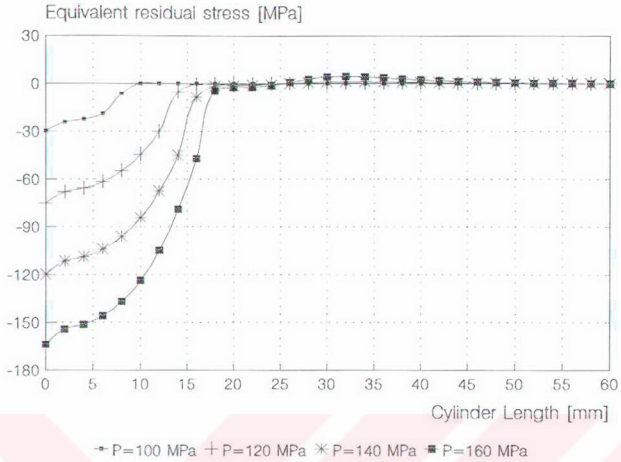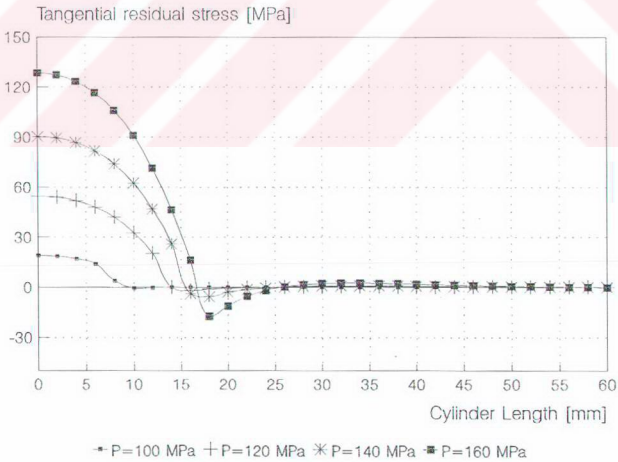
84

Figure 7.71. Variations of the tangential stress through the length of the circular cylinder with a hole (a=10mm) under different band pressure along the inner surface
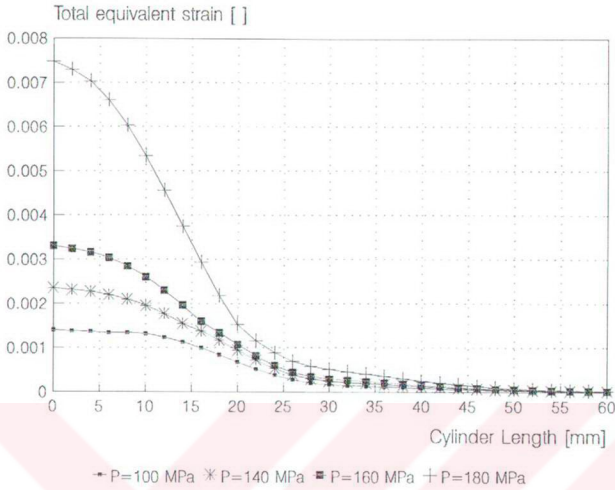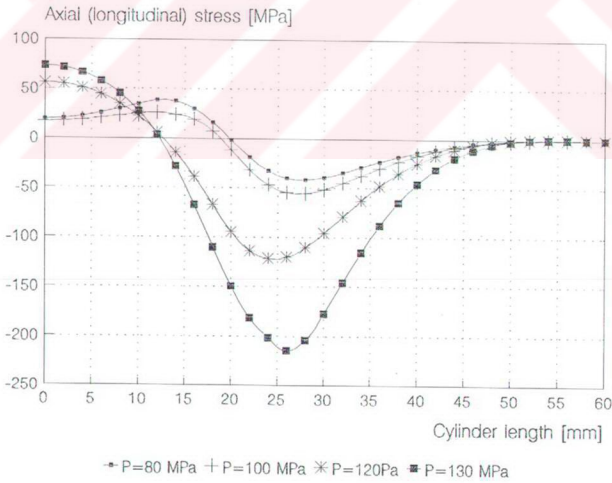

Figure 7.72. Variations of the axial stress through the length of the circular cylinder with a hole (a=10mm) under different band pressure along the inner surface
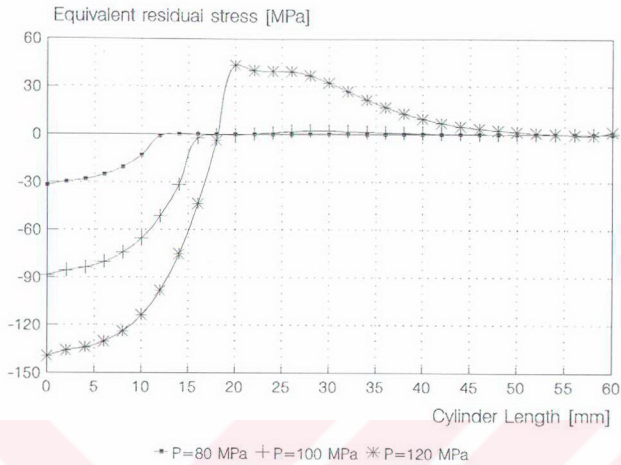
Figure 7.73. Variations of the equivalent residual stress through the length of the circular cylinder with a hole (a=10mm) under different band pressure along the inner surface
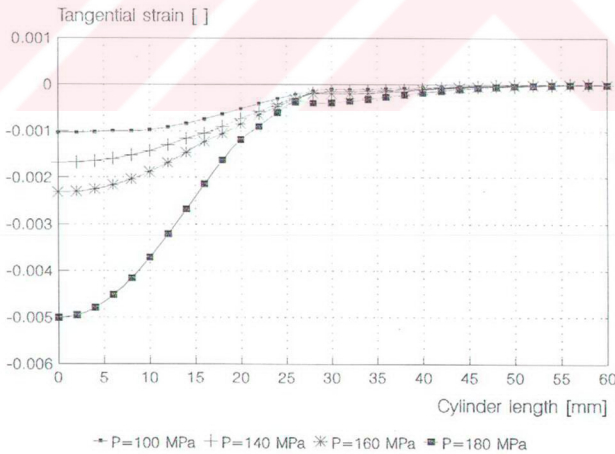

Figure 7.74. Variations of the tangential residual stress through the length of the circular cylinder with a hole (a=10mm) under different band pressure along the inner surface
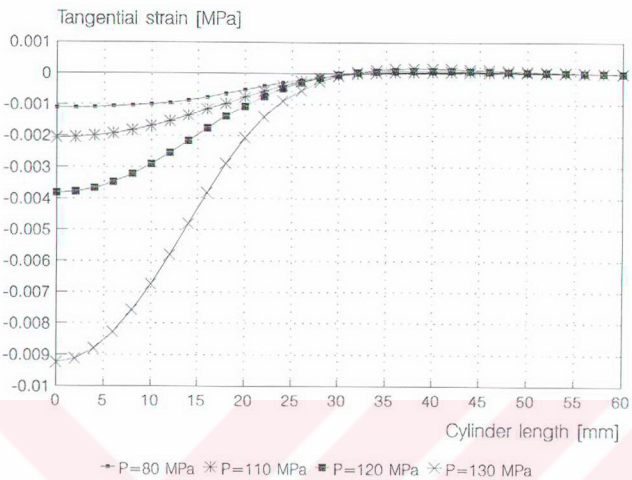
Figure 7.75. Variations of the tangential strain through the length of the circular cylinder with a hole (a=10mm) under different band pressure along the inner surface
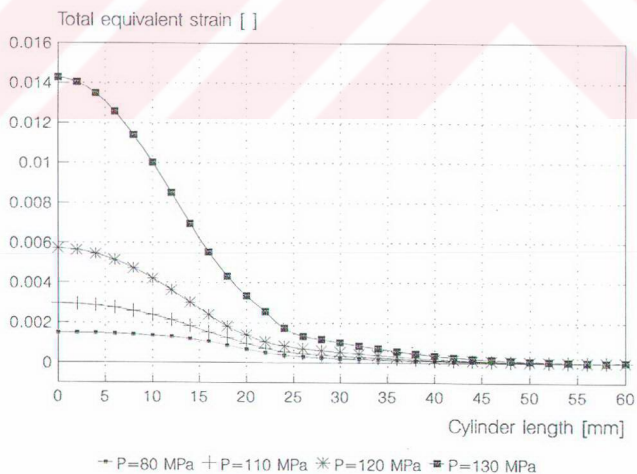

Figure 7.76. Variations of the total equivalent strain through the length of the circular cylinder with a hole (a=10mm) under different band pressure along the inner surface
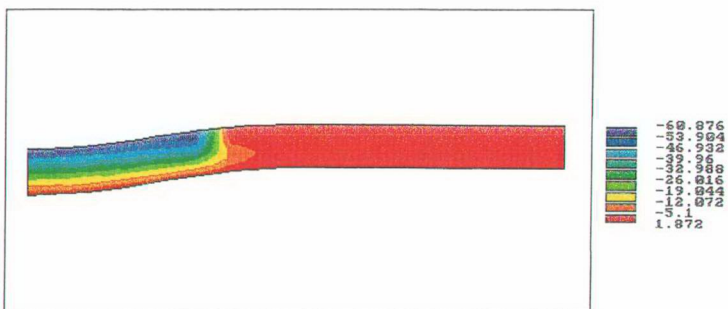
Figure 7.77. Radial stress contour on the longitudinal section of the circular cylinder with a hole (a=15mm) subjected to band pressure P=60 MPa
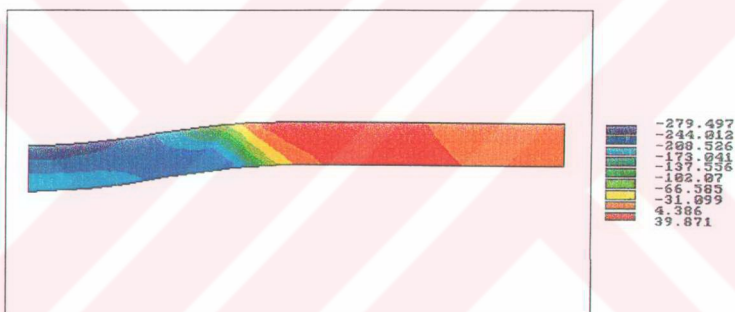
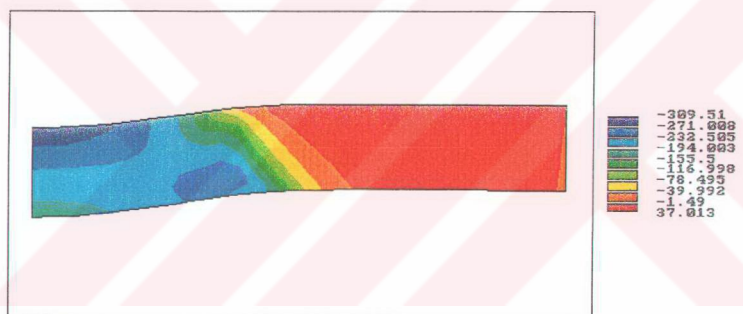
Figure 7.78. Tangential stress contour on the longitudinal section of the circular cylinder with a hole (a=15mm) subjected to band pressure P=60 MPa
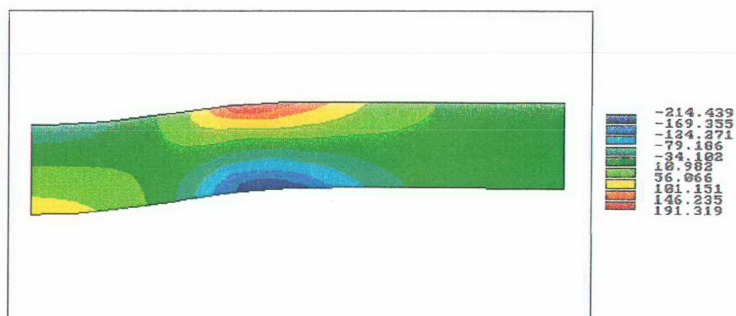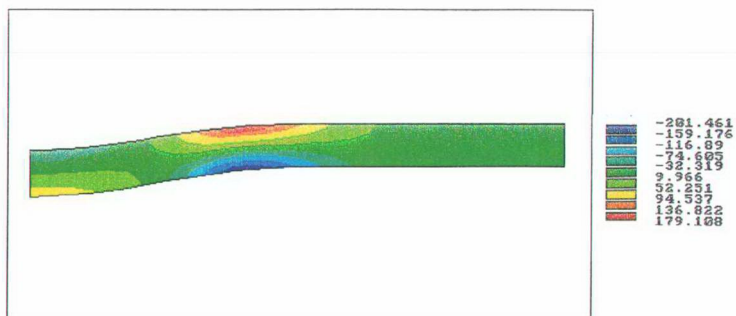

Figure 7.79. Axial stress contour on the longitudinal section of the circular cylinder with a hole (a=15mm) subjected to band pressure P=60 MPa
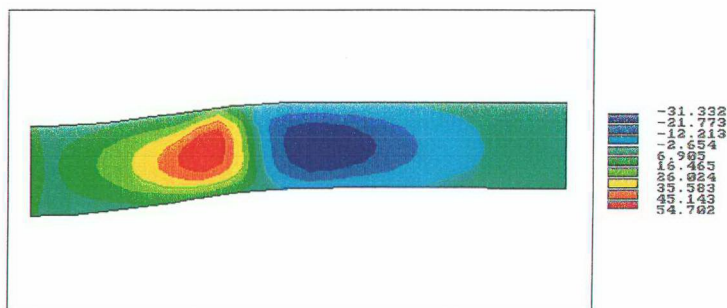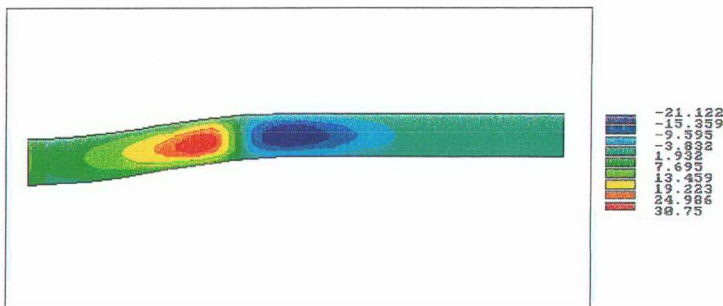
Figure 7.80. Shear stress contour on the longitudinal section of the circular cylinder with a hole (a=15mm) subjected to band pressure P=60 MPa
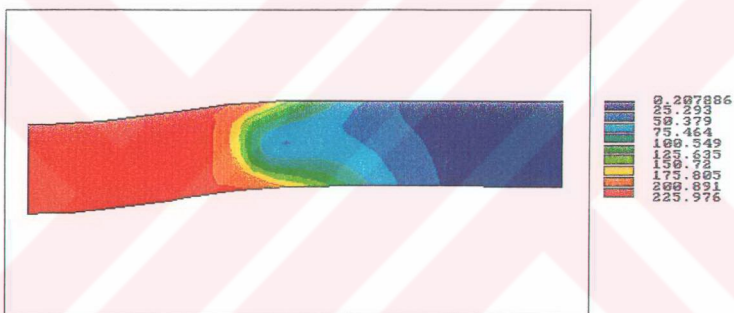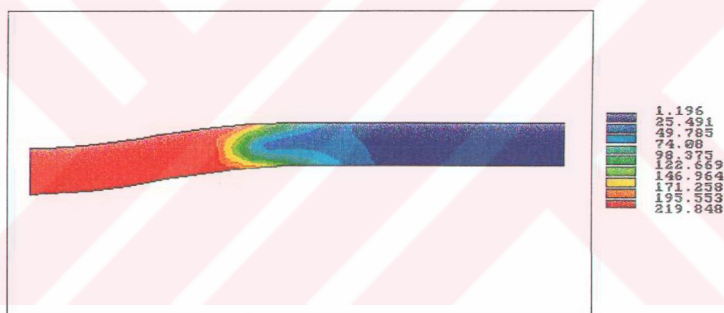

Figure 7.81. Equivalent stress contour on the longitudinal section of the circular cylinder with a hole (a=15mm) subjected to band pressure P=60 MPa
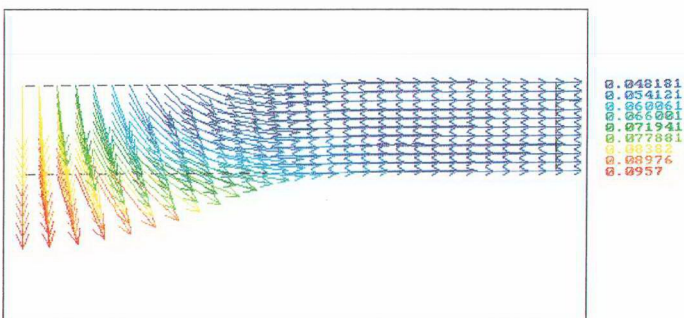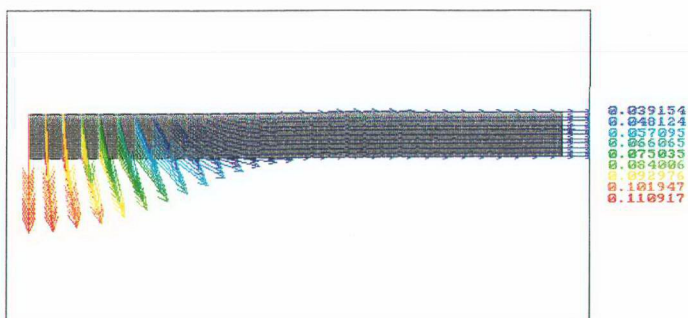

Figure 7.82. Vector plot of displacement on the longitudinal section of the circular cylinder with a hole (a=15mm) subjected to band pressure P=60 MPa
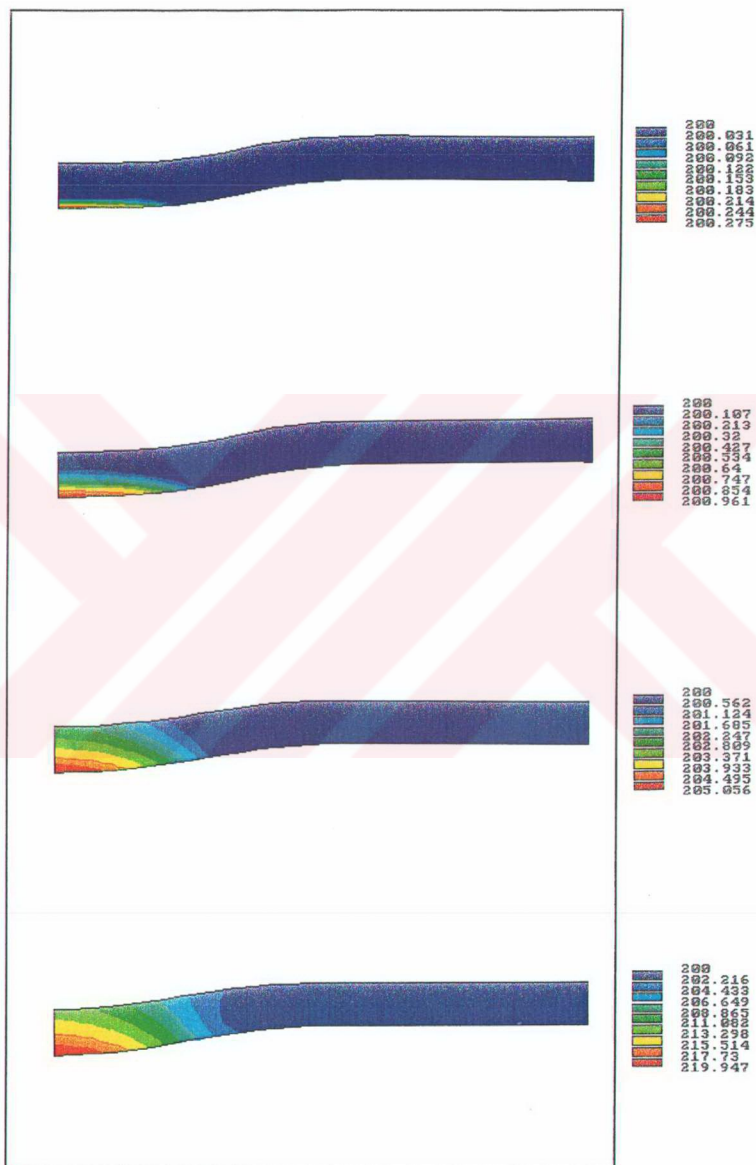
Figure 7.83. Elasto-plastic equivalent stress contour on the longitudinal section of the circular cylinder with a hole (a=15mm) subjected to band pressure respectively, P=45 MPa, P=50 MPa, P=55 MPa, P=60 MPa
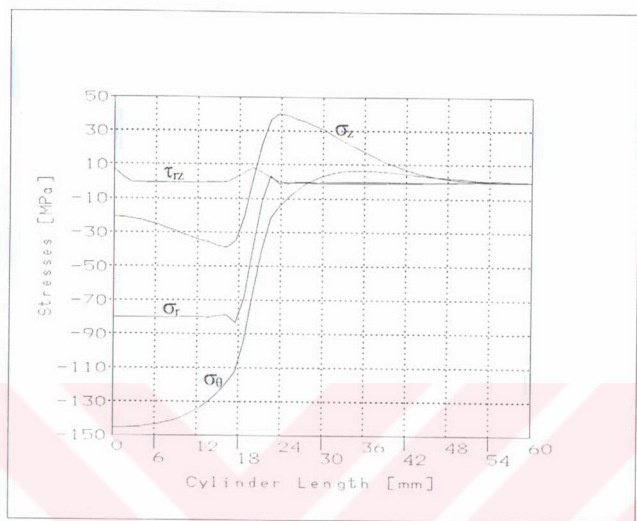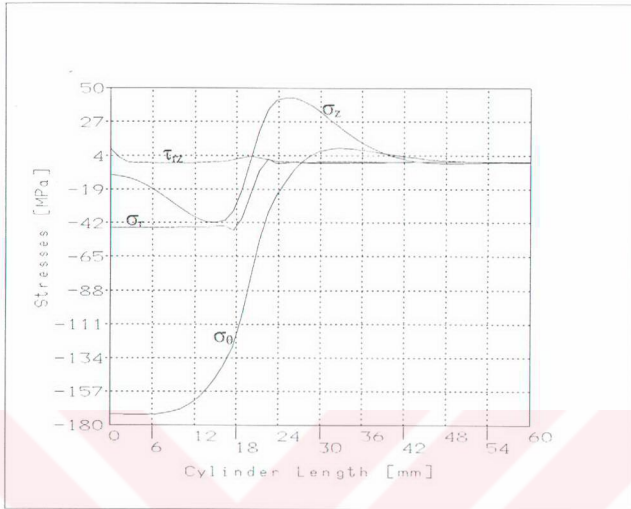
Figure 7.84. The stress distributions through the length of the circular cylinder with a hole (a=15mm) under band pressure P=45 MPa at a=0.75b along the outer surface

Figure 7.85. The stress distributions through the length of the circular ylinder with a hole (a=15mm) under band pressure P=45 MPa at a=0.75b along the inner surface
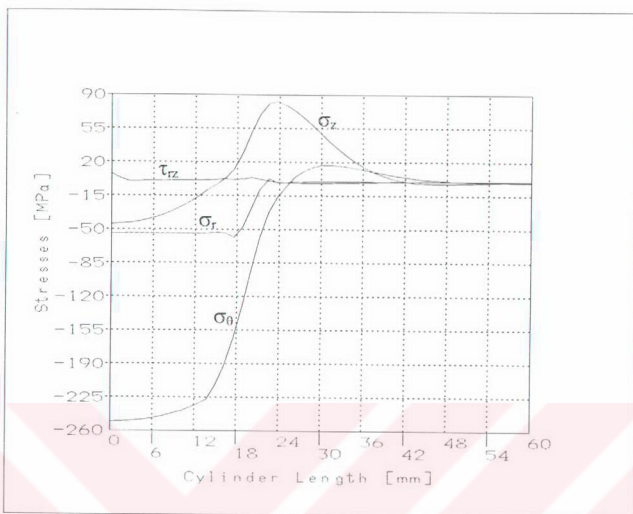
Figure 7.86. The stress distributions through the length of the circular cylinder with a hole (a=15mm) under band pressure P=55 MPa at a=0.75b along the outer surface
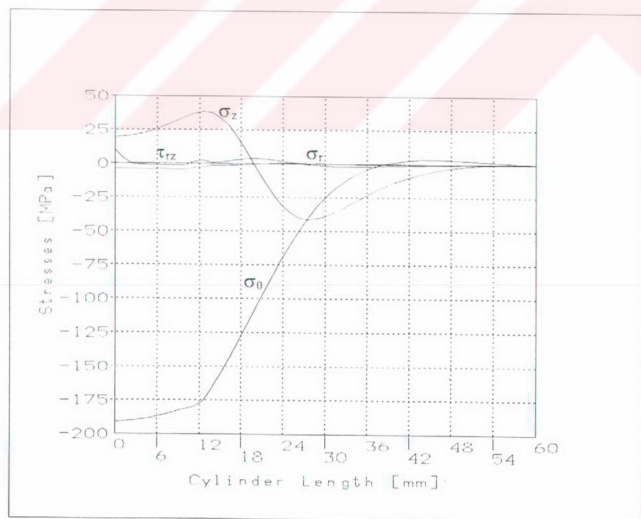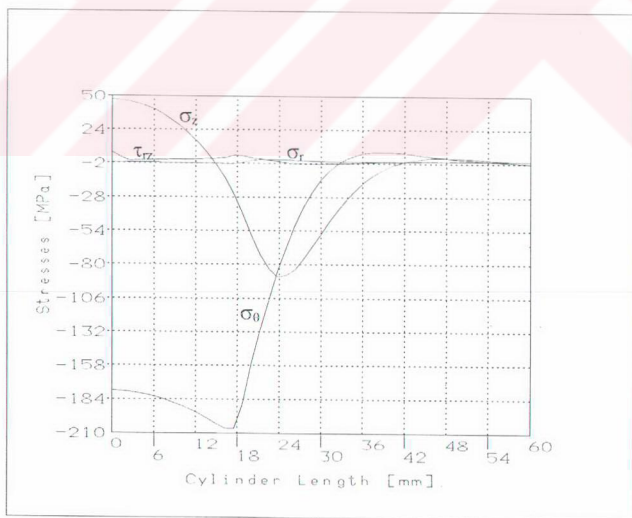

Figure 7.87. The stress distributions through the length of the circular cylinder with a hole (a=15mm) under band pressure P=55 MPa at a=0.75b along the inner surface
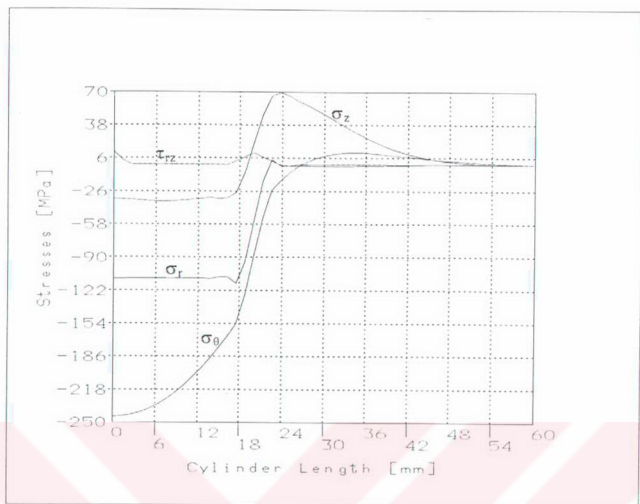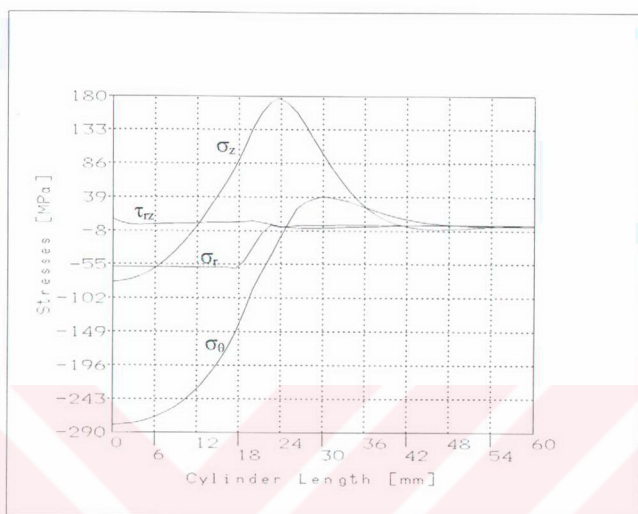
Figure 7.88. The stress distributions through the length of the circular cylinder with a hole (a=15mm) under band pressure P=60 MPa at a=0.75b along the outer surface
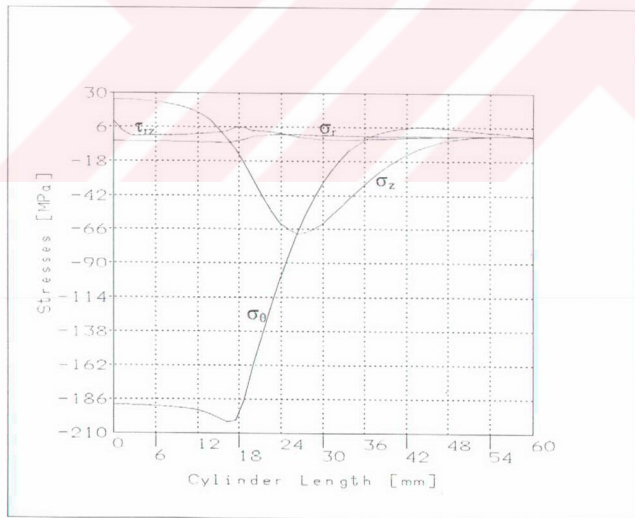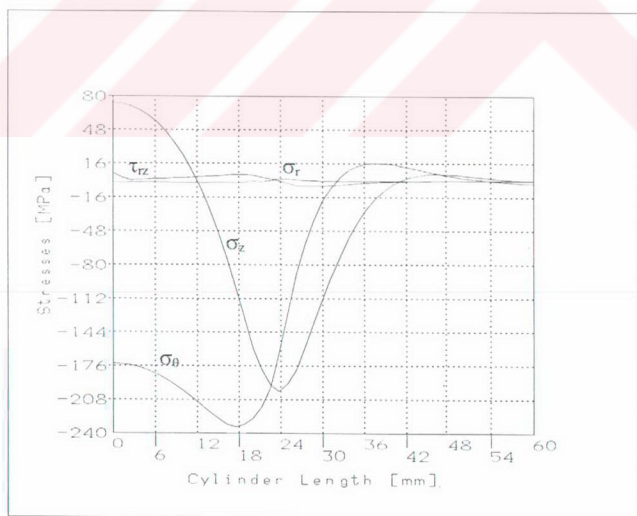

Figure 7.89. The stress distributions through the length of the circular cylinder with a hole (a=15mm) under band pressure P=60 MPa at a=0.75b along the inner surface

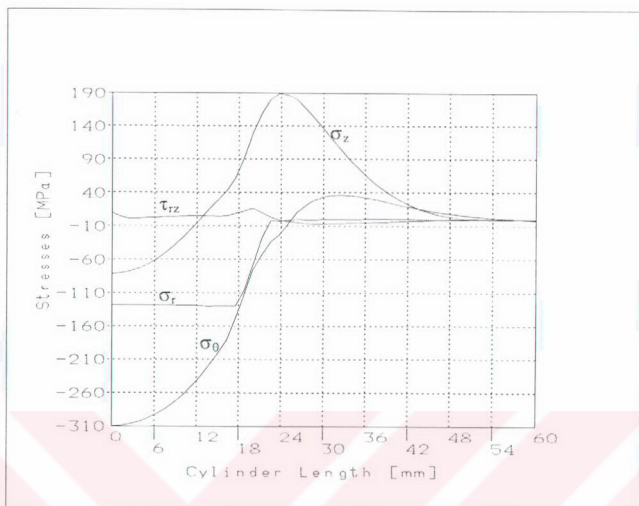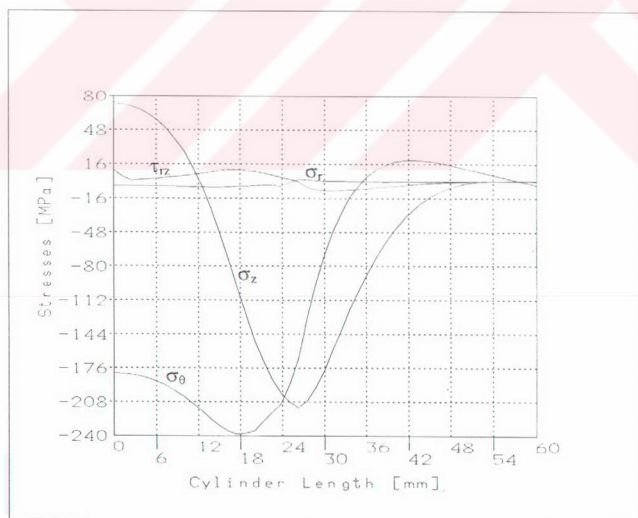**Figure 7.90.** Variations of the elasto-plastic stress through the length of the circular cylinder with a hole (a=15mm) under different band pressure along the inner surface

Figure 7.91. Variations of the equivalent stress through the length of the circular cylinder with a hole (a=15mm) under different band pressure along the inner surface

94
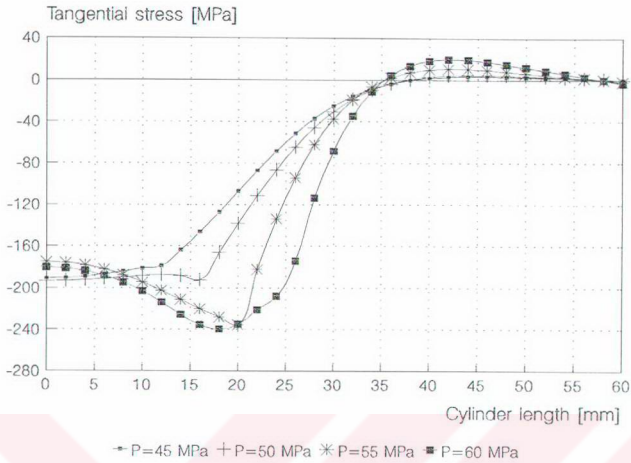
Figure 7.92. Variations of the tangential stress through the length of the circular cylinder with a hole (a=15mm) under different band pressure along the inner surface
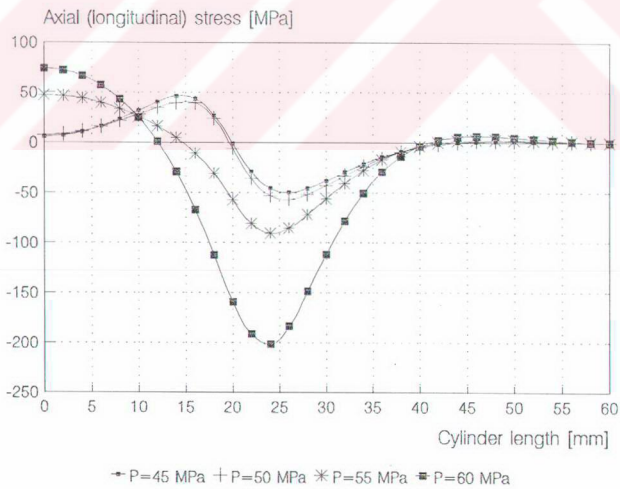
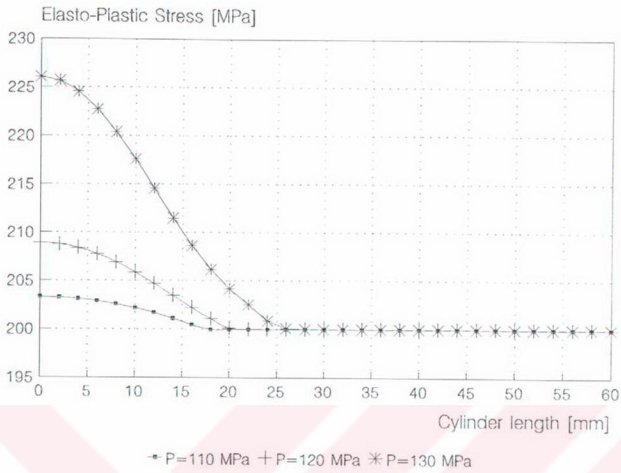Figure 7.93. Variations of the axial stress through the length of the circular cylinder with a hole (a=15mm) under different band pressure along the inner surface
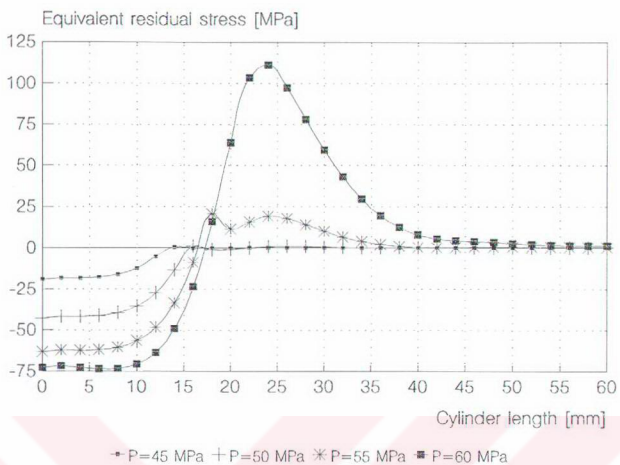
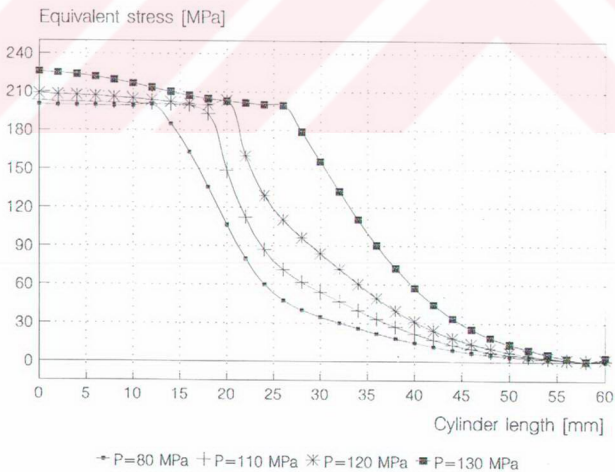**Figure 7.94.** Variations of the equivalent residual stress through the length of the circular cylinder with a hole (a=15mm) under different band pressure along the inner surface
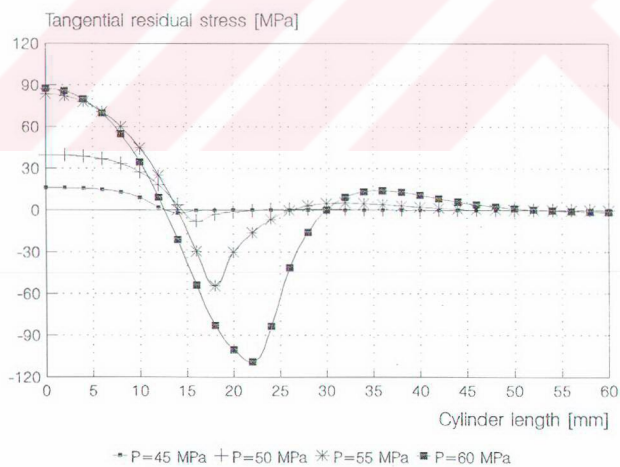
Figure 7.95. Variations of the tangential residual stress through the length of the circular cylinder with a hole (a=15mm) under different band pressure along the inner surface

96
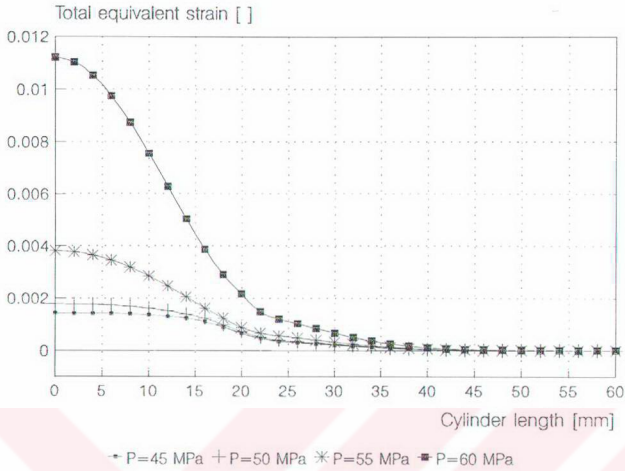
Figure 7.96. Variations of the total equivalent strain through the length of the circular cylinder with a hole (a=15mm) under different band pressure along the inner surface
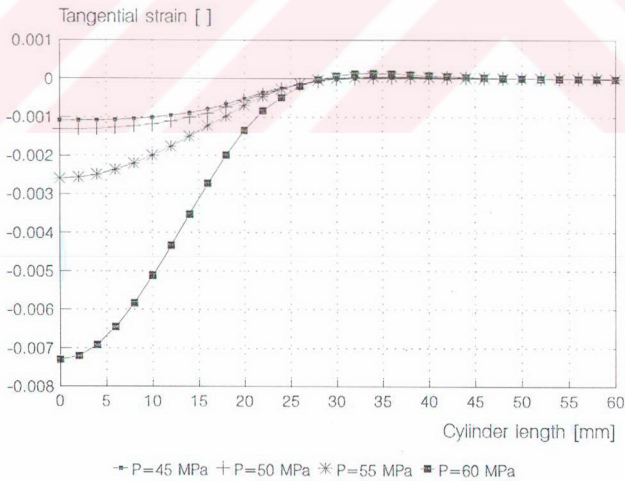
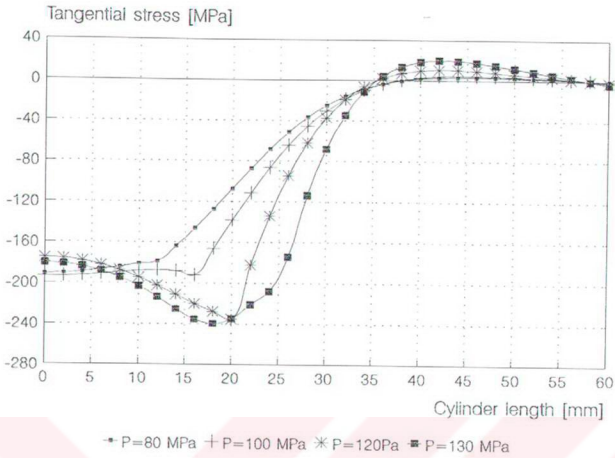**Figure 7.97.** Variations total tangential strain of the through the length of the circular cylinder with a hole (a=15mm) under different band pressure along the inner surface

97
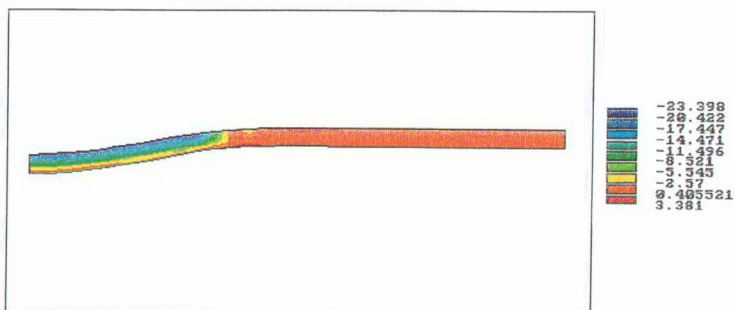
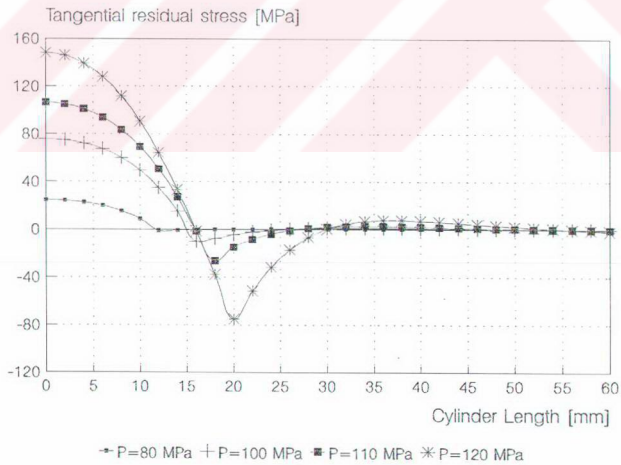Figure 7.98. Radial stress contour on the longitudinal section of the circular
cylinder with a hole (a=18mm) subjected to band pressure P=23 MPa
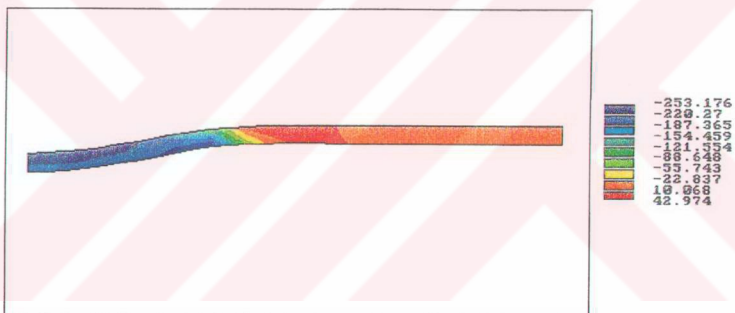
Figure 7.99. Tangential stress contour on the longitudinal section of the circular
cylinder with a hole (a=18mm) subjected to band pressure P=23 MPa
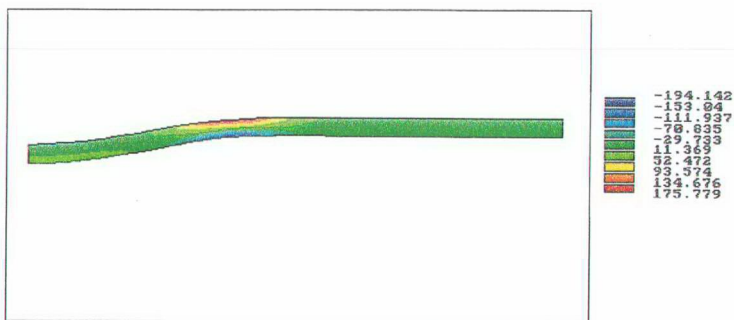
Figure 7.100. Axial stress contour on the longitudinal section of the circular
cylinder with a hole (a=18mm) subjected to band pressure P=23 MPa
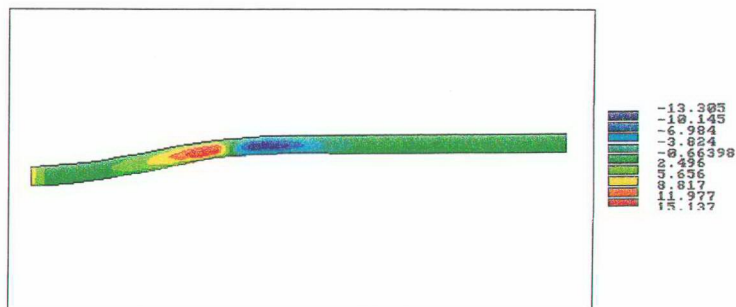
Figure 7.101. Shear stress contour on the longitudinal section of the circular cylinder with a hole (a=18mm) subjected to band pressure P=23 MPa

Figure 7.102. Equivalent stress contour on the longitudinal section of the circular cylinder with a hole (a=18mm) subjected to band pressure P=23 MPa
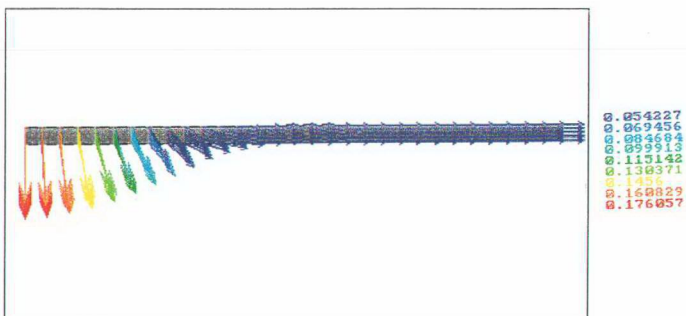
Figure 7.103. Vector plot of displacement on the longitudinal section of the circular cylinder with a hole (a=18mm) subjected to band pressure P=23 MPa
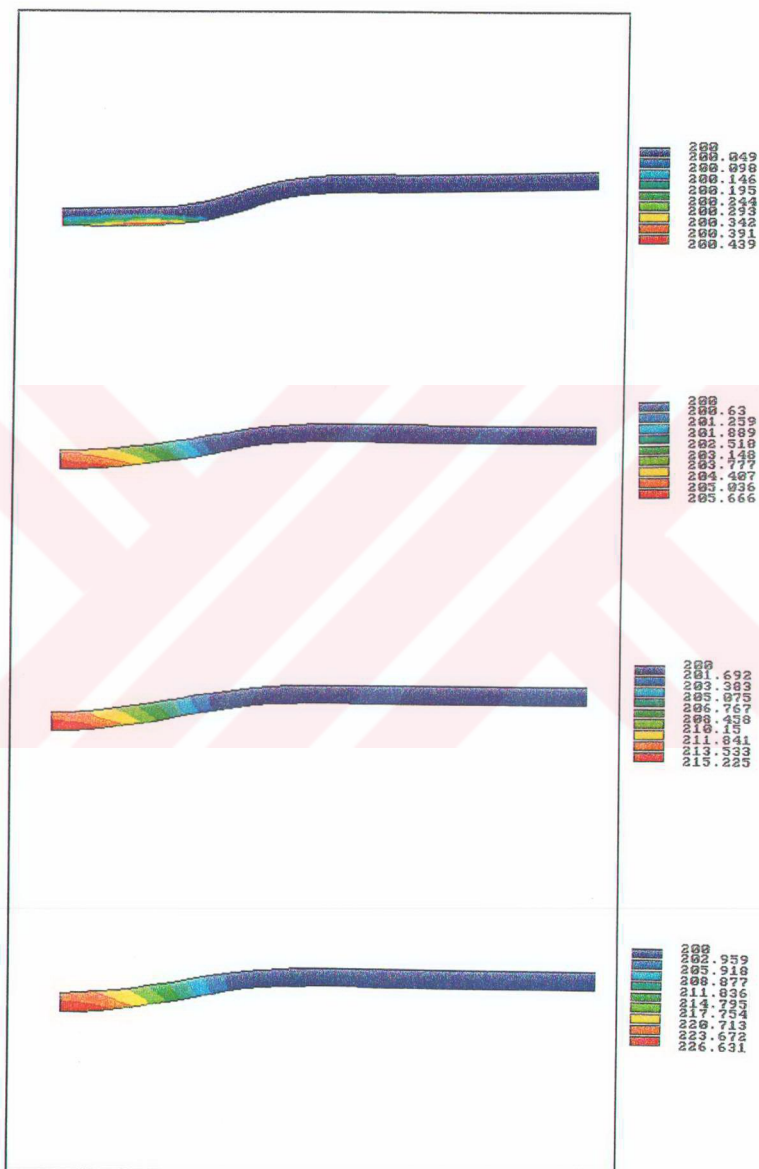
Figure 7.104. Elasto-plastic equivalent stress contour on the longitudinal section of the circular cylinder with a hole (a=18mm) subjected to band pressure respectively, P=20 MPa, P=21 MPa, P=22 MPa, P=23 MPa
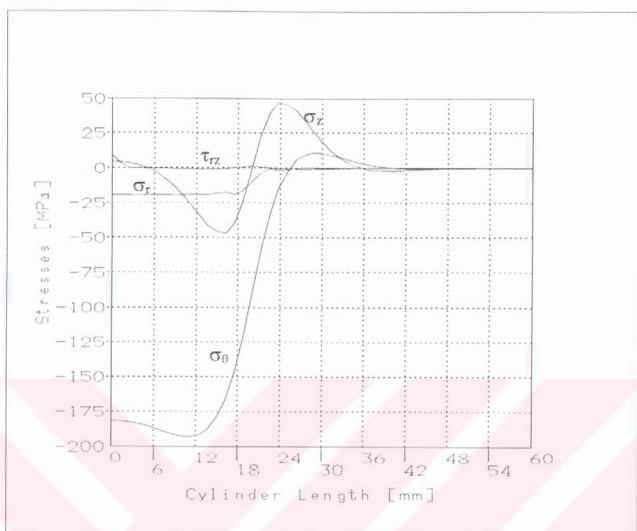
Figure 7.105. The stress distributions through the length of the circular cylinder with a hole (a=18mm) under band pressure P=19 MPa at a=0.9b along the outer surface
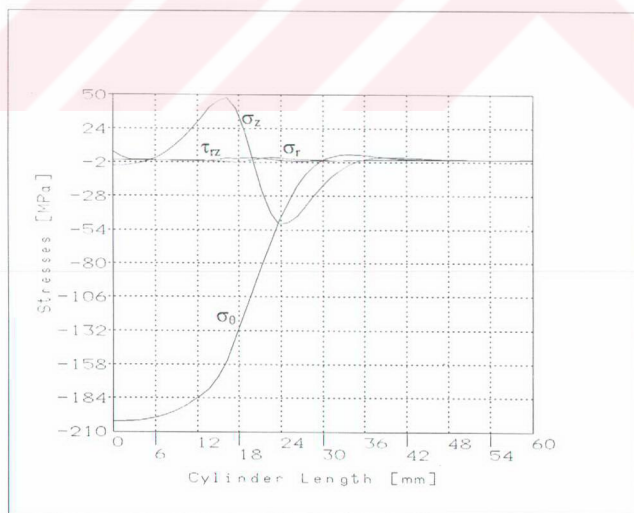

Figure 7.106. The stress distributions through the length of the circular cylinder with a hole (a=18mm) under band pressure P=19 MPa at a=0.9b along the inner surface

101
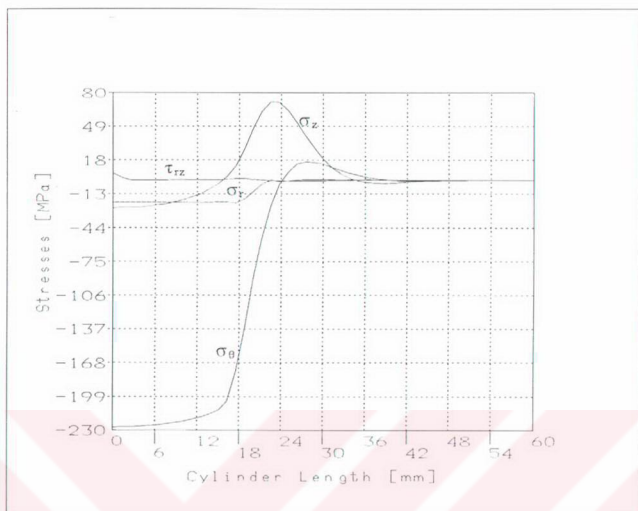
Figure 7.107. The stress distributions through the length of the circular cylinder with a hole (a=18mm) under band pressure P=21 MPa at a=0.9b along the outer surface
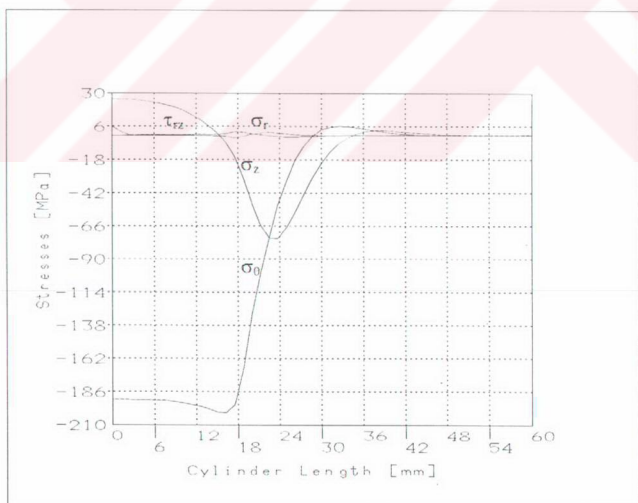
Figure 7.108. The stress distributions through the length of the circular cylinder with a hole (a=18mm) under band pressure P=21 MPa at a=0.9b along the inner surface
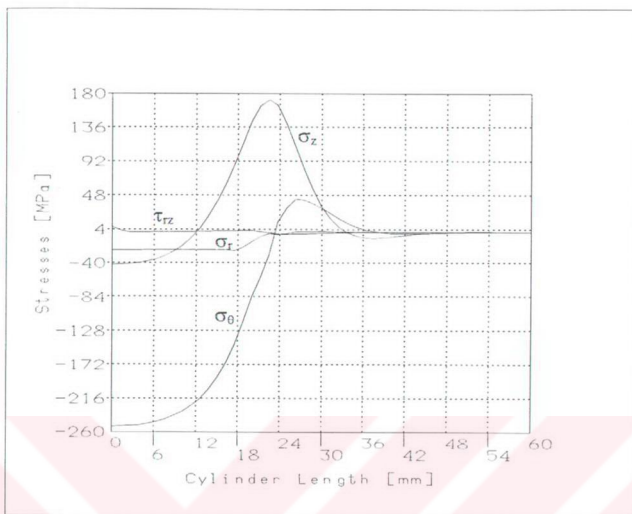
Figure 7.109. The stress distributions through the length of the circular cylinder with a hole (a=18mm) under band pressure P=23 MPa at a=0.9b along the outer surface
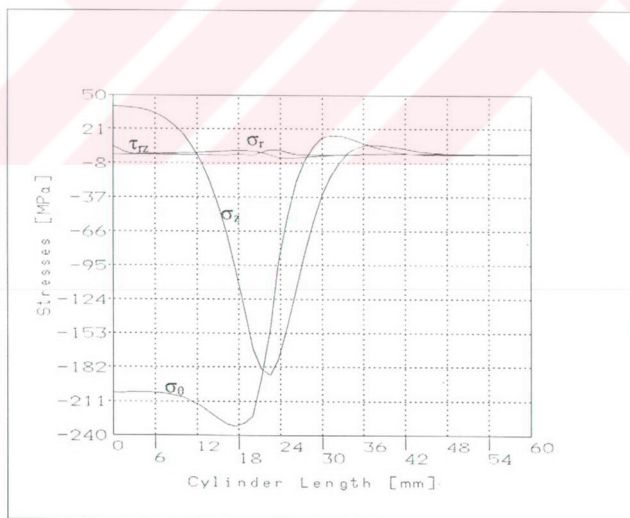
Figure 7.110. The stress distributions through the length of the circular cylinder with a hole (a=18mm) under band pressure P=23 MPa at a=0.9b along the inner surface

103
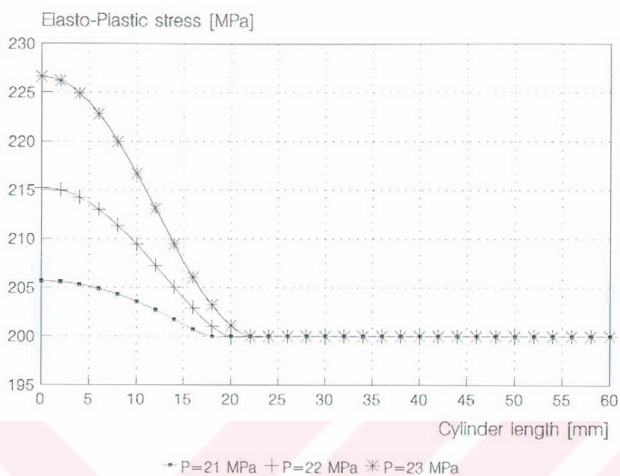
Figure 7.111. Variations of the elasto-plastic stress through the length of the cylinder with a hole (a=18mm) under different band pressure along the inner surface
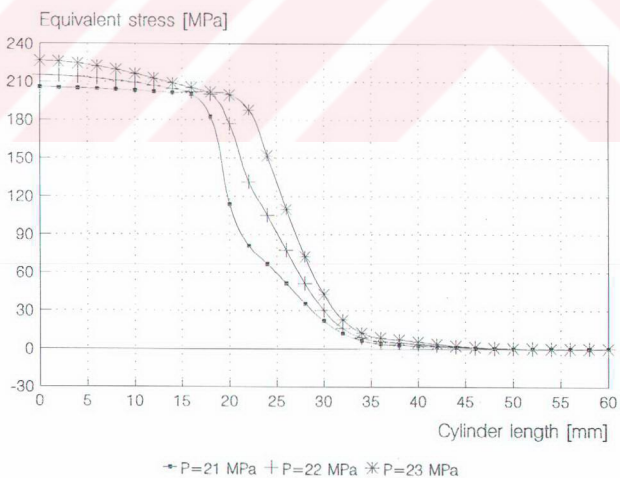
Figure 7.112. Variations of the equivalent stress through the length of the cylinder with a hole (a=18mm) under different band pressure along the inner surface
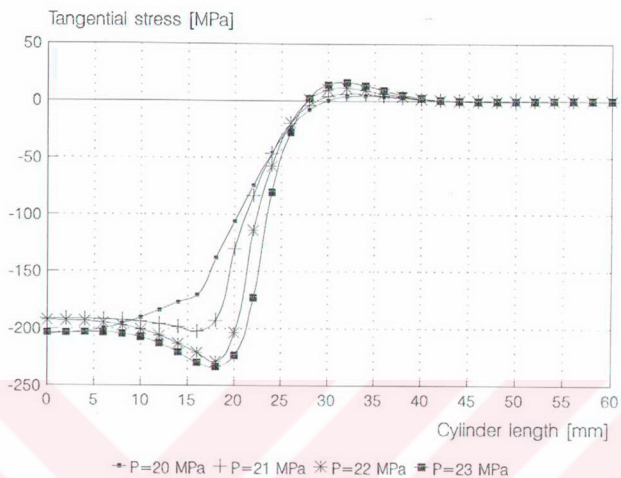
Figure 7.113. Variations of the tangential stress through the length of the cylinder with a hole (a=18mm) under different band pressure along the inner surface
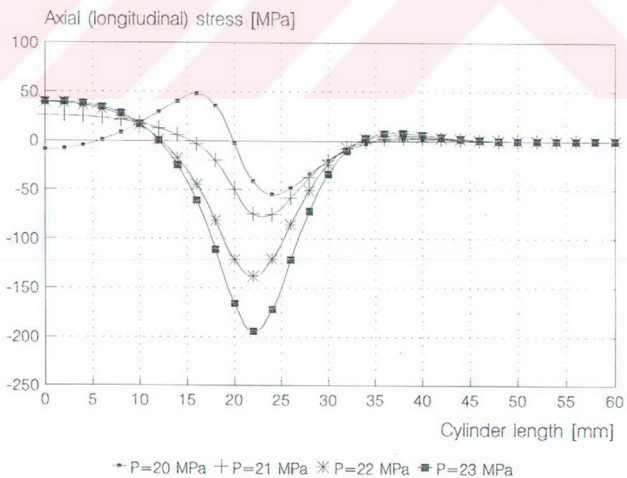
Figure 7.114. Variations of the axial stress through the length of the cylinder with a hole (a=18mm) under different band pressure along the inner surface

Equivalent residual stress [MPa]

→ P=21 MPa + P=22 MPa ✳ P=23 MPa
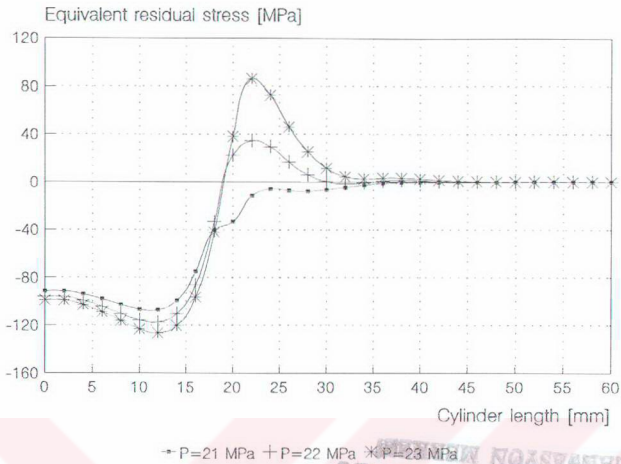
Figure 7.115. Variations of the equivalent residual stress through the length of the cylinder with a hole (a=18mm) under different band pressure along the inner surface

Tangential residual stress [MPa]

→ P=21 MPa + P=22 MPa ✳ P=23 MPa
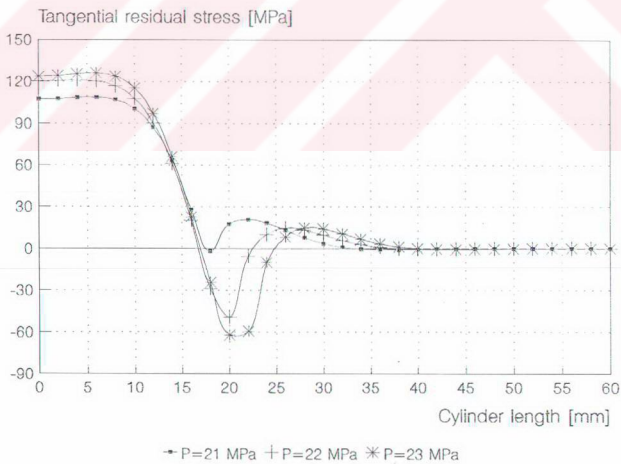
Figure 7.116. Variations of the tangential residual stress through the length of the cylinder with a hole (a=18mm) under different band pressure along the inner surface

106
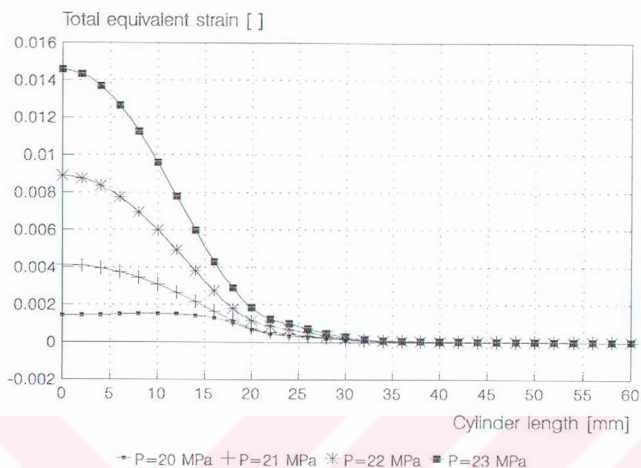
Figure 7.117. Variations of the total equivalent strains through the length of the cylinder with a hole (a=18mm) under different band pressure along inner surface
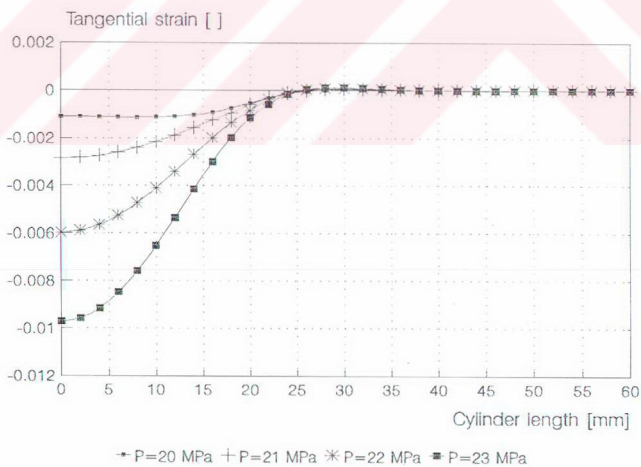
Figure 7.118. Variations of the tangential strains through the length of the cylinder with a hole (a=18mm) under different band pressure along the inner surface

In the circular cylinder with a hole, we have investigated all region and especially critical local region (surface of cylinder and center of cylinder). Therefore, distributions of the stress components are plotted inner and outer surface of the circular cylinder for different band pressure in figures. The stress components (tangential stress σ_θ, radial stress σ_r, axial stress σ_z and shear stress τ_{rz}) distributions through the length of the circular with a hole cylinder under band pressure along outer surface and inner surface of cylinder are shown on the same graph in figures. Variations of the elasto-plastic stress over the yielding stress through the length of the circular cylinder with a hole subjected to different band pressure along outer and inner surface of the cylinder are plotted in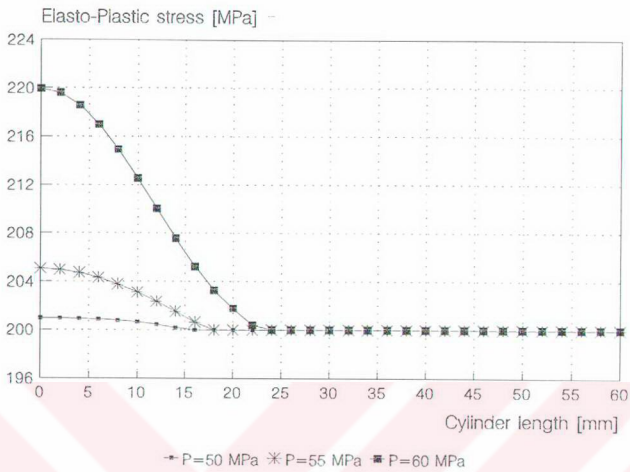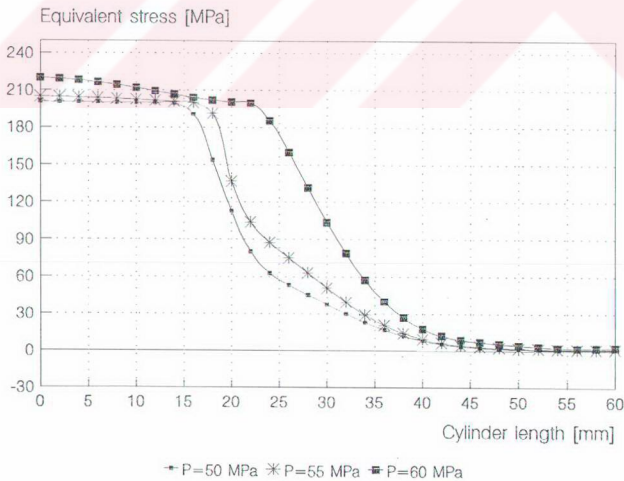 figures. Variations of the equivalent stress through the length of the circular cylinder with a hole under different band pressure along outer and inner surface of the cylinder are shown in figures. Variations of the tangential and axial stress through the length of the circular cylinder with a hole under different band pressure along outer and inner surface of the cylinder are shown in figures.

Variations of the total equivalent and tangential strain through the length of the circular solid cylinder under different band pressure along outer and inner surface of the cylinder are plotted in figures.

Variations of the tangential and equivalent residual stress through the length of the circular cylinder with a hole under different band pressure along outer and inner surface of the cylinder are shown in figures.

7.4. BAND PRESSURE TO START YIELDING IN THE CIRCULAR CYLINDER SOLID AND WITH A HOLE

In solid cylinder, yielding begins at the symmetry axis for band pressure P=176 MPa. In the hallow section cylinders, yielding begin on the inner surface for different band pressure which are given in the table 7.4. For different ratios a/b where a is inner diameter and b is outer diameter are investigated band pressure magnitude to begin yielding. Considered outer diameter b=20mm, and inner diameter are a=0=solid, a=1mm, a=2mm, a=5mm, a=10mm, a=15mm a=18mm.

Table 7.6 Band pressure that to begin yielding for different diameter ratio inner diameter to outer diameter

a/b	solid 0	0.025	0.1	0.25	0.5	0.75	0.9
Band Pressure MPa	176	155	119	100	76	45	19.25

Variation of the band pressure to start yielding in the circular cylinder with a hole for different ratios inner diameter to outer diameter in figure 7.119.
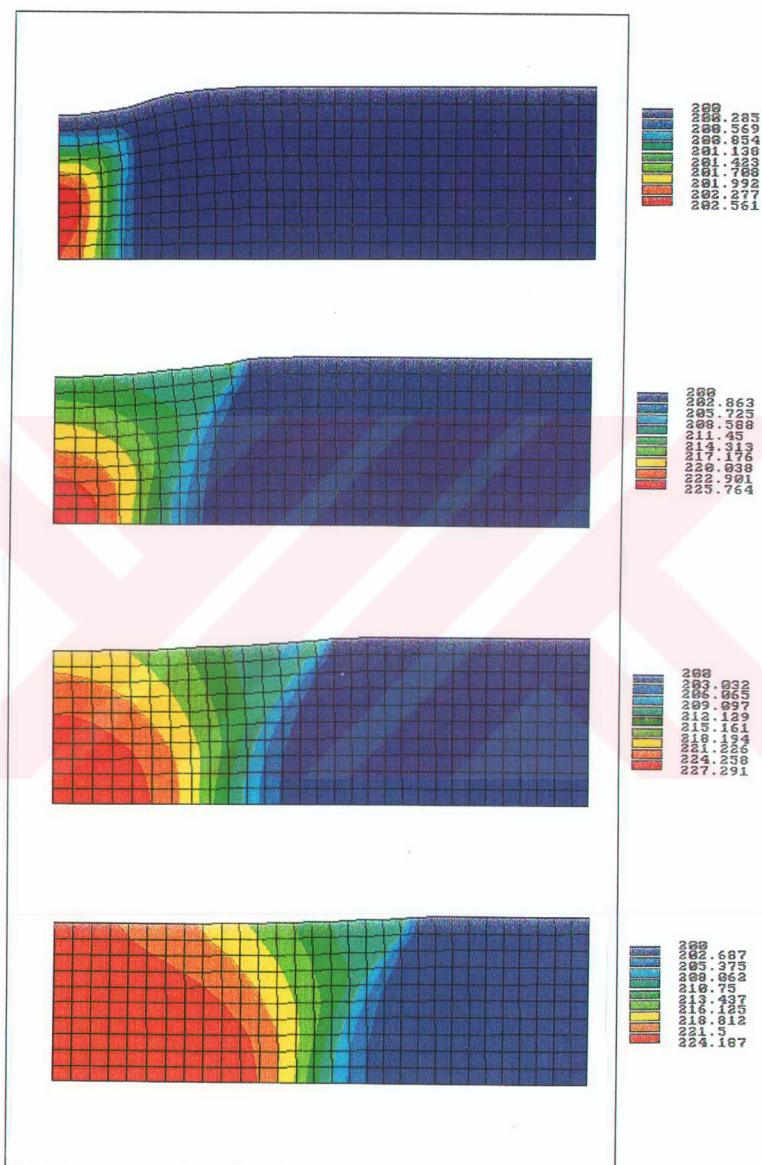
Figure 7.120. Elasto-plastic equivalent stress contour on the longitudinal section of the circular solid cylinder subjected to band pressure P=220 MPa for different band width, respectively C=10 mm, C=20 mm, C=30 mm, C=40 mm
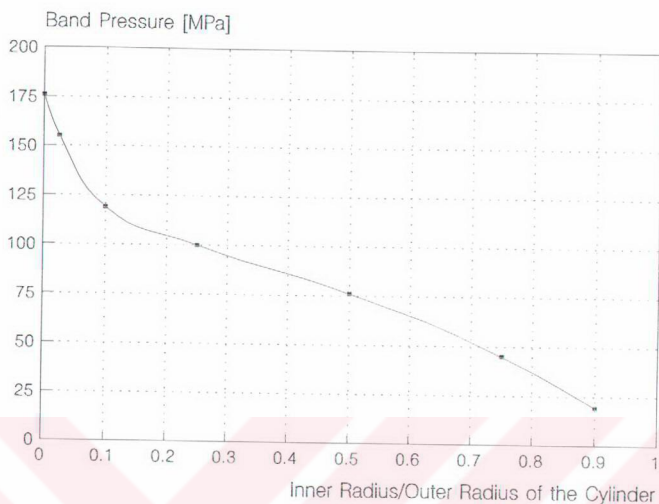
Figure 7.119. Variation of the band pressure to start yielding in the circular cylinder with a hole for different ratios inner diameter to outer diameter

7.5 ELASTO-PLASTIC ANALYSIS IN THE CIRCULAR SOLID AND HALLOW CYLINDER SUBJECTED TO DIFFERENT WIDTH BAND PRESSURE

In the circular solid and hallow cylinder, stress components are investigated for different band width.

In the solid cylinder, variations of the elasto-plastic stress distribution and stress components are investigated under band pressure P=220 MPa for different band width that are c=10mm, c=20mm, c=30mm and c=40mm. Variations of the elasto-plastic stress distributions are shown as contour legend with different color on longitudinal section of the circular solid cylinder in figure 7.120. Distributions of the stress components (elasto-plastic, equivalent, tangential and axial) are plotted in the symmetry axis of the cylinder in figure 7.121-7.124.

In the hallow cylinder that is dimensions a=10mm and b=20mm, variations of the elasto-plastic stress distribution and stress components are investigated under band pressure P=130 MPa for different band width that are c=10mm, c=20mm, c=30mm and c=40mm. Variations of the elasto-plastic stress distributions are shown as contour legend with different color on longitudinal section of the circular hallow cylinder in figure 7.125. Distributions of the stress components (elasto-plastic, equivalent, tangential and axial) are plotted in the inner surface axis of the cylinder in figure 7.126-7.129.
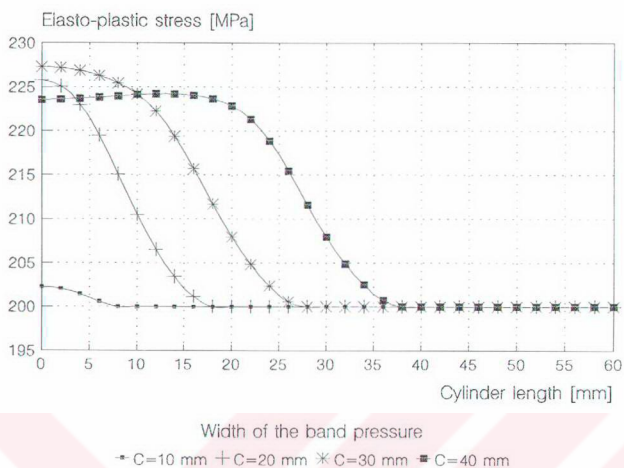
Figure 7.121. Variations of the elasto-plastic stress trough the length of the circular solid cylinder under band pressure P=220 MPa for different band width along symmetry axis of the cylinder
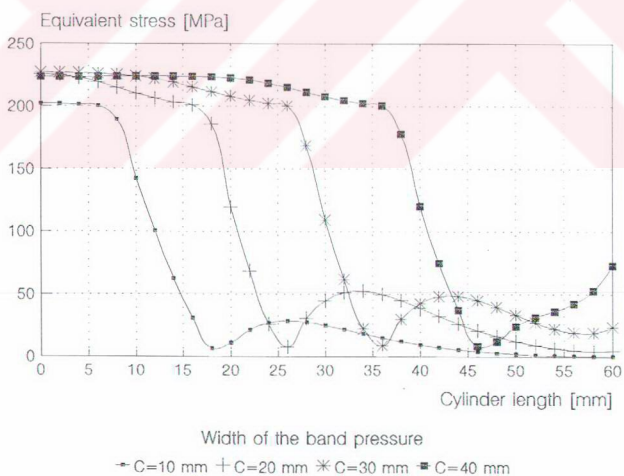
Figure 7.122. Variations of the equivalent stress through the length of the circular solid cylinder under band pressure P=220 MPa for different band width along symmetry axis of the cylinder
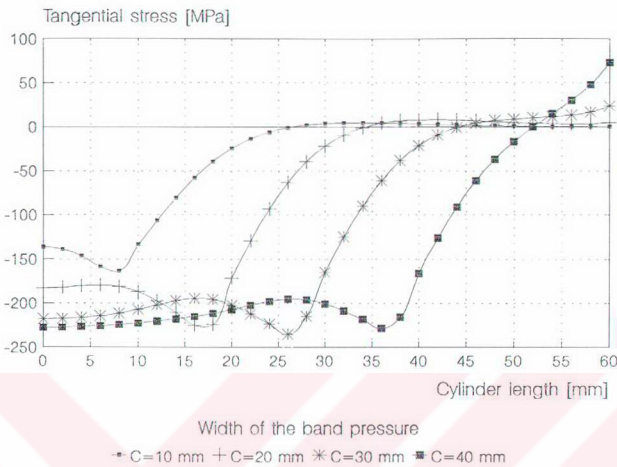
Figure 7.123. Variations of the tangential stress through the length of the circular solid cylinder under band pressure P=220 MPa for different band width along symmetry axis of the cylinder
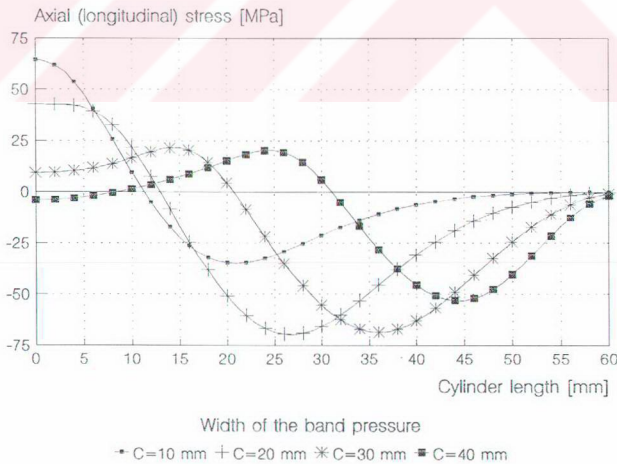
Figure 7.124. Variations of the axial stress through the length of the circular solid cylinder under band pressure P=220 MPa for different band width along symmetry axis of the cylinder

Figure 7.125. Elasto-plastic equivalent stress contour on the longitudinal section of
the circular cylinder with a hole (a=10 mm) subjected to band pressure P=130 Pa
for different band width, respectively C=10 mm, C=20 mm, C=30 mm, C=40 mm
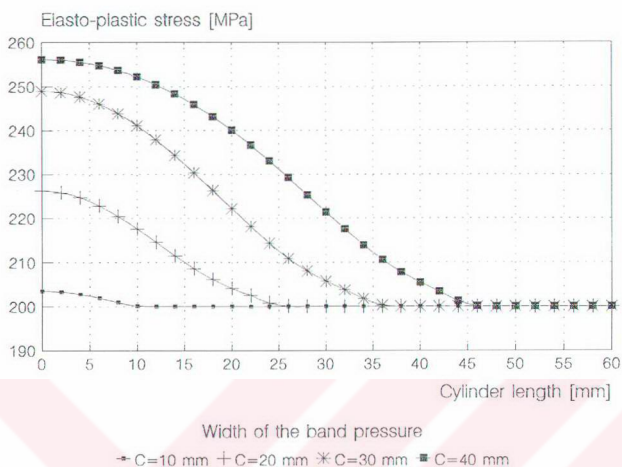
Figure 7.126. Variations of the elasto-plastic stress trough the length of the circular cylinder with a hole (a=10 mm) under band pressure P=220 MPa for different band width along inner surface of the cylinder
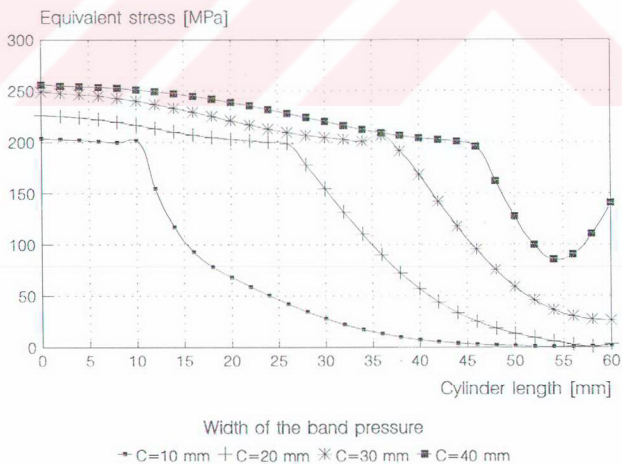
Figure 7.127. Variations of the equivalent stress trough the length of the circular cylinder with a hole (a=10 mm) under band pressure P=220 MPa for different band width along inner surface of the cylinder
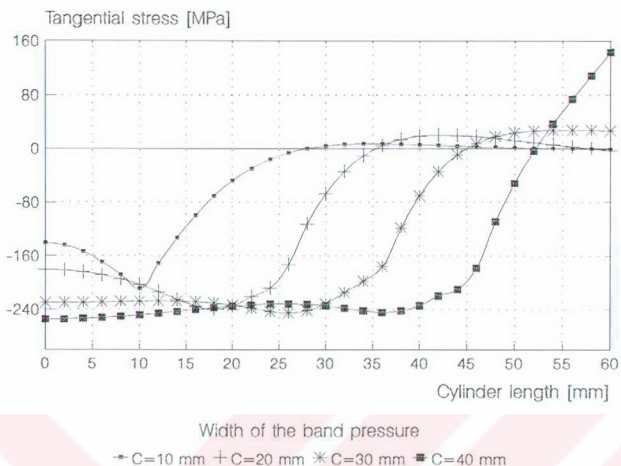
Figure 7.128. Variations of the tangential stress trough the length of the circular cylinder with a hole (a=10 mm) under band pressure P=220 MPa for different band width along inner surface of the cylinder
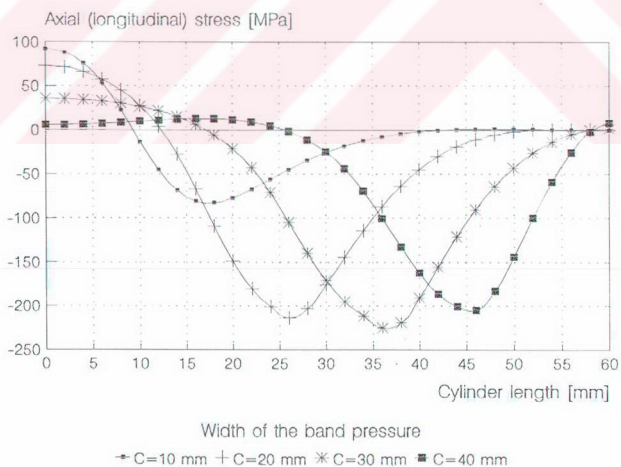
Figure 7.129. Variations of the axial stress trough the length of the circular cylinder with a hole (a=10 mm) under band pressure P=220 MPa for different band width along inner surface of the cylinder

115

CHAPTER EIGHTH

RESULTS AND CONCLUSIONS

In this study, elasto-plastic analysis is made in the circular solid and hallow cylinder under band pressure for isotropic material. Band pressure acts as uniform loading. External band pressure is loaded on the surface of the circular cylinder in the radial direction.

In the solution, finite element method was used It is assumed that deformations are small $\varepsilon_t \cong 0.02$. Circular cylinder with a band of pressure has symmetry with respect to loading, boundary condition, geometry and material properties. Because of the symmetry only quarter of the circular cylinder was analysed. Finite element model of the quarter of the solid and hallow cylinder consist of 300 elements and 341 node. An isoparametric rectangular ring shape element having four nodes is used. The automatic mesh generation is used. General purpose computer program that is mention ANSYS is used to solve the problem.

To control whether the computer program gives true results, tangential and radial stresses are obtained from the literature in the circular cylinder has hallow cross section under external pressure. Then, these stresses are compared with the exact solution.

Two form circular cylinder that are solid and hallow cross section are investigated. Equivalent stress is calculated by means of von Mises criterion. If the equivalent stress is greater than yielding point of material, yielding begins. Values of the band pressure initiating plastic deformation are determined for different diameters by von Mises criterion. Obtained results show that value of the band pressure is decreasing when inner radius of the cylinder is increasing. Yielding begins in the inner surface or symmetry axis of the cylinder then expansion grows from the inner surface to outer surface around the band pressure.

The stress that remains in a circular cylinder upon removal of external load is called residual stress. The magnitude of residual stresses can be obtained by superposition of the stresses due to loading and unloading. The unloading or reverse stress pattern is assumed to be fully elastic and hence can be obtained using Hook's law. The residual stresses are obtained for different diameter of the circular cylinder. Distributions of the residual stress components are plotted in figures for different band pressure along the inner surface of the circular solid and hallow cylinder.

Obtained Results in the Circular Solid Cylinder:

We have investigated all region of the problem and especially critical local region (surface and center of cylinder). Therefore, distributions of the stresses components are plotted center and outer surfaces of the circular cylinder.

Yielding begins in the symmetry axis in the circular solid cylinder and expansions grows from the symmetry axis to outer surface. Maximum equivalent stress (σ_{eq}) that is obtained from von Mises criterion occurs in the symmetry axis of the cylinder. Tangential (σ_θ) and radial (σ_r) stress distributions are same each other in the symmetry axis. Shear stress (τ_{rz}) distribution is around zero in the symmetry axis. Therefore, it may be neglect. Axial or longitudinal (σ_z) stress distribution is not important other stress component.

The greatest stress component is tangential and stress and occurs as compression on outer surface of cylinder. Radial stress component is equal to band pressure in the outer surface as compression. Shear stress distribution is approximately zero on outer surface. Therefore, it may be neglect.

Maximum equivalent strain and maximum tangential strain occurs in the symmetry axis of the solid cylinder.

The residual stress are obtained for different band pressure in the symmetry axis through the length of the cylinder. First, elasto-plastic stress components are calculated then, elastic stress components are calculated by finite element method at each node and then residual stresses obtained by means of elastic solving are subtract from the elasto-plastic solving. The greatest equivalent residual stress occurs around the band pressure on the surface of the cylinder.

Obtained Results in the Hallow Section Cylinder:

Yielding begins in the inner surface of the circular cylinder with a hole and expansions grow from the inner surface to outer surface applied pressure increases. Maximum equivalent stress (σ_{eq}) occurs on the inner surface of the cylinder. Tangential (σ_θ) stress distributions is the maximum on the inner surface and outer surface. Radial stress is equal to band pressure on the outer surface of the cylinder. In contrast, radial stress distribution is, around zero on the inner surface of the cylinder. Shear stress (τ_{rz}) distribution is around zero on the inner wall of the cylinder with a hole. Axial or longitudinal stress (σ_z) distribution is not important compared with the other stress component.

The greatest stress component is tangential stress on inner surface and around end of the band pressure of the hallow cylinder as compression. Radial stress component is equal to

band pressure on the outer surface as compression. Shear stress distribution is around zero on outer surface. Therefore, it may be neglect.

Maximum equivalent and tangential strain occur on the inner surface of the hallow cylinder.

The greatest equivalent residual stress occurs around the band pressure on the inner surface of the cylinder.

After yielding point, as band pressure is increased, elasto-plastic region is getting growing up.

Variation of the band pressure to start yielding in the circular cylinder that are solid or with a hole for different ratios inner diameter to outer diameter is shown in figure. When diameter of the hole is increasing band pressure to start yielding is decreases. Therefore, if it is not need a hole for design purpose, circular hallow cylinder should not be used under band pressures.

In the circular solid and hallow cylinder, stress components are investigated for different band width. Variations of the elasto-plastic stress distribution and stress components are investigated under constant band pressure for different band width. Variations of the elasto-plastic stress distributions are shown as contour legend with different colour on longitudinal section of the circular solid and hallow cylinder in figures. Distributions of the stress components (elasto-plastic, equivalent, tangential and axial) are plotted in the symmetry axis and inner surface of the cylinder in figures.

It can be done elasto-plastic analysis of composite circular solid and hallow cylinder for different diameter and band pressures.

And also It can be investigated large deformation elasto-plastic of isotropic circular solid and hallow cylinder for different diameter and band pressure.

REFERENCES

1. Gamer, U., Lance, R..H., "Residual stress in shrink fit", Int. Journal of Applied Mechanics Sci, Vol.25, pp.465, 1983.

2. Gamer, U., "The shrink fit with nonlinearly hardening elastic-plastic hub", Journal of Applied Mechanics, Vol.54, pp.474, 1987.

3. Gallegher, R.H., Padlog, J. Bijlard, P.B., "Stress analysis of heated complex shape", J. Am. Rocket Soc., Vol.32, pp.700-707, 1962.

4. Argyris, J.H., "Elasto-plastic matrix displacement analysis of three dimensional continua", Jl. R. Aeronaut. Soc., Vol.69, pp.663, 1962.

5. Pope, G.G., "A discrete element method for analysis of plane elasto-plastic strain problems", R.A.F. Farnborough, T.R.65028, 1965.

6. Swedlow, M.L., Williams, M.L., Yang, W.M., "Elasto-plastic stresses in cracked plates", Calcit, Report SM, pp.15, 1965.

7. Marcal, P.V., King, I.P., "Elasto-plastic analysis of two dimensional stress systems by the finite element method", Int. Journal of Applied Mechanics Sci, Vol.9, pp.143-155, 1967.

8. Reyes, S.F., Deere, D.U., "Elasto-plastic analysis of underground openings by the finite element method", Proc. 1st. Int. Congr. Rock Mechanics, Vol.11, pp.447-486, Lizbon, 1966.

9. Popov, E.P., Khojasteh-Bakth, M., Yaghmai, S., "Bending of circular plates of hardening material", Intern. J. Sol. Struct., Vol.3, pp.975-988, 1968.

10. Ergataoudis, I., Irons, B.M., Zienkiewicz, O.C., "Curved isoparametric quadrilateral elements for finite element analysis", International Journal of Solid Structures, Vol.4, pp.31-42, 1968.

11. Clough, R.W., Abeyaratne, R., "A finite element approximation for the analysis of thin shell", International Journal of Solid Structures, Vol.4, pp.43-60, 1968.

12. Owen, D.R.J. and Salonen, E.M., "Three-dimensional elasto-plastic finite element analysis", International Journal for Numerical Methods in Engineering, Vol.9, pp.209-218, 1975.

13. Yamada, Y., Yoshimura, H., and Sakurai, T., "Plastic stress-strain matrix and its application elastic-plastic problems by the finite element method", Int. Journal of Mechanics Sci., Vol.10, pp.343-354, 1968.

14. Nayak, G.C., Zienkiewicz, O.C., "Elasto-plastic stress analysis. A generalization for various constituve relations including strain softening", International Journal for Numerical Methods in Engineering, Vol.5, pp.113-115, 1972.

15. Meguid, S.A., Klair, M.S., "Elasto-plastic co-indendation analysis of a bounded solid using finite element method", Int. Journal of Mechanics Sci., Vol.27, pp.157-168, 1983.

16. Barton, M.V., "The circular cylinder with a band of pressure", Journal of Applied Mechanics, Vol.8, pp.A-97, 1941.

17. Okubo, H., Angew, Z., "An analysis of an elastic collar shrunk onto a long elastic shaft, without friction", Mathematical Mechanics, Vol.32, pp.178-186, 1952.

18. ANSYS Procedures, "Engineering Analysis System Verification Manual", Swanson Analysis System Inc., Volume.1, Houston, PA, United Stated of America, 1993.

19. ANSYS Command, "Engineering Analysis System Verification Manual", Swanson Analysis System Inc., Volume.2, Houston, PA, United Stated of America, 1993.

20. ANSYS Elements, "Engineering Analysis System Verification Manual", Swanson Analysis System Inc., Volume.3, Houston, PA, United Stated of America, 1993.

21. ANSYS Theory, "Engineering Analysis System Verification Manual", Swanson Analysis System Inc., Volume.4, Houston, PA, United Stated of America, 1993.

22. ANSYS Structural Nonlinearities, "Engineering Analysis System Verification Manual", Swanson Analysis System Inc., Volume.1, Houston, PA, United Stated of America, 1993.

23. ANSYS workbook, "Engineering Analysis System Verification Manual", Swanson Analysis System Inc., Volume.1, Houston, PA, United Stated of America, 1993.

24. ANSYS Getting Started, "Engineering Analysis System Verification Manual", Swanson Analysis System Inc., Houston, PA, United Stated of America, 1993.

25. Weidmann, G., Lewis, P., and Reid, N., "Structural Material", Alden Press Ltd., London, United Kingdom, 1990.

26. Bathe, K.J., "Finite Element Procedures in Engineering analysis", Prentice Hall, New Jersey, 1982.

27. Mendelson, A., "Plasticity: Theory and Application", The Macmilan Company, United Stated of America, 1968.

28. Dieter, George E., "Mechanical Metallurgy", MacGraw-Hill Company, Singapore 1968.

29. Belegundu, A.D., Chandrupatla, T.R., "Introduction to Finite Elements in Engineering", Prentice Hall, New Jersey, 1991.

30. Boressi, A.P., Sidebottom, Omar M., "Advenced Mechanics of Materials", John Wiley and Sons, Canada, 1985.

31. Zbigniew, D.J., "The Nature and Properties of Engineering Materials", John Wiley and Sons, Canada, 1987.

32. Hearn, E.J., "Mechanics of Materials", International Series on Materials Science and Thecnology, Volume.19, Pergamon Press Ltd., Oxford OX3 OBW, England, 1985.

33. Black, P.H., Adams, O.E., "Machine Design", MacGraw-Hill Company, New York, 1981.

34. Shigley, J.E., Mischake, C.R., "Mechanical Engineering Design", MacGraw-Hill Company, New York, 1989.

35. Baker, A.J., Pepper, D.W., "Finite Elements 1-2-3", MacGraw-Hill Company, Singapore 1991

36. Chakrabatry, J., "Theory of Plasticity", MacGraw-Hill Company, New York, 1988.

37. Zienkiewicz, O.C., Taylor, R.L., "The Finite Element Method", MacGraw-Hill Company, England, 1989.

38. Fung, Y.C., "Foundations of Solid Mechanics", Prentice Hall of India Private Limited, New Delhi, 1968.

39. Ottosen, N., Peterson, H., " Introduction to Finite Element Method", Prentice Hall, Great Britain, 1992.

40. Timoshenko, S.P., Goodier, J.N., "Theory of Elasticity", MacGraw-Hill Company, Singapure, 1987.

41. Wait, R., Mitchell, A.R., " Finite Element Analysis and Applications of ", John Wiley and Sons, Great Britain, 1985.

42. Ford, H., "Advanced Mechanics of Materials", John Wiley and Sons, New York, 1963.

43. Shames, H.I, "Introduction to Solid Mechanics", Prentice Hall Inc, New Jarsey, 1989.

44. Ugural, A.C., Fenster, S.U.,"Advanced Strength and Applied Elasticity", Elsevier North Holland, 1981.

45. Timoshenko, S.P., Young, D.H., "Theory of Structures", MC Graw Hill Company, United Stated.1965.

46. Edwards, K.S., Mckee, B., Robert, J.R.,"Fundamentals of Mechanical Component Design", MC Graw Hill Company, United Stated.1991.

47. Cook, R.D., Malkus, D.S., Plesha, M.E., "Consept and Applications of Finite Element Analysis", John Wiley and Sons, Canada, 1989

48. Karakuzu, Ramazan., "Increasing angular velocity of rotating discs with holes by residual stresses", Ph.D. Thesis, Dokuz Eylül Üniversity, Graduate School of Natural and Applied Sciences, İzmir, 1992.

APPENDIX A

PRESS AND SHRINK FITS

Shrink fits are found frequently in mechanical engineering. The importance of shrink fits rests on the fact that they are capable of transmitting high moments at low production costs. To better utilize the hub material, plastic deformation is admitted in many cases.

When two cylindrical parts are assembled by shrinking or press-fitting one part upon another, a contact pressure is created between two parts. The stress resulting from this pressure may easily be determined with the equations.

Figure 1.2 shows two cylindrical members which have been assembled with a shrink fit. A contact pressure P exists between the members at the transition radius R, causing radial stress $\sigma_r = -P$ in each member at the contacting surfaces. The tangential stress at the transition radius of the outer member is determined in outer surface,

$$\sigma_T (\text{at R}) = -P \frac{R^2 + r_i^{\,2}}{R^2 - r_i^{\,2}} \qquad (A.1)$$

In the same manner, the tangential stress at the inner surface of the outer member is

$$\sigma_T (\text{at R}) = P \frac{r_0^{\,2} + R^2}{r_0^{\,2} - R^2} \qquad (A.2)$$

These equation can not be solved until the contact pressure is known. In obtaining a shrink fit, the radius of the male member is made larger than the radius of the female member. The difference in these dimensions is called the radial interference and is the radial deformation which the two members must experience. Since these dimensions are usually known, the deformation should be introduced in order to evaluate the stresses. As shown in figure A.1 δ_i and δ_0 symbolize the changes in the radii of the inner and outer members, respectively. The total radial interference is, therefore,

$$\delta = |\delta_i| - |\delta_0| \qquad (A.3)$$
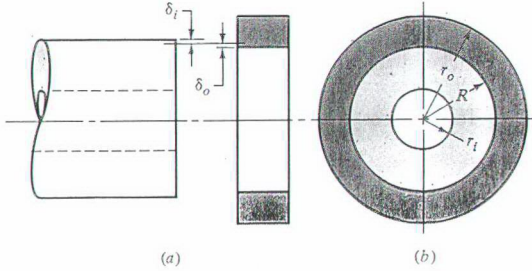
Figure A.1 Notation for press and shrink fits. a- Unassembled circular
cylinder with a hole parts   b- after assembly

The tangential strain at the transition radius of outer cylinder is measured by the change
in circumference, and is

$$\varepsilon_{ot} = \frac{2\pi(R+\delta_0) - 2\pi R}{2\pi R} = \frac{\delta_0}{R} \tag{A.4}$$

and so $\delta_0 = R\,\varepsilon_{ot}$ but, since

$$\varepsilon_{ot} = \frac{\sigma_{ot}}{E_o} - \frac{\upsilon_o \sigma_{or}}{E_o} \tag{A.5}$$

then, from equation (1.1) and (1.2), we have

$$\delta_o = \frac{PR}{E_o}\left(\frac{r_o^2 + R^2}{r_o^2 - R^2} + \upsilon_o\right) \tag{A.6}$$

This is the change in radius of the outer member. In a similar manner, the change in
radius of inner member is found to be

$$\delta_i = -\frac{PR}{E_i}\left(\frac{R^2 + r_o^2}{R^2 - r_o^2} - \upsilon_o\right) \tag{A.7}$$

Then, from equation (1.3), we have total deformation

$$\delta = \delta_o - \delta_i = \frac{PR}{E_o}\left(\frac{r_o^2 + R^2}{r_o^2 - R^2} + \upsilon_o\right) + \frac{PR}{E_i}\left(\frac{R^2 + r_o^2}{R^2 - r_o^2} + \upsilon_i\right) \tag{A.8}$$

123

This equation can be solved for the pressure P when the radial interference δ is given. If the two members are of the same materials, $E_o=E_i=E$, $\upsilon_o=\upsilon_i$ and the relation simplifies to

$$P = \frac{E\delta}{R}\left[\frac{\left(r_o^2 - R^2\right)\left(R^2 - r_i^2\right)}{\left(r_o^2 - r_i^2\right)}\right] \tag{A.9}$$

The value of interface pressure P from either Eq. (1.8) or Eq. (1.9) can now be used to obtain the stress state at the stress state at the specified radius in either cylinder.

In addition to the assumptions both stated and implied by the development, it is necessary to assume that both members have the same length. In the case of a hub which has been press-fitted to a shaft, this assumption would not be true, and there would be increased pressure at each end of hub. It is customary to allow for this condition by the employment of a stress concentration factor. The value of this factor depends upon the contact pressure and the design of the female member, but its theoretical value is seldom greater than 2.

APPENDIX B

STRESSES IN CYLINDER

Cylindrical pressure vessels, hydraulic cylinders, gun barrels, and pipes carrying fluids at high pressures developed both radial and tangential stresses with values that are depended upon the radius of the element under consideration. In determining the radial stress σ_r and the tangential stress σ_t we make use of the assumption that the longitudinal elongation is constant around the circumference of the cylinder. In other words, a right section of the cylinder remains plane after stressing.

Referring to figure B.1 we designate the inside radius of the cylinder by r_i, the outside radius r_o, the internal pressure P_i, and the external pressure P_o. Than it can be shown that tangential and radial stresses exist whose magnitudes are

$$\sigma_t = \frac{P_i r_i^2 - P_o r_o^2 - r_i^2 r_o^2 \left(P_o - P_i \right) / r^2}{r_o^2 - r_i^2} \tag{B1.1}$$

$$\sigma_r = \frac{P_i r_i^2 - P_o r_o^2 + r_i^2 r_o^2 \left(P_o - P_i \right) / r^2}{r_o^2 - r_i^2} \tag{B1.2}$$

As usual, positive values indicate tension and negative values, compression. The special case of $P_o = 0$ gives

$$\sigma_t = \frac{r_i^2 P_i}{r_o^2 - r_i^2} \left(1 + \frac{r_o^2}{r^2} \right) \tag{B1.3}$$

$$\sigma_r = \frac{r_i^2 P_i}{r_o^2 - r_i^2} \left(1 - \frac{r_o^2}{r^2} \right) \tag{B1.4}$$
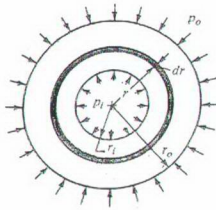
Figure B.1 A cylinder subjected to both internal and external pressure

It should be realized that longitudinal stresses exist when the end reactions to be internal pressure are taken by the pressure vessel itself. This stress is found to be

$$\sigma_l = \frac{P_i r_i^2}{r_o^2 - r_i^2} \qquad (B1.5)$$

We further note that equations (B1.1), (B1.2), (B1.3) and (B1.4) apply only to sections a significant distance from the ends and away from any areas of stress concentration.
An other special case $P_i=0$ gives

$$\sigma_t = -\frac{r_i^2 P_o}{r_o^2 - r_i^2}\left(1 + \frac{r_o^2}{r^2}\right) \qquad (B1.6)$$

$$\sigma_r = -\frac{r_i^2 P_o}{r_o^2 - r_i^2}\left(1 - \frac{r_o^2}{r^2}\right) \qquad (B1.7)$$

126

APPENDIX C

THE COMPUTER PROGRAM

C.1. INTRODUCTION

ANSYS program is a general-purpose computer program for finite element analysis that was used in the solution. The ANSYS program is a general-purpose program, meaning that you can use it for almost any type of finite element analysis in virtually any industry: automobiles, aerospace, railways, machinery, electronics, electromagnetic, sporting goods, power generation, power transmission, and biomechanics to mentioned just a few. General purpose also refers to the fact that the program can be used in all disciplines of engineering: structural, mechanical, electrical, electromagnetic, electronic, thermal, fluid, and biomedical. The ANSYS program is also used as an educational tool in universities and other academic institutions.

The procedure for typical ANSYS analysis can be devided into three distinct steps:

♦ Build the model
♦ Apply loads and obtain the solution
♦ Review the results

C.2. BUILD THE MODEL

C.2.1. Defining Element Type

Element types are considered. The ANSYS program element library contains over 100 types element. It may be that are span, beam, plane, volume, shell, axisymmetric etc. The element type determines, among other thing, the degree of freedom set which is implies the discipline (structural ,thermal, magnetic etc.), the characteristic shape of the element (line, quadrilateral, brick etc.), and the whether the element lies in 2-D space or 3-D space.

C.2.2. Defining Material Properties

Material properties are required for most element types. Depending on the application, material properties may be linear, nonlinear, and/or anisotropic. Material properties are stress-strain curve, modulus of elasticity, Poisson's ratio in all direction.

C.2.3. Creating the Model Geometry and Meshing

The main objective of this step is to generate a finite element model -nodes and elements-that adequately describes model geometry. With solid modeling, you describe the geometric boundaries of your model and than instruct the ANSYS program to automatically mesh the geometry with nodes and elements. You can control the size and shape of the elements that the program creates.

C.2.4. Defining Element Real Constants

Element real constants are properties that are specific to a given element type, such as cross-sectional properties of a beam element. For example, real constants for 2-D beam element are area of cross-section, moment of inertia, etc.

C.3. APPLY LOADS AND OBTAIN THE SOLUTION

C.3.1. Applying Forces and Pressure

Forces (F_X, F_Y, F_Z) and moment (M_X, M_Y, M_Z) are concentrated loads usually specified on the model exterior. The direction implied by the labels are in the nodal coordinate system. Pressures are surface loads, also usually applied on the model exterior. Positive values of pressure act towards the element face(resulting in a compressive effect).

C.3.2. Applying Boundary Condition

Displacements (U_X, U_Y, U_Z, ROT_X, ROT_Y, ROT_Z) are DOF constraints usually specified at the model boundaries to define rigid support points. They are also used to indicate symmetry boundary conditions and points of known motion. The directions implied by the labels are in the nodal coordinate system.

C.3.3. Obtaining Solution

Before the solution of the problem, some of the options are need to define. Define analysis type static or dynamic or any other. Specify load step options that is need to incremental loading. Program runs Newton-Raphson procedure and load external force incrementally. The program will continue to do equilibrium iterations until the convergence criteria are satisfied. Convergence checking is used two parameter. One of them is force, other is displacement. Using tighter convergence criteria will improve the accuracy of the results, but at the cost of more equilibrium iterations. These iterations will continue until to obtain results for all node.

C.4. REVIEW THE RESULTS

Postprosesing is that phase of any analysis in which you review the results. Results from a nonlinear static analysis consist mainly of displacement, stresses, strains and reactions forces.

PLDISP to display the deformed shape of the model
PLNSOL to display contours of stresses, strains and displacement etc.
PRNSOL to obtain tabular listing of data each node element.

(TÜBİTAK / TÜRDOK'un Abstrakt Hazırlama Kılavuzunu kullanınız.)

İNGİLİZCE ABSTRAKT (en fazla 250 sözcük): Circular cylindrical element with strip pressure in radial direction has widely applications in engineering such as bearings, gears, pulleys and shrink fit. In these machine elements, small permanent deformations occur under the working loads. Determination of elasto-plastic deformations, stress components and residual stresses after removal of loads would make possible the utilization of ultimate level of material capacity.

In the study, elasto-plastic stresses and residual stresses in the isotropic circular cylinder with the strip pressure in radial direction are investigated by the finite element method.

As the stress-strain relationship of the material is nonlinear after the yielding point, in the non-linear region successive incremental loading are carried out, the material is assumed linear, and for each incremental that material behaves linearly. Namely, successive linear analysis carried out for non-linear behavior.

In the investigation, because of the symmetry with respect to geometry, support condition and material properties of the problem, the problem is analyzed by four nodes isoparametric rectangular ring shape finite elements. Finite element mesh generation is carried out on computer automatically. General purpose computer program is used to solve the problem.

In the solution, it is assumed that deformations are small. Solid and hallow sectional cylinders with ratios inner diameter to outer diameter are considered. Stress and strain components are determined for different band pressures. And in the removal of the band pressure residual stresses are calculated. The magnitude of the residual stress can be obtained by superposition of the stresses due to loading and unloading. Values of the band pressure initiating plastic deformation are determined for different diameters by using von-Mises criterion.

Distributions of stress components (equivalent, tangential, radial, axial and shear stress) and residual stress components are plotted along the longitudinal axis on the outer and inner surfaces of the circular cylinder. Deformed shape and displacement of the model are given on the longitudinal section in the circular cylinders. Variations of stress contour components are presented on the longitudinal section along the circular cylinder for different diameter.

TÜRKÇE ABSTRAKT (en fazla 250 sözcük): Çevresi boyunca band basıncına maruz dairesel silindirik elemanlar mühendislik uygulamalarında yaygın kullanım alanı bulmaktadır (rulman, kasnak ve dişli makina elemanlarının sıkı geçme ile bağlanmasında olduğu gibi). Bu form birleştirmelerde, silindirik elemanlar üzerinde, büyük olmayan kalıcı şekil değişiklikleri meydana gelir. Makina elemanlarının bu bölgelerindeki, elasto-plastik şekil değişikliklerinin, gerilme bileşenlerinin ve band basıncının kaldırılmasıyla oluşan artık gerilmelerin önceden belirlen- mesi, malzemenin mukavemetinden maksimum seviyede faydalanılmasına imkan sağlar.

Bu çalışmada, çevresi boyunca band basıncı etkisine maruz, izotrop malzemeye sahip dairesel silindirik (dolu ve simetri ekseni boyunca boşaltılmış) elemanlarda meynada gelen elasto-plastik gerilmeler ve artık gerilmeler sonlu elemanlar metodu ile incelendi.

Akma noktasından sonra malzemenin gerilme-zorlanma ilişkisi non-lineer olduğundan, küçük artırımlarla ardışık yükleme yapılmış ve her bir aralıkta malzemenin lineer davrandığı kabul edilmiştir. Diger bir ifade ile nonlineer analizde çok tekrarlı lineer analiz yapılmıştır. Sonlu eleman modeli, geometri, sınır şartları ve yükleme simetrisinden dolayı izoparametrik dört düğümlü dörtgen halka elemanlardan oluşturulmuştur. Sistemin sonlu sayıda elamana bölümlenmesi bilgisayarda otomatik olarak yapılmıştır.

Çözümde, şekil değişimlerinin küçük olduğu durumlar incelenmiştir. Çözümler, dolu ve farklı oranlarda içi boşaltılmış silindirler için yapılmıştır. Farklı band basıncı değerlerinde meydana gelen zorlanma ve gerilme bileşenleri değerleri hesaplanmıştır. Bununla birlikte, silindire etki eden band basıncının kaldırılması halinde silindirde meydana gelen artık gerilmeler hesaplanmıştır. Plastik şekil değişimini başlatan band basıncı değerleri von-Mises akma kriteri esas alınarak belirlenmiş ve grafik olarak sunulmuştur..

Elasto-plastik gerilme analizi sonucunda, farklı band basıncı etkisinde dairesel silindirlerin iç ve dış yüzeylerinde hesaplanan gerilme bileşenlerinin (eşdeğer, teğetsel, radyal, eksenel ve kayma) ve artık gerilme bileşenlerinin değişimleri simetri ekseni boyunca grafikler halinde gösterildi. Modelin şekil değiştirmiş formu ve modeli oluşturan sonlu elemanların yerdeğiştirmeleri kesit üzerinde gösterildi. Elasto-plastik gerilme bileşenlerinin dağılımları ve band basıncın artırılması ile plastik deformasyonun derinleşmesi silindirin boylamasına kesiti üzerinde farklı renklerle gösterildi.